MOLECULAR AND CELLULAR MECHANISMS CONTRIBUTING TO THE ACCELERATED AGING PHENOTYPE IN HUTCHINSON-GILFORD PROGERIA SYNDROME

Dan Constantinescu

B.S., Haverford College, 1999

Submitted to the Graduate Faculty of

The School of Medicine in partial fulfillment of

the requirements for the degree of
Doctor of Philosophy

University of Pittsburgh

2008

UNIVERSITY OF PITTSBURGH

SCHOOL OF MEDICINE

This dissertation was presented

by

Dan Constantinescu

It was defended on

December 8th, 1008

and approved by

Dr. Richard Wood, Professor, MD Anderson Cancer Center

Dr. Laura Niedernhofer, Assistant Professor, Microbiology and Molecular Genetics

Dr. Simon Watkins, Professor, Cell Biology and Physiology

Dr. William Walker, Associate Professor, Cell Biology and Physiology

Thesis Advisor: Dr. Gerald Schatten, Professor, Obstertics, Gynecology and Reproductive Sciences

MOLECULAR AND CELLULAR MECHANISMS CONTRIBUTING TO THE ACCELERATED AGING PHENOTYPE IN HUTCHINSON-GILFORD PROGERIA SYNDROME

Dan Constantinescu, Ph.D.

University of Pittsburgh, 2008

Hutchinson-Gilford Progeria Syndrome (HGPS) is an autosomal dominant disorder caused by de novo mutations in the gene (LMNA) encoding lamin A that results in “premature aging” and early death. HGPS belongs to a group of disorders collectively referred to as, segmental progeroid syndromes, because multiple organs and tissues exhibit premature degenerative phenotypes consistent with physiological aging. The results presented here indicate that HGPS cells exhibit an elevated steady-state level of DNA double-stranded breaks (DSBs) and impaired repair of ionizing radiation (IR)-induced DSBs, both of which correlate strongly with the nuclear structural irregularities observed in a fraction of HGPS cells. These DNA damage-associated defects are due to the presence of Progerin in a dominant gain of function manner. Accordingly, reduction of Progerin levels by treatment with a farnesyl transferase inhibitor (FTI) improves repair of IR-induced DSBs. Interestingly, MRN (MRE11/Rad50/Nbs1) repair complex factors, involved in DSB repair, exhibit delayed localization to IR-induced DSBs, which may contribute to the repair defect. Furthermore, many segmental progeroid syndromes including HGPS exhibit phenotypes consistent with pre-natal developmental defects. These developmental defects are significant in their own right, but also because they may contribute to the post-natal progressive degeneration observed in HGPS. To begin investigating whether the HGPS mutation has adverse effects during pre-natal development, the expression of nuclear lamins was characterized in mouse (mESCs) and human (hESCs) embryonic stem cells which have been shown to be representative of pluripotent inner mass cells of blastocyst-stage embryos. This study shows that lamin A is not expressed in undifferentiated mESCs and hESCs, but becomes expressed quickly during in vitro hESC differentiation. Theses results suggest that Progerin is absent during early pre-natal development, but becomes expressed at later stages when the LMNA gene is activated, perhaps adversely affecting the

developmental process. Altogether, theses studies identify impaired DNA DSB repair as a molecular mechanism that may contribute to the progressive degeneration phenotype and suggest that at least some of the pathophysiology may begin before birth.

TABLE OF CONTENTS

1.0 INTRODUCTION ……... 1

1.1 Physiological Aging and DNA damage…….. 1

1.2 Hutchinson-Gilford Progeria Syndrome……. 3

1.3 LMNA and nuclear lamins…… 5

1.4 A-type lamin function…… 7

1.5 HGPS mutation……. 10

1.6 HGPS cellular and molecular phenotypes…… 11

1.7 DNA double-strand break repair……. 15

2.0 CHAPTER ONE: LAMIN A/C EXPRESSION IS A MARKER OF MOUSE AND HUMAN EMBRYONIC STEM CELL DIFFERENTIATION 18

2.1 Rationale…… 18

2.2 Abstract…….. 19

2.3 Introduction…… 20

2.4 Results……... 22

2.4.1 Undifferentiated mES and hES cells do not express A-type lamins… 22

2.4.2 Undifferentiated mES and hES cells express B-type lamins…… 24

2.4.3 hES cells express A-type lamins upon differentiation to neuronal….. lineages and cardiomyocytes 24

2.5 Discussion…… 26

2.6 Materials and Methods…….. 31

2.6.1 Cell Culture…….. 31

2.6.2 RNA Isolation and RT-PCR…….. 32

2.6.3 Wide-Field and Confocal Microscopy and Immunocytochemistry….. 32

2.7 Acknowledgements…… 33

3.0 CHAPTER TWO: DEFECTIVE DOUBLE-STRAND BREAK REPAIR…….. 34
CORRELATES WITH ABNORMAL NUCLEAR MORPHOLOGY AND IS
IMPROVED WITH FTI TREATMENT IN HUTCHINSON-GILFORD PROGERIA
SYNDROME FIBROBLASTS.

3.1 Rationale……. 34

3.2 Abstract…… 34

3.3 Introduction……. 35

3.4 Results……. 38

3.4.1 HGPS fibroblasts with an abnormal nuclear morphology have…….. 38
elevated steady-state levels of DSBs and impaired repair of
γ-irradiation induced DSBs.

3.4.2 Impaired repair of γ-irradiation induced DSBs is due to production.... 43
of Progerin and is present only in Progerin positive cells with an
abnormal nuclear morphology.

3.4.3 FTI treatment improves nuclear morphology and repair of…….. 46
γ-irradiation induced DSB, but does not reduce the steady-state
level of DSBs in HGPS fibroblasts.

3.4.4 MRN complex localization to γ-irradiation induced DSBs is……. 50
delayed in HGPS cells and GFP-Progerin positive hCAECs.

3.5 Discussion…… 54

3.6 Materials and Methods…….. 58

3.6.1 Cell Culture…….. 58

3.6.2 FTI treatment……... 59

3.6.3 Western Analysis…… 59

3.6.4 Immunocytochemistry……. 60

3.6.5 Lentivirus Production and Transduction…….. 60

3.7 Acknowledgements…… 61

4.0 CHAPTER THREE: SUMMARY AND CONCLUSIONS…… 62

4.1 Summary of Results…… 62

4.2 Mechanistic Hypotheses…… 65

BIBLIOGRAPHY…… 69

LIST OF FIGURES

FIGURE 1..... 4
FIGURE 2..... 5
FIGURE 3..... 9
FIGURE 4..... 22
FIGURE 5..... 23
FIGURE 6..... 25
FIGURE 7..... 26
FIGURE 8..... 27
FIGURE 9..... 38
FIGURE 10..... 40
FIGURE 11..... 42
FIGURE 12..... 45
FIGURE 13..... 47
FIGURE 14..... 53

INTRODUCTION

1.1 PHYSIOLOGICAL AGING AND DNA DAMAGE

Physiological aging is commonly described as a progressive decline in tissue functionality with increased mortality and is believed to be caused by a combination of genetic and environmental influences. Although multiple theories have been proposed, there is no unified theory for why and how organisms age. At the cellular and molecular levels, progressive decline in tissue functionality is believed to occur in large part due to the accumulation of damage to various cellular components and biomolecules that can lead to cell loss or loss of function. The body copes with such continuous damage, maintaining tissue homeostasis and function, by recycling cells through regeneration from stem cell pools. It is believed that the physiological decline that defines aging is due to an inability of the body to support regeneration indefinitely. This is the basis for the "Disposable Soma" evolutionary theory of aging which states that organisms have evolved to invest only enough energy to regenerate the soma to maintain proper tissue function to reach reproductive age, since energy devoted to regeneration of the soma reduces the energy devoted to development and reproduction (reviewed in (Kirkwood, 1977; Kirkwood and Holliday, 1979)). This hypothesis demands that the optimal level of energy invested in maintenance is below the minimum required for immortality (indefinite regeneration) and implies natural rates of tissue deterioration and eventual death. It is important to note that physiological aging and pathological disease are different phenomena even though one may contribute to the other. For example, many disease states such as atherosclerosis, cancer, etc…arise preferentially during old age and are believed to be caused at least in part by the loss of proper cellular or tissue function. Alternatively, genetic mutations can lead to diseases such as the segmental progeroid that appear to accelerate aging.

It is believed that damage to various cellular components, such as nuclear and mitochondrial DNA, RNA, and proteins contributes to physiological aging. However, it is thought that the accumulation of nuclear DNA damage is particularly detrimental because cells only have two copies of nuclear DNA, whereas several thousand copies of the mitochondrial genome exist and damaged proteins, RNA, and other cellular components can be replaced (reviewed in (Lombard et al., 2005)). Thus, damage to nuclear DNA can be particularly harmful to cellular function and survival. Even repair of nuclear DNA damage via the multiple repair mechanisms that exist usually results in changes to the local DNA sequence, producing mutations that may have significant consequences for the cell. There are several lines of evidence suggesting a mechanistic link between nuclear DNA damage and physiological aging (Reviewed in (Lombard et al., 2005)). It has been shown that the steady-state level of DSBs increases with age and that a higher proportion of radiation-induced DSBs remain unrepaired in cells from older individuals (Sedelnikova et al., 2004), which suggests that DSB repair mechanisms become less efficient with age. Similarly, multiple studies have shown that older individuals exhibit a higher mutation frequency (Reviewed in (Vijg, 2000)). Lastly, there is the observation that multiple progeroid syndromes are caused by mutations in DNA maintenance proteins and exhibit impaired DNA damage repair (Reviewed in (Puzianowska-Kuznicka and Kuznicki, 2005)).

Segmental Progeroid syndromes are a category of diseases characterized by the premature appearance of features consistent with physiological aging and early death (Reviewed in (Hofer et al., 2005; Navarro et al., 2006; Puzianowska-Kuznicka and Kuznicki, 2005). Because of the premature appearance of age-associated features, these diseases have been referred to as “accelerated aging” disorders. Such syndromes are referred to as “segmental” because they affect multiple organs and tissues, although no progeroid syndrome affects all organs and tissues, identifying a major difference with physiological aging. However, even if these syndromes do not mimic aging in its full extent, the mechanisms responsible for the tissue-specific progressive deterioration observed in these syndromes may help us to better understand the fundamental mechanisms responsible for physiological aging.

1.2. Hutchinson-Gilford Progeria Syndrome

HGPS is a rare segmental progeroid syndrome first clinically described by Hutchinson (Hutchinson, 1886) and later by Gilford (Gilford, 1904). It results from de novo mutations in the LMNA gene and has an estimated incidence of 1 in 4,000,000. It is considered the most severe of the progeroid syndromes affecting multiple tissues and resulting in a median lifespan of ~13 years. Until the recent discovery of the mutated gene (De Sandre-Giovannoli et al., 2003; Eriksson et al., 2003), diagnosis was based solely on clinical features, an approach that current genetic analysis has shown to be imperfect. Misdiagnoses have occurred because segmental progeroid syndromes share many clinical features. Unfortunately, misdiagnoses have resulted in some early research studies on HGPS being performed on cells from individuals that since been shown to harbor different mutations. A clear consensus on the clinical features specific to HGPS is important for disease diagnosis, understanding disease progression, and for determining success criteria in current clinical trials. A recent study of HGPS patients harboring the correct mutations systematically described a variety of pathological features that patients exhibit (Merideth et al., 2008). This study showed that HGPS patients are characterized by abnormalities that may be associated with developmental/growth defects, such a hypodontia (7/11), ankyloglossia (7/14), circumoral cyanosis (13/15), ogival palate (8/15), delayed tooth eruption (12/15), and double row of teeth (3/15), as well as conditions reminiscent of physiological aging, including, alopecia (15/15), altered skin pigment (15/15), and sclerotic skin (12/15) (Merideth et al., 2008). Individuals afflicted with HGPS exhibit growth retardation. Mean body mass at birth is normal, but falls below the third percentile shortly after birth, resulting in an average gain of 0.65kg per year between the ages of two and ten, compared to 1.80 kg per year for healthy children (Merideth et al., 2008). Individuals receiving hormone therapy gained 1.01kg per year (Merideth et al., 2008). Similarly, height falls below the third percentile for healthy children by 15 months of age, resulting in an average gain of 3.58 cm per year compared with 5.84 cm per year for healthy children (Merideth et al., 2008). HGPS patients receiving growth hormone gained 3.98 cm per year (Merideth et al., 2008). Contributing to low body mass is decreased bone density and

percent body fat (Merideth et al., 2008). Impaired growth does not appear to be due to inadequate nutrition, abnormal growth hormone production, or insulin resistance (Merideth et al., 2008). HGPS patients also exhibit various physical and functional cardiovascular abnormalities, resulting in overall reduced vascular function with age. Particularly, patients exhibit medial smooth-muscle cell loss, maladaptive vascular remodeling, intimal thickening, disrupted elastin fibers, deposition of extracellular matrix, and stenosis associated with sclerotic plaques in the aortic and coronary arteries (Merideth et al., 2008). The cardiovascular irregularities are of particular interest, considering that 90% of HGPS patients die because of atherosclerosis associated myocardial infarct or stroke. Patients exhibited various musculoskeletal physical abnormalities including decreased spinal flexation (11/11), stooped shoulders (11/11), calcaneovalgus (9/11), subluxed finger joints (7/11), genu valgum (4/11), kyphosis (3/11), and calcaneo varus (1/11), resulting in functional impairments (Merideth et al., 2008). Muscle strength and muscle volume to body mass is normal (Merideth et al., 2008). Blood tests revealed elevated platelet counts (14/15), prolonged prothrombin time (8/11), elevated levels of serum phosphorus (8/15), serum triglycerides (5/14), total cholesterol (elevated low-density lipoprotein cholesterol (4/14) and reduced high-density lipoprotein cholesterol (10/14)) (Merideth et al., 2008).

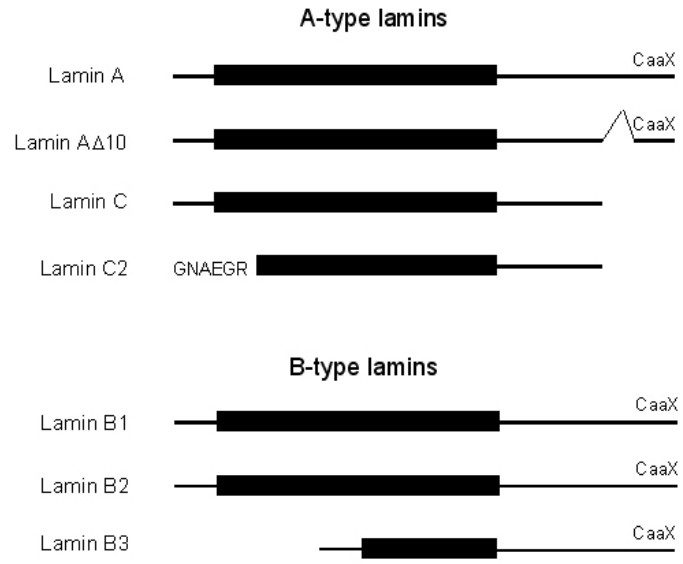

Figure 1. A-type and B-type lamins.

1.3. LMNA AND NUCLEAR LAMINS

The HGPS mutation occurs in the LMNA gene which encodes the A-type nuclear lamins: lamin A, lamin C, lamin AΔ10, and lamin C2. Lamin AΔ10 and the male germ cell specific C2 are minor isoforms that have been minimally investigated (Figure 1). The A-type lamins, together with the B-type lamins, lamin B1 encoded by the LMNB1 gene and lamins B2 and B3 encoded by the LMNB2 gene (Figure 1), form the nuclear lamina, a scaffold-like structure that lines the inside of and interacts with the inner nuclear membrane. There is evidence that nuclear lamins are also present throughout the nucleoplasm, contributing to a nuclear matrix (Hozak et al., 1995). Nuclear lamins are type-V intermediate filament proteins that are categorized into the A- and B-subtypes based on sequence homologies. The nuclear lamins consist of a globular N-terminal head domain, followed by a central α-helical coiled-coil rod domain, and a C-terminal tail domain (Figure 1). Lamins A, B1, and B2, the primary nuclear lamin isoforms contain a CAAX motif at the C terminus that is post-translationally modified. Lamin proteins form parallel coiled-coil homodimers, which then align head to tail to form protofilaments, that interact laterally to form higher-order filaments. A recent report suggests that lamins do not form heterodimers (Delbarre et al., 2006). Little is known about how the lamin

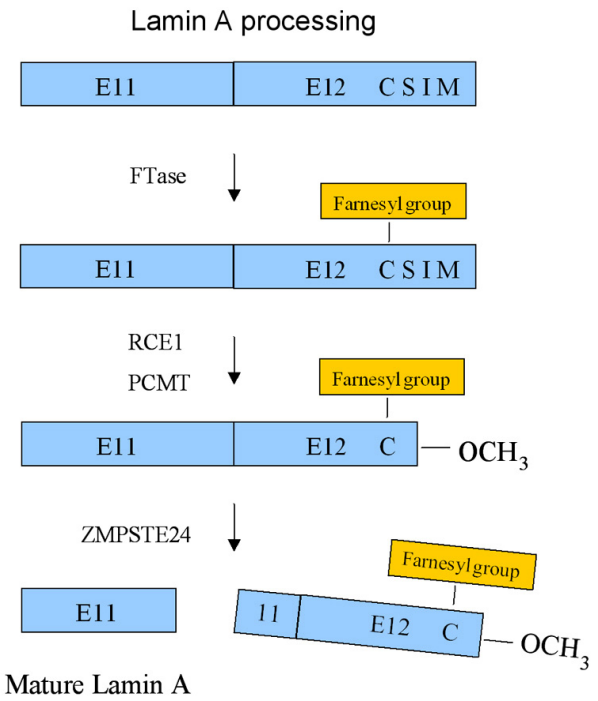

Figure 2. Pre-lamin A Processing. The image shows exon 11 (E11) and exon 12 (E12) in blue not drawn to scale. Exon 12 ends in the CaaX motif, CSIM. FTase = farnesyl transferase.

filaments associate in vivo to form the nuclear lamina, or their nucleoplasmic organization.

Lamin A is synthesized as prelamin A, a precursor molecule consisting of exons 1-12 that is subsequently modified in four steps to yield mature lamin A (Figure 2). The first step is farnesylation of the cysteine residue within the CaaX motif by protein farnesyltransferase (Sinensky et al., 1994). Subsequently, the protein undergoes endonuclease cleavage by RCE1 which removes the last three amino acids (Bergo et al., 2002; Corrigan et al., 2005). The exposed farnesylcysteine is then methylated by isoprenylcysteine carboxyl methyltransferase (Bergo et al., 2002). The last processing step is internal proteolytic cleavage by ZMPSTE24, removing the last 15 carboxy-terminal amino acids, including the farnesylcysteine methyl ester to generate mature lamin A (Bergo et al., 2002; Corrigan et al., 2005; Sinensky et al., 1994). The initial farnesylation step is necessary for the subsequent proteolytic modifications (Bergo et al., 2002). Evidence suggests that farnesylation targets farnesyl-prelamin A to the inner nuclear membrane and that the final ZMPSTE24 endoproteolytic step releases mature lamin A, allowing it to properly incorporate into the nuclear lamina.

Whereas lamins B1 and B2 are present ubiquitously, lamins A and C are expressed primarily in differentiated cells. Mouse studies have shown that during development lamin A is fist detected in the trophectoderm around day 9 and in the embryo proper around day 12 (Prather et al., 1991; Prather et al., 1989; Rober et al., 1989; Schatten et al., 1985; Stewart and Burke, 1987). In most tissues it is not detected until late development and in some LMNA expression is only observed post-natally. Lamins A and C are absent or expressed at low levels in undifferentiated cells such as embryonic carcinoma (EC) (Stewart and Burke, 1987). Further, studies have produced mixed results regarding the expression of lamin A in undifferentiated adult cells and certain adult stem cell populations (Broers et al., 1997; Lourim and Lin, 1989a; Rober et al., 1989; Scaffidi and Misteli, 2008). Further, lamin A is not expressed in mouse (mES) or human (hES) embryonic stem cells, but is upregulated upon hES cell differentiation ((Presented here; (Constantinescu et al., 2006)). These expression patterns indicate a correlation between differentiation and lamin A expression, and some have proposed that lamin A may be involved in

maintaining the differentiated state, perhaps by stabilizing chromatin patterns and hence gene expression. However, a specific study in which chicken lamin A was stably expressed in undifferentiated human embryonic carcinoma cells resulted in no detectable affect on differentiation (Peter and Nigg, 1991). The presence of lamin A neither induced differentiation, nor maintained the pluripotent state. Ideally, this experiment should be performed with the expression of human lamin A in non-tumor derived undifferentiated cells such as human embryonic stem cells. My own attempts to stably express a GFP-Lamin A construct in hES cells failed despite, despite consistent success in stably expressing GFP alone in hES cells (non-published results) and the GFP-Lamin A construct in differentiated cells (Figure 11). This raises the possibility that the presence of lamin A in undifferentiated ES cells is toxic resulting in cell death. More extensive studies are needed to fully identify the role of lamin A/C with respect to differentiation.

1.4. A-TYPE LAMIN FUNCTION

A-type lamins provide nuclear structural support and have been shown to be important for chromatin organization and nuclear positioning as well as DNA replication (Kennedy et al., 2000; Shumaker et al., 1998; Spann et al., 1997) and transcription (Spann et al., 2002), processes which are believed to be dependent on proper nuclear structural and chromatin organization. *LMNA* -/- mice develop normally, but exhibit growth retardation and muscular dystrophy after birth, resulting in early death (Sullivan et al., 1999). The nuclei in embryonic fibroblasts from *LMNA*-/- mice display abnormal nuclear shapes and mislocalization of B-type lamins and emerin, a lamin-binding inner nuclear membrane protein (Clements et al., 2000). Interestingly, expression of lamin C, in the absence of lamin A, appears to be sufficient to maintain relatively normal cellular characteristics (Fong et al., 2006b).

The nuclear lamins appear to be important for nuclear assembly post-mitosis and there appear to be differences in the functions of A-type and B-type lamins. During the transition from late prophase to metaphase the nuclear envelope breaks down in preparation for cell division. Disassembly of the nuclear lamina is activated through phosphorylayion of lamin subunits by p34sdc2, resulting in the formation of lamin monomers, dimers, and tetramers (Dessev et al., 1991; Gerace and Blobel, 1980; Newport and Spann, 1987; Ottaviano and Gerace, 1985; Peter et al., 1990). Disassembly of the different lamin isoforms appears to occur at different rates; A-type lamins are released during early prophase, whereas B-type lamins are remain at the nuclear periphery until prometaphase (Georgatos et al., 1997). The manner of nuclear lamina assembly following mitosis and the role of in nuclear assembly is more controversial. It is believed that nuclear lamin dephosphorylation, perhaps by the PP1 family of serine/threonie phosphotases (Steen et al., 2000; Thompson et al., 1997), is necessary for reassembly of the nuclear envelope after mitosis. There is evidence to suggest that lamins interact with NE components and have a functional role in envelope formation early during assembly (Burke and Gerace, 1986; Dabauvalle et al., 1991; Lourim and Krohne, 1993). Alternatively there is also evidence indicating that lamins have no functional role in nuclear assembly and are imported into nuclear vesicles that have formed around chromatin and have functional nuclear pores (Meier et al., 1991; Newport et al., 1990). Both scenarios can be reconciled by a model in which only a small fraction of the total amount of lamins takes part in envelope formation and the remaining lamins are imported into the nucleus when nuclear pore complexes become functional. Further research is necessary to fully elucidate the order of events of lamina reassembly and any functional role lamins may have in nuclear envelope assembly.

Multiple lines of evidence suggest that A-type lamins are important for local chromatin organization and positioning throughout the nucleus. The first line of evidence is the multiple direct and indirect interactions between A-type lamins and chromatin. A-type lamins have been shown to bind mitotic chromosomes (Burke, 1990; Glass et al., 1993; Glass and Gerace, 1990) and polynucleosomal particles in vitro (Yuan et al., 1991). Specifically, A-type lamins have been shown to interact with chromatin by binding histones (Glass et al., 1993; Hoger et al., 1991; Schmidt and Krohne, 1995; Taniura et al., 1995;

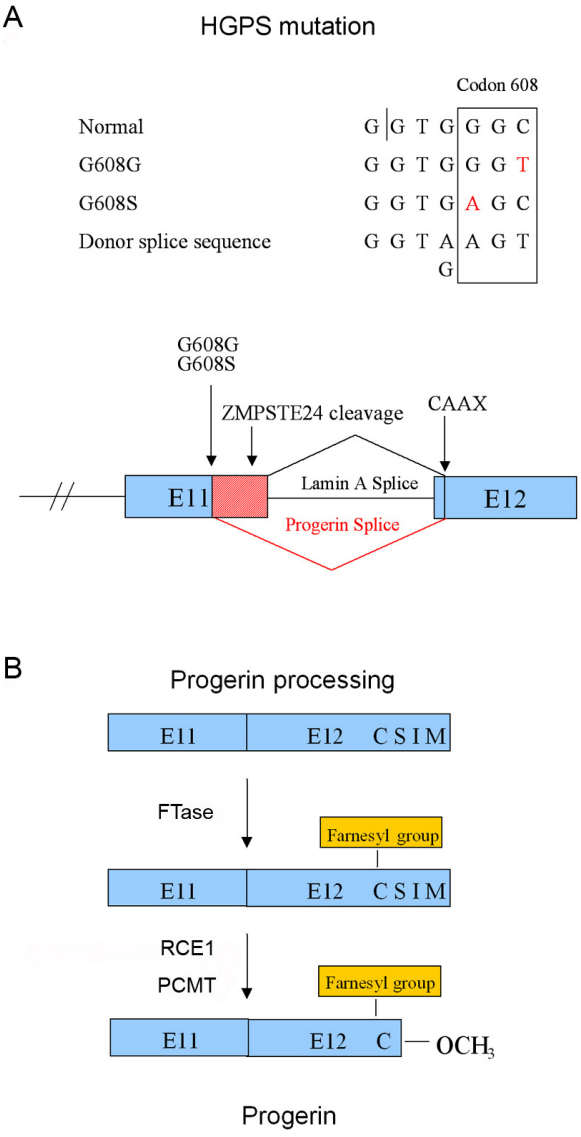

Figure 3. HGPS mutations and abnormal post-translational processing. A) The G608G and G608S HGPS mutations within exon 11 increase the sequence similarity between the wildtpye sequence and the indicated donor splice sequence. The mutations can result in aberrant splicing within exon 11, removing 50 amino acids including the ZMPSTE cleavage site. B) Processing of the mutated form of lamin A. Interference with ZMPSTE cleavage leaves "Progerin" as the final processing product.

Yuan et al., 1991) and DNA directly (Shoeman and Traub, 1990; Stierle et al., 2003). A-type lamins also interact with chromatin indirectly through lamin-binding proteins, including LAP2α (Dechat et al., 2000) and barrier-to-autointegration (BAF) (Holaska et al., 2003). The second line of evidence comes from cells with various LMNA mutations that exhibit irregularities in chromatin organization. LMNA-/- fibroblasts have regions exhibiting a dissociation of heterochromatin from the nuclear envelope (Nikolova et al., 2004; Sullivan et al., 1999). Cells from patients with AD-EDMD (Sabatelli et al., 2001), FPLD (Capanni et al., 2003), MAD (Filesi et al., 2005), and HGPS (Columbaro et al., 2005; Goldman et al., 2004) exhibit a similar dissociation or loss of heterochromatin. Cells from patients with MAD also exhibit changes in H3K9me3 patterns, a marker of constitutive heterochromatin (Filesi et al., 2005). A third line of evidence shows that LMNA mutations result in chromatin repositioning. LMNA-/- cells exhibit altered localization of a genetic locus on human chromosome 4 associated with acioscapulohumeral muscular dystrophy (FSHD) (Masny et al., 2004). Further, chromosome territories, 13 and 18, are repositioned form the

nuclear periphery to the interior of the nucleus in some diseases caused by LMNA mutations (Meaburn et al., 2007).

1.5. HGPS MUTATION

The most prevalent mutation associated with HGPS is a single nucleotide substitution, 1824C>T in codon 608 within exon 11 of the LMNA gene (Figure 3A). This mutation along with another less prevalent mutation, 1822G>A results in partial activation of a cryptic splice site (Figure 3A), and removal of the 150 carboxy-terminal nucleotides in exon 11 (De Sandre-Giovannoli et al., 2003; Eriksson et al., 2003) (Figure 3A). This aberrant splicing event maintains the CAAX motif, but removes the internal ZMPSTE24 cleavage site that is needed for lamin A maturation, resulting in permanent farnesylation and carboxymethylation (Figure 3B). This protein product, termed Progerin/LAdelta50 remains preferentially localized to the nuclear lamina, since it cannot undergo the final ZMPSTE24-mediated endoproteolytic cleavage step (Goldman et al., 2004). It has been estimated that only 10-50% of the mRNA from the mutated allele is spliced incorrectly, and since the second LMNA allele is normal, the majority on mRNA results in the production of wildtype lamin A, albeit at lower levels (De Sandre-Giovannoli et al., 2003). Multiple other mutations in LMNA, collectively termed laminopathies, appear to produce an variety of diseases (Rankin and Ellard, 2006). Some of these mutations are responsible for a growing class of laminopathies, referred to as Atypical HGPS, which exhibit a similar clinical phenotype to classical HGPS (Csoka et al., 2004a). However, the mechanism of action is probably different since these mutations do not result in the production of Progerin.

1.6. HGPS CELLULAR AND MOLECULAR PHENOTYPES

Various pathological cellular and molecular phenotypes have been described for HGPS cells. First, HGPS cells exhibit multiple nuclear structural irregularities including an abnormal nuclear shape, characterized by lobes and invaginations in the nuclear envelope (De Sandre-Giovannoli et al., 2003; Eriksson et al., 2003; Goldman et al., 2004), thickening of the lamina (Goldman et al., 2004), and altered spatial distribution of NPCs (Goldman et al., 2004). These abnormal structural characteristics are accompanied by functional changes, including loss of structural nuclear integrity under mechanical stress (Lammerding et al., 2004) as well as mitotic defects, including abnormal chromosome segregation, delays in cytokinesis and nuclear reassembly, and binucleation (Cao et al., 2007; Dechat et al., 2007).
HGPS cells also exhibit altered chromatin organization in interphase nuclei, similar to changes observed in other diseases caused by LMNA mutations as previously discussed. Particularly, HGPS cells exhibit loss of peripheral heterochromatin (Columbaro et al., 2005; Goldman et al., 2004) that may be due to epigenetic changes, including upregulation of H3K9me3 and H4K20me3, which define constitutative heterochromatin and downregulation of H3K27me3 which defines facultative heterochromatin (Columbaro et al., 2005; Goldman et al., 2004; Scaffidi and Misteli, 2005). In addition to epigenetic changes, HP1alpha, which is usually associated with H3K9me3 is down-regulated and partially dissociated (Scaffidi and Misteli, 2005; Shumaker et al., 2006). The decrease in H3K27me3 may due to a reduction in the expression of enhancer of zeste homolog (EZH2), the histone methyltransferase responsible for H3K27 trimethylation (Shumaker et al., 2006). The retinoblastoma gene product (pRb), which binds A-type lamins in vitro (Ozaki et al., 1994) and whose hyperphosphorylated form is reduced in HGPS cells (Dechat et al., 2007) may also be responsible for epigenetic changes. pRB regulates expression of EZH2 (Bracken et al., 2003) and associates with and regulates the HMTs, SUV39H1 and Suv4-20h, responsible for H3K9 and H4k20 trimethylation, respectively (Gonzalo et al., 2005; Isaac et al., 2006; Nielsen et al., 2001). Changes in constitutative and facultative heterochromatin, which are associated with gene expression inhibition, are expected to result in gene expression changes, especially gene activation.

There is some evidence to suggest that these epigenetic chromatin alterations do bring about gene expression changes. The decrease in H3K9Me3 in pericentric regions of HGPS cells coincides with upregulation of pericentric chromosome 9 sat III transcripts (Shumaker et al., 2006). Further, loss of H3K27me3 on the inactive X chromosome (Xi) due to expression of Progerin leads to decondensation of Xi (Shumaker et al., 2006), although it remains unknown if this is accompanied by transcriptional upregulation.

Telomere length has been shown to correlate inversely with age and senescence and directly with replicative capacity in vitro (Reviewed in (Aubert and Lansdorp, 2008)). It has been reported that primary cells derived from individuals diagnosed with HGPS have shorter telomeres than age matched controls (Allsopp et al., 1992). However, this study was performed prior to identification of the HGPS mutation so it is not known for certain whether the donors were afflicted with classical HGPS (608 mutation). Since it has been shown that diagnosis of classical HGPS based on clinical features is not always accurate, these results have to be regarded with skepticism. Furthermore it has been reported that primary HGPS cells can be immortalized with telomerase (Ouellette et al., 2000; Wallis et al., 2004), but that clonogenic variance exists (Wallis et al., 2004). It was reported that one third of HGPS clones did not immortalize even though telomerase levels and telomeres lengths were within appropriate ranges (Wallis et al., 2004). This variability may be due to occasional loss of the mutated allele and subsequent selection of these cells during proliferation, but this has not been confirmed.

Interestingly, multiple lines of evidence indicate that HGPS cells exhibit elevated levels of DNA damage. First, HGPS cells demonstrate limited proliferative capacity in culture, early onset of senescence, and increased apoptosis (Bridger and Kill, 2004), all of which can be caused by DNA damage. Second, HGPS cells exhibit elevated activity of DNA damage response pathways (Liu et al., 2006). Lastly, the most direct evidence of elevated DNA damage comes from a study which showed that HGPS and ZMPSTE24-/- cells have a DSB repair defect that may be specific to homologous recombination (HR) repair (Liu et al., 2005). Furthermore, both HGPS and ZMPSTE24-/- cells exhibited less localization of

the DSB repair factors Rad50 and Rad51 and prolonged association of 53BP1, a DNA damage signaling molecule. Altogether, these studies indicate that Lamin A is important for proper DNA damage repair and that DSB repair in compromised in HGPS cells, but the extent and the manner of the DSB repair impairment has not been fully elucidated.

It has been demonstrated that the nuclear morphological changes and some of the altered chromatin characteristics are not caused by lamin A haploinsufficiency, but by the presence of Progerin in a dominant gain-of-function fashion, possibly through its accumulation at the INM (Goldman et al., 2004; Scaffidi and Misteli, 2005), where it appears to alter nuclear lamina structure (Dahl et al., 2006). Furthermore, the observation that ZMPSTE24-/- MEFs results in a similar DNA damage repair phenotype as HGPS cells (Liu et al., 2005) suggests that the DNA damage repair defect is due to the over-accumulation of Progerin at the INM, perhaps also in a dominant gain-of-function manner.

Accordingly, studies aimed at reducing the level of Progerin have shown improvement in many HGPS cellular phenotypes. One successful approach has been to use progerin specific aintisense morpholinos, which target the aberrant splice site, inhibiting splicing (Scaffidi and Misteli, 2005). Although, this approach is biologically and mechanistically ideal since it specifically inhibits the production of Progerin without affecting lamin A production, clinical application is thwarted by the inability to safely and accurately deliver desired quantities of morpholinos to all the tissues affected by HGPS in vivo. Another successful approach has been to treat HGPS cells with farnesyl transferase inhibitors (FTIs), which inhibit farnesyl transferase and thus post-translational modification of Progerin. This approach is based on the hypothesis that HGPS pathology is caused by the modified form of Progerin which aggregates at the INM. FTI treatment can improve some of the nuclear abnormalities in vitro as well as the overall health in LMNA HG/+ mice (Capell et al., 2005; Fong et al., 2006a; Glynn and Glover, 2005; Liu et al., 2006; Toth et al., 2005; Yang et al., 2006; Yang et al., 2008), but one report suggests that FTIs do not reduce the elevated levels of DNA damage response pathways in HGPS cells (Liu et al., 2006). FTIs do not specifically inhibit modification of Progerin, resulting in inhibition of lamin A as well as the modification of

other unrelated proteins that are farnesylated. Although this makes FTI treatment less than ideal, FTIs do not appear to have major adverse effects as shown by clinical studies aimed at treating cancer. Their apparent safety and ease of administration, as well as the lack of any other therapeutic treatment, has led to a current phase II clinical trial to treat HGPS patients (ClinicalTrials.gov identifier: NCT00425607).

Two groups have created mouse models to study HGPS. Yang et al. have created targeted $Lmna^{HG/+}$ and $Lmna^{HG/HG}$ mouse models, using a Lmna targeting vector missing the last 150 nucleotides from exon 11, so that that the construct produces a mouse version of progerin, exclusively (Yang et al., 2005; Yang et al., 2006). The authors show that a higher percentage of embryonic fibroblasts from $Lmna^{HG/+}$ mice display an abnormal nuclear morphology. The $Lmna^{HG/+}$ mice developed normally, but began exhibiting reduced weight gain by 6-8 weeks. The mice also displayed lypodystrophy and various skeletal abnormalities, similar to HGPS patients. Survival rate for $Lmna^{HG/+}$ was severely reduced. 50% of the $Lmna^{HG/+}$ mice died or were euthenized due to severity of phenotype by 27 weeks of age. $Lmna^{HG/HG}$ exhibited similar phenotypes, but more severe, and died by 5-6 weeks after birth. It is important to note that because the targeting construct produces progerin exclusively, $Lmna^{HG/+}$ mice likely express a higher level of progerin than is present in HGPS patients. Varga et al. have also created an HGPS mouse model by introducing a bacterial artificial chromosome expressing the mutated (G608G) human genomic sequence (Varga et al., 2006). Thus the transgenic mice have two wildtype mouse Lmna alleles, and a mutated (G608G) human LMNA allele that was reported to express human lamin A, C and progerin. No external characteristics associated with HGPS or lifespan differences were detected by 20 months of age. The transgenic mice did show a progressive degeneration of vascular tissue, characterized by loss of smooth muscle cells and changes in extracellular matrix composition. Similar vascular changes have been described in HGPS patients, which display a rapid onset of atherosclerosis. The lack of a severe HGPS phenotype in this model may be due to the low levels of human progerin relative to wildtype mouse lamin A or a less potent effect of human progerin in mouse cells despite the high level of sequence homology

1.7. DNA DOUBLE-STRAND BREAK REPAIR

Cellular DNA is under constant attack from endogenous and exogenous agents resulting in various type of DNA damage, including single- (SSBs) and double-strand breaks (DSBs), DNA-protein crosslinks, and various base damage. DNA DSBs are the most dangerous form of DNA damage since such lesions can result in loss or rearrangement of genetic information as well as cell death. DSBs are produced naturally as part of the mechanisms for various biological processes such as V(D)J recombination (Franco et al., 2006), class-switch recombination (Chaudhuri et al., 2007), and meiosis (Keeney and Neale, 2006). They can also occur during DNA replication when replication forks encounter blocking lesions that can be produced by reactive oxygen species (ROS), chemical agents, and UV radiation (Bosco et al., 2004; Limoli et al., 2002). Further, they can be produced by ionizing radiation, either directly or indirectly through production of reactive oxygen species (ROS). Cells have developed DNA damage response pathways that detect DSBs, transiently arrest the cell cycle, and activate repair mechanisms (Reviewed in (Kobayashi et al., 2008; Shrivastav et al., 2008)). If repair is successful cells re-enter the cell cycle, but if DSBs are irreparable cells can undergoe apoptosis to prohibit inheritance of genomic lesions.

Eukaryotic cells have developed two primary mechanisms for repair of DSBs: non-homologous end joining (NHEJ) and homologous recombination (HR) (Reviewed in (Shrivastav et al., 2008)). It is believed that DSBs produced during replication through replication fork collapse are primarily repaired via HR, whereas other DSBs can be repaired by either mechanism. NHEJ exhibits variable accuracy depending on the type of DSB being repaired, but generally results in small deletions or insertion at the DSB, and thus in alteration of the local nucleotide sequence. HR utilizes a homologous region (sister chromatid, homologous chromosome, or repeated regions on the same or different chromosome) to prime repair synthesis. The accuracy of repair depends on the homology of the repair template which is often not 100% accurate if the sister chromatid is not used, resulting in transfer of information form the donor locus

to the recipient locus. Further evidence form yeast suggests that the repair polymerase used in HR is not as accurate as those involved in DNA replication, resulting in a higher rate of point mutations (Strathern et al., 1995). Nonetheless, HR is considered to be more accurate than NHEJ.

It is thought that both NHEJ and HR compete for repair of DSBs. This was suggested by experiments showing that both mechanisms actively repair plasmid DNA transfected into mammalian cells. It has also been shown that when NHEJ is defective HR capacity increases, consistent with a competitive model (Reviewed in (Shrivastav et al., 2008)). There are differences in which repair pathway is preferentially used from cell type to cell type and throughout the cell cycle that appear to be due to both active and passive mechanisms (Reviewed in (Shrivastav et al., 2008)). Active mechanisms include differing expression levels or functionality of proteins involved in or in control of either type of repair. For example, RAD51 and RAD52, repair factors involved in HR are overexpressed during S phase (Chen et al., 1997) in which HR capacity has been shown to be increased. Further, p53 has been shown to be a suppressor of HR (Reviewed in (Gatz and Wiesmuller, 2006)). Accordingly, mouse ES cells which have decreased p53 function (Chen et al., 1997) have greater HR capacity. Passive mechanisms include the different accessibility of a homologous template throughout the cell cycle. It has been shown that sister chromatids are the preferred template in mammalian cells (Dronkert et al., 2000; Kadyk and Hartwell, 1992), probably due to the close physical proximity until separation in anaphase. Accordingly, HR appears to be the predominant repair pathway during S and G2 phases of the cell cycle although NHEJ repair is still active during these phases (Reviewed in (Shrivastav et al., 2008)).

The repair machinery involved in HR repair includes various proteins. One such component is the MRN complex (MRE11, RAD 50, and NBS1). The MRN complex is essential for DSB repair as shown by the observation that null mutations in any of the three component proteins results in embryonic lethality in mice (Luo et al., 1999; Xiao and Weaver, 1997; Zhu et al., 2001). Furthermore, Nijmegen breakage syndrome (Carney et al., 1998; Varon et al., 1998) and ataxia telangiectasia-like disorder (Stewart et al., 1999), which are characterized by radiation hypersensitivity, are caused by mutations in the NBS1 and

MRE11 genes, respectively. In humans, MRN acts both as a damage sensor and is believed to be involved in the early steps of HR repair (Reviewed in (Williams et al., 2007)). The MRN complex is believed to function as both a long range tethering scaffold to hold large chromosomal domains in place as well as short range DNA synaptic structures that hold the two broken chromosome ends at a DSB in close proximity (Reviewed in (Williams et al., 2007)). Reports indicate that other factors are also involved at least in the long range tethering scaffolds (Sjogren and Nasmyth, 2001; Strom et al., 2007). The MRN complex is also important in activation of DNA damage response pathways through activation of ATM. The current understanding is that NBS1 binds ATM physically recruiting it to DSBs and also helps to activate ATM kinase activity (Lee and Paull, 2005; You et al., 2005). Once activated, ATM phosphorylates numerous targets that regulate cell cycle checkpoints and DNA damage repair, including H2AX, Chk2, and p53 (reviewed in (Kurz and Lees-Miller, 2004). Lastly, the MRN complex has been implicated in chromatin remodeling near DSBs. MRE11 is important for histone removal in the area surrounding DSBs (Reviewed in (Williams et al., 2007)). Similalry, MRN has been linked with the recruitment and/or activity of various chromatin remodeling proteins (reviewed in (Williams et al., 2007).

CHAPTER II: LAMIN A/C EXPRESSION IS A MARKER OF MOUSE AND HUMAN EMBRYONIC STEM CELL DIFFERENTIATION

2.1 RATIONALE

The rational for examining the expression of nuclear lamins in mouse and human ESCs was two fold. One purpose of the experiments was to determine whether Progerin is present during early human development. Since Progerin acts in a dominant gain-of-function manner it can only exert its adverse effects if the LMNA gene is expressed. Although HGPS has traditionally been described as an "accelerated aging" disorder because it exhibits many characteristics associated with old age prematurely, it also manifests multiple pathologies that point to developmental defects. For example, a recent study categorizing HGPS clinical phenotypes identified the following developmental abnormalities: hypodontia (7/11), ankyloglossia (7/14), circumoral cyanosis (13/15), ogival palate (8/15), delayed tooth eruption (12/15). Interestingly, it is possible that some of the characteristics associated with aging may be causally rooted in more fundamental developmental defects. Irrespective of such a putative relationship, investigating developmental defects in HGPS is important for fully understanding the pathophysiology and progression of the disease. Examination of LMNA expression in ESCs, which are representative of pluripotent inner mass cells, allows us to determine whether Progerin is present and whether HGPS pathology begins during early human embryonic development.

The second rationale was to further examine whether there is a correlation between LMNA expression and an undifferentiated state in human cells. It is commonly accepted that most, if not all, human tissues maintain cellular homeostasis through continual regeneration from tissue-specific multipotent adult stem cell pools. It has even been hypothesized that functional loss of adult tissue-specific stem cell pools

contributes to normal aging (Reviewed in (Rossi et al., 2008; Sharpless and DePinho, 2007)). If LMNA is expressed and Progerin is present in undifferentiated adult stem cells, the cells may experience increased rates of apoptosis and early onset of senescence, which may contribute to the accelerated aging phenotype observed in HGPS.

2.2 ABSTRACT

Nuclear lamins comprise the nuclear lamina, a scaffold-like structure that lines the inner nuclear membrane. B-type lamins are present in almost all cell types, but A-type lamins are expressed predominantly in differentiated cells, suggesting a role in maintenance of the differentiated state. Previous studies have shown that lamin A/C is not expressed during mouse development before day 9, nor in undifferentiated mouse embryonic carcinoma (EC) cells. To further investigate the role of lamins in cell phenotype maintenance and differentiation, we examined lamin expression in undifferentiated mouse and human embryonic stem (ES) cells. Wide-field and confocal immunofluorescence microscopy and semi-quantitative RT-PCR analysis revealed that undifferentiated mouse and human ES cells express lamins B1 and B2, but not lamin A/C. Mouse ES cells display high levels of lamins B1 and B2 localized both at the nuclear periphery and throughout the nucleoplasm, but in human ES cells, B1 and B2 expression is reduced and localized primarily at the nuclear periphery. Lamin A/C expression is activated during human ES cell differentiation, prior to down-regulation of the pluripotency marker, Oct-3/4, but not before the down-regulation of the pluripotency markers Tra-1-60, Tra-1-81, and SSEA-4. Our results identify the absence of A-type lamin expression as a novel marker for undifferentiated ES cells and further support a role for nuclear lamins in cell maintenance and differentiation.

2.3 INTRODUCTION

Nuclear lamins are intermediate filament proteins that were originally identified as components of the nuclear lamina (Aebi et al., 1986; McKeon et al., 1986), a 10-50 nm thick meshwork of proteins that underlies the inner nuclear membrane (Fawcett, 1966). It had traditionally been thought that the nuclear lamina functions primarily to provide structural support and organization to the nuclear envelope (Csoka et al., 2004a; Lammerding et al., 2004; Lenz-Bohme et al., 1997; Newport et al., 1990; Smythe et al., 2000; Sullivan et al., 1999; Vigouroux et al., 2001), but recent reports have documented that lamins exist throughout the nucleoplasm, suggesting structural contributions to a nuclear matrix (Bridger et al., 1993; Goldman et al., 1992; Hozak et al., 1995) and roles in DNA replication (Moir et al., 2000), transcription (Spann et al., 2002), and RNA processing (Jagatheesan et al., 1999; Kumaran et al., 2002; Muralikrishna et al., 2001). Mutations in lamins have also been assigned a causative role in the group of diseases collectively called laminopathies (Reviewed in (Burke and Stewart, 2002; Mounkes et al., 2003)).

In mammals, seven lamin proteins, which are the products of three genes, have been identified and can be divided into two subtypes. B-type lamins include B1, encoded by the *LMNB1* gene, and B2 and B3, splice variants of the *LMNB2* gene (Biamonti et al., 1992; Furukawa and Hotta, 1993; Pollard et al., 1990). A-type lamins, A, AΔ10, C, and C2 are all splice variants of the *LMNA* gene (Fisher et al., 1986; Furukawa et al., 1994; Machiels et al., 1996). Lamins B3 and C2 are expressed only in male germ cells (Furukawa and Hotta, 1993; Furukawa et al., 1994). The remaining B-type lamins are present ubiquitously in embryonic and adult cell types. At the cellular level, lamins B1 and B2 are essential for cell growth and survival (Harborth et al., 2001). *lmnB1* knock-out mice exhibit abnormal lung and bone development and die at birth (Vergnes et al., 2004). Contrastingly, A-type lamins are primarily found in differentiated cells. During mouse embryonic development, expression of A-type lamins is first detected on day 9 in extra-embryonic tissues and on day 12 in the embryo itself (Prather et al., 1991; Prather et al., 1989; Rober et al., 1989; Schatten et al., 1985; Stewart and Burke, 1987). Embryonic carcinoma cells

generally express little or no A-type lamins (Peter and Nigg, 1991; Stewart and Burke, 1987). Lastly, certain adult cell types that are not fully differentiated also express little or no A-type lamins (Lourim and Lin, 1989b; Rober et al., 1989). Consistent with these findings, lamin A/C is not essential for cell growth and survival (Harborth et al., 2001). Although *lmna* knock-out mice exhibit normal development at birth, they soon develop retarded postnatal growth and a muscular dystrophy phenotype that results in death by eight weeks of age (Sullivan et al., 1999). The detection of A-type lamins primarily in differentiated cells suggests that they might function to limit developmental plasticity by maintaining a cell's differentiated phenotype (Rober et al., 1989).

ES cells are obtained from the inner cell mass of blastocyst stage embryos and exhibit unlimited proliferative capacity and pluripotency (Magnuson et al., 1982; Thomson et al., 1998). The ability of ES cells to differentiate into all cell types of the embryo suggests that they are ideal candidates for therapeutic use. However, the specific differentiation of ES cells toward desired lineages remains ineffective, resulting in mixtures of differentiated cells. Further, due to the proliferative capacity of ES cells and their tendency to form teratomas when transplanted into animals (Gropp et al., 2003; Reubinoff et al., 2000), it is important to ensure that differentiated cells do not revert back to an ES cell phenotype after transplantation. Such reversion has been reported for mouse muscle-derived stem cells after differentiation into hematopoietic lineages (Cao et al., 2003), and for drosophila spermatogonial stem cells that have differentiated into spermatogonia (Brawley and Matunis, 2004). Thus, prior to clinical applications, it is necessary to understand the mechanisms controlling ES cell differentiation and the maintenance of the differentiated state. Given the possible role of nuclear lamins in cell maintenance and differentiation, we decided to characterize their expression in mouse (mES) and human (hES) ES cells. We report that 129/SVEV mES cells and HSF-6 hES cells express lamins B1 and B2, but not lamin A/C, and that as HSF-6 hES cells begin to differentiate into neuronal lineages and cardiomyocytes, lamin A/C expression is activated. Our results demonstrate that lamin A/C expression is a reliable marker of ES cell differentiation.

2.4 RESULTS

2.4.1 Undifferentiated mES and hES cells do not express A-type lamins.

Semi-quantitative RT-PCR analysis with human-specific primers was used to examine lamin A/C expression levels in HSF-6 hES cells. The centers of several HSF-6 hES cell colonies were scraped 5 days after passage to isolate undifferentiated cells and exclude peripheral cells that might be differentiating (Figure 4A, B). Whole colonies were also scraped 10 days after passage to examine whether lamin A/C expression is activated in some peripheral cells. Using this method, we show that HSF-6 hES cells, obtained by center colony scraping that are undifferentiated by morphological appearance (Figure 4A), express Oct-4, but little or no detectable lamin A/C (Figure 4C, lane 2). In contrast, differentiated WI-38 control cells express lamin A/C (Figure 4C, lane 1). However, lamin A/C was detected in whole colony scrapings (Figure 4C, lane 3), suggesting that lamin A/C expression is activated in some peripheral ES cells that are, presumably, differentiating. Immunocytochemistry experiments corroborated the RT-PCR results, demonstrating a lack of lamin A/C in HSF-6 hES cells and 129SV/EV mES (Figure 5). The pluripotency markers, Oct-4, (Pesce et al., 1998; Reubinoff et al., 2000; Thomson et al., 1998), TRA-1-60 (Andrews et al., 1984; Thomson et al., 1998), TRA-1-81

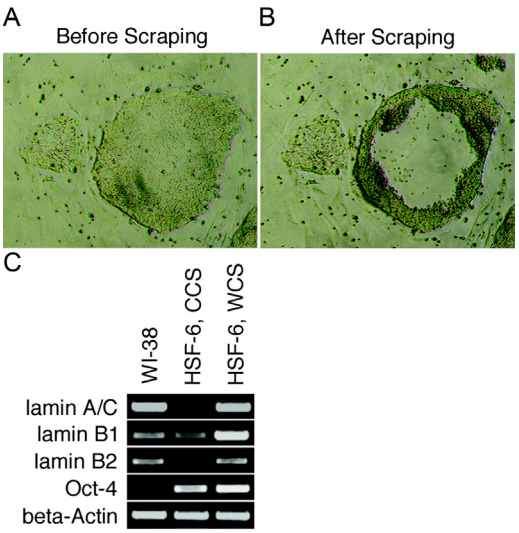

Figure 4. Detection of lamin mRNA in hES cells. HSF-6 hES cells were cultured for 5 days after passage and the centers of colonies were scraped to obtain a pure population of undifferentiated HSF-6 hES cells for RNA isolation (A, B). Whole HSF-6 hES cell colonies cultured for 10 days after passage, consisting of undifferentiated and differentiated cells were also scraped for RNA isolation (not shown). (C) RT-PCR of WI-38 fibroblasts (lane 1), HSF-6 center colony scrapings (CCS) (lane 2), and HSF-6 whole colony scrapings (WCS) (lane 3).

(Andrews et al., 1984; Thomson et al., 1998), and SSEA-4 (Kannagi et al., 1983; Thomson et al., 1998) were used to identify undifferentiated cells along with morphological observations (undifferentiated ES cells are relatively small (8-10 micrometers diameter) with a high nucleus/cytoplasm ratio). Undifferentiated HSF-6 hES cells, that are positive for Oct-4 (Figure 5B), TRA-1-60 (Figure 5E), TRA-1-81 (Figure 5H), and SSEA-4 (Figure 5K), lack lamin A/C (Figure 5C, F, I, and L), but adjacent CF-1 MEF feeder cells that are negative for each of the pluripotency markers are lamin A/C positive. Similar results were obtained with the H1 hES cell line (not shown). Further, 129/SVEV mES cells, as identified by Oct-4 labeling (Figure 5N), do not express lamin A/C (Figure 5O). In contrast, differentiated SNL mouse embryonic fibroblast (MEF) feeder cells adjacent to the mES cells

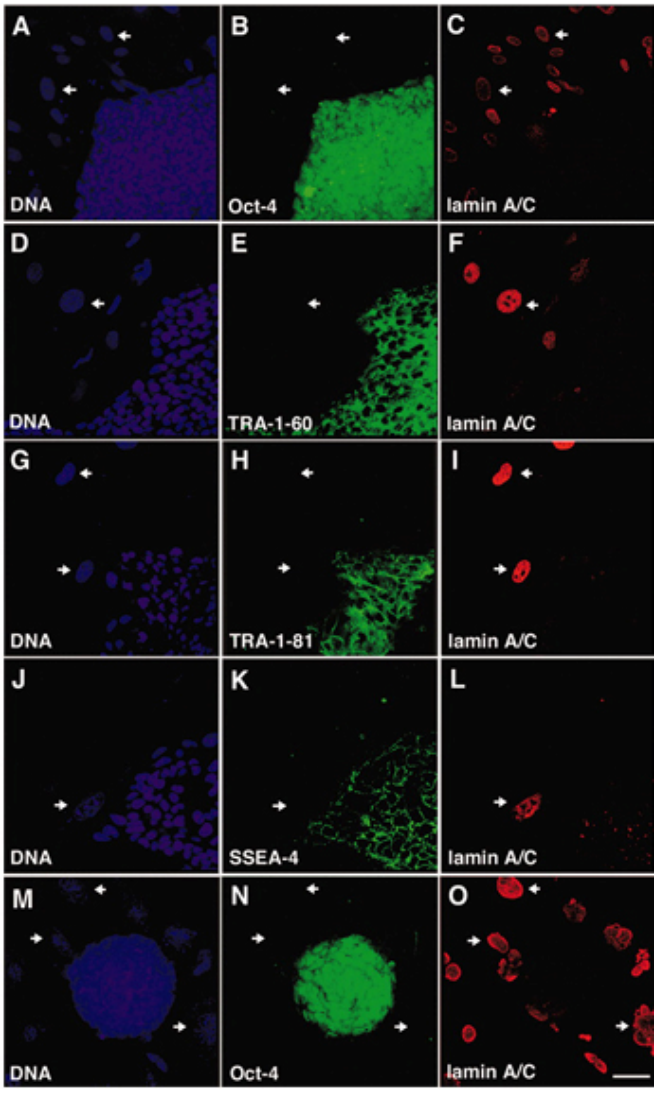

Figure 5. hES and mES cells do not contain lamin A/C. HSF-6 hES cells were fixed with 100% methanol (A-C) or 2% formaldehyde (D-L) 4-5 days after passage. 129/SVEV mES cells were fixed with 100% methanol (M-O) 2 days after passage. Cells were co-labeled for and lamin A/C (C, F, I, L, and O) and the pluripotency markers Oct-4 (B, N), TRA-160 (E), TRA-180 (H), and SSEA-4 (K). Undifferentiated HSF-6 hES cells growing in a colony are positive for Oct-4 (B), TRA-160 (E), TRA-180 (H), and SSEA-4 (L), but negative for lamin A/ C (C, F, I, and L). Conversely, adjacent differentiated CF-1 MEF feeder cells are negative for the pluripotency markers, but positive for lamin A/C. Undifferentiated 129/SVEV mES cells within a colony are positive for Oct-4 (N), but negative for lamin A/C (O), whereas adjacent differentiated SNL MEF feeder cells are negative for Oct-4, but positive for lamin A/C. DNA was visualized with TOTO-3 (A, D, G, J, and M). Representative MEF feeder cells are identified with arrows. Images were captured using confocal microscopy. Scale bar equals 50 microns.

that are negative for Oct-4 labeling, contain lamin A/C. Collectively, these observations indicate that undifferentiated ES cells do not express lamin A/C.

2.4.2 Undifferentiated mES and hES cells express B-type lamins

Next, we used RT-PCR analysis to investigate the expression of lamins B1 and B2 in HSF-6 hES cells and report that HSF-6 hES cells express lamin B1 (Figure 4C, lane 2), but under the conditions utilized, we could not detect the presence of lamin B2 mRNA (Figure 4C, lane 2). Immunocytochemistry experiments showed that undifferentiated HSF-6 hES cells and 129/SVEV mES cells contain lamins B1 and B2 (Figure 6). Since we previously demonstrated that undifferentiated HSF-6 hES cells and 129/SVEV mES cells do not express lamin A/C, we utilized this feature along with morphological characteristics to identify undifferentiated ES cells. Undifferentiated HSF-6 hES cells that are lamin A/C negative (Figure 6B and E) express lamins B1 (Figure 6C) and B2 (Figure 6F). Similarly, undifferentiated 129/SVEV mES cells that are lamin A/C negative (Figure 6H and K) express lamin B1 (Figure 6I) and lamin B2 (Figure 6L). Interestingly, lamins B1 and B2 levels are low in HSF-6 hES cells relative to the differentiated CF-1 MEF feeder cells. Further, lamin B2 is localized primarily at the nuclear envelope (Figure 7F), whereas lamin B1 demonstrates a peripheral and punctate labeling pattern throughout the nucleoplasm, (Figure 7C). These results indicate that mouse and human ES cells express both B-type lamins, although expression and/or protein levels may be lower than in differentiated cell types, and localization may differ.

2.4.3 hES cells express A-type lamins upon differentiation to neuronal lineages and cardiomyocytes

Our RT-PCR results from whole HSF-6 hES cell colony scrapings suggested that lamin A/C expression is

activated in some peripheral hES cells, suggesting that expression is activated in differentiating cells. Further, some HSF-6 hES cell colonies that we examined exhibited peripheral cells that labeled for both Oct-4 (Figure 8B) and lamin A/C (Figure 8C) and probably represent cells that are beginning to differentiate. To investigate this further, we used immunocytochemistry to examine if lamin A/C expression is activated in neuronal lineages and cardiomyocytes derived from HSF-6 hES cells. Neuronal cells as identified by either nestin (Figure 8E) or β-III tubulin (Figure 8H) labeled for lamin A/C (Figure 8F, I). Similarly, beating cardiomyocytes, as identified by α-actinin (Figure 8K) or light meromyosin (MF 20) (Figure 8N), also demonstrated lamin A/C expression (Figure 8L, O). Our results indicate that, upon differentiation to neuronal lineages and cardiomyocytes, hES cells begin to express lamin A/C. Further, the detection of cells at the periphery of some HSF-6 hES cell colonies that label for both Oct-4 and lamin A/C suggests that lamin A/C expression is activated prior to down-regulation of Oct-4 so that there is a transient overlap in expression. We did not observe similar co-labeling of lamin A/C with Tra-1-60, Tra-1-81, and SSEA-4.

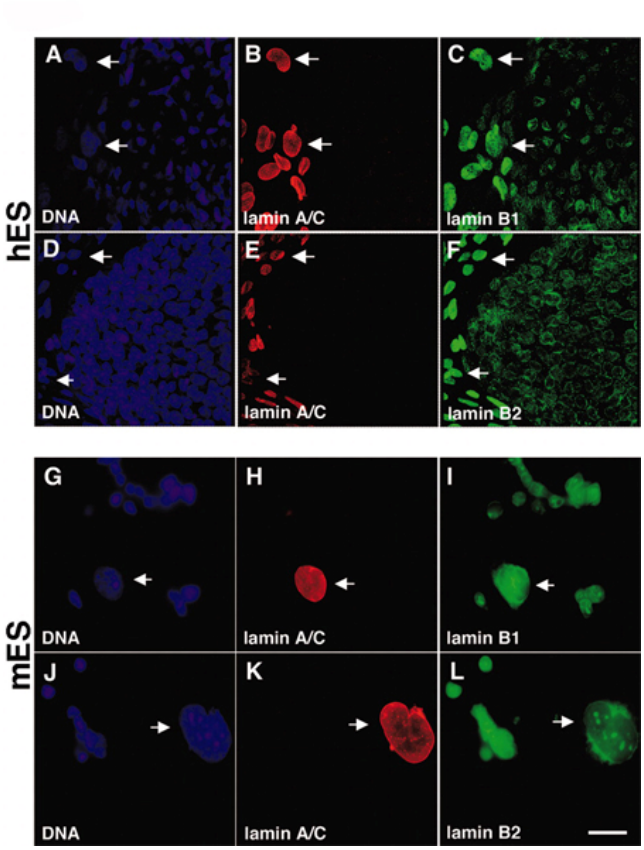

Figure 6. hES and mES cells contain lamin B1 and B2. HSF-6 hES cells were fixed with methanol 5 days after passage. Cells were co-labeled for lamin A/C (B, E, H, and K) in conjunction with either, lamin B1 (C, I), or lamin B2 (F, L). Undifferentiated HSF-6 hES cells are negative for lamin A/C (B, E), but positive for lamin B1 (C) and B2 (F). Adjacent differentiated CF-1 MEF feeder cells, are positive for lamin A/C, lamin B1 and lamin B2. Lamin B1 (F) and B2 (I) levels are low in hES cells relative to the MEF feeder cells. DNA was visualized with TOTO-3 (A, D, G, and J). Representative MEF feeder cells are identified with arrows. Images were captured using confocal microscopy. Scale bar equals 50 microns (A-C and G-J) or 5 microns (D-F and J-L).

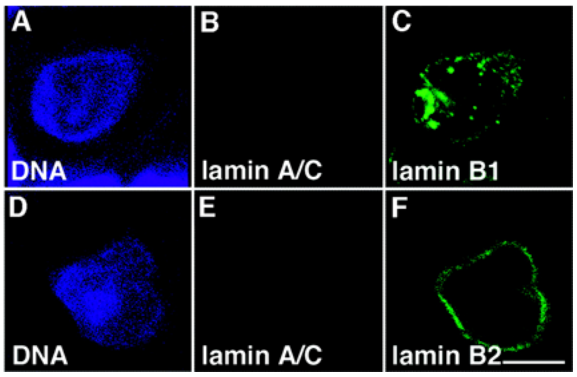

Figure 7. Lamins B1 and B2 localize primarily to the nuclear envelope of undifferentiated hES cells. HSF-6 hES cells were co-labeled for lamin A/C (B, E) in and lamin B1 (C) or lamin B2 (F). Undifferentiated HSF-6 hES cells that are lamin A/C negative (B, E) exhibit low levels of lamins B1 (C) and B2 (F). Lamin B2 is present primarily at the nuclear periphery (F). Lamin B1 is present at the periphery as well as in punctate structures throughout the nucleoplam. DNA was visualized with TOTO-3 (A, E). Images were captured with confocal microscopy. Scale bar equals 5 microns.

2.5 DISCUSSION

Nuclear lamins are components of the nuclear envelope that are involved in nuclear structural support and organization (Csoka et al., 2004a; Lammerding et al., 2004; Lenz-Bohme et al., 1997; Newport et al., 1990; Smythe et al., 2000; Sullivan et al., 1999; Vigouroux et al., 2001), DNA replication (Moir et al., 2000), transcription (Spann et al., 2002), and RNA processing (Jagatheesan et al., 1999; Muralikrishna et al., 2001). B-type lamins are present in most cell types from the first zygotic cell division through adulthood (Rober et al., 1989). In Contrast, A-type lamins are detected primarily in cells that are differentiated, as demonstrated by the lack of expression for the majority of mouse embryonic development (Rober et al., 1989), in various adult cells that are not fully differentiated (Rober et al., 1989), and in EC cell lines (Peter and Nigg, 1991; Stewart and Burke, 1987). The observation that B-type lamins are present in all cell types, but that A-type lamins are present primarily in differentiated cells suggests that A-type lamins could function to maintain the differentiated state. To begin investigating this possibility, we examined lamin expression in embryonic stem cells and differentiated derivatives. Since ES cells are isolated from blastocyst stage embryos and are pluripotent (Magnuson et al., 1982), we

hypothesized that undifferentiated ES cells should express B-type, but not A-type lamins, and that as ES cells differentiate lamin A/C expression would be activated.

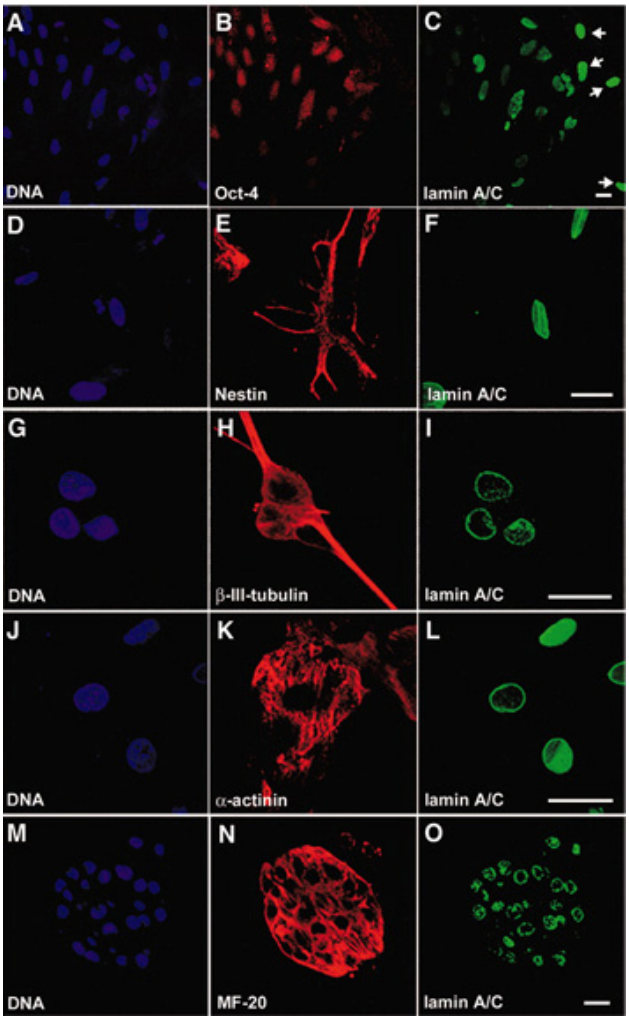

Using semi-quantitative RT-PCR with human-specific primers, we show that undifferentiated HSF-6 cells express lamin B1 (Figure 4, lane 2), but lamin B2 (Figure 4, lane 2) could not be detected using two different sets of primers (only one shown). Interestingly, immunocytochemistry analysis identified the presence of both lamin B1 (Figure 6C, I) and B2 (Figure 6F, L) in HSF-6 hES and 129/SVEV mES cells. However, HSF-6 hES cells appear to have lower B-type lamin levels relative to differentiated CF-1 MEF feeder cells. Further lamin B2 localization appears to be primarily peripheral with little or no labeling throughout the nucleoplasm (Figure 7F), whereas lamin B1 appears to be localized both to the periphery and in nuclear foci (Figure 7C). This

Figure 8. Lamin A/C is activated upon hES cell differentiation to neuronal lineages and cardiomyocytes. Some HSF-6 hES cell colonies contained peripheral cells that co-labeled for Oct-4 (B) and lamin A/C (C) with varying intensity. HSF-6 hES cells were cultured for five weeks on CF-1 MEF feeder cells without passage to obtain neuronal lineages (D-I) and cardiomyocytes (J-O). Differentiated cells were labeled for lamin A/C (F, I, L, and O) in conjunction with either nestin (E), β-III tubulin (H), α-actinin (K), or light meromyosin (MF-20) (N). DNA was labeled with TOTO-3 (A, D, G, J). Neuronal lineages, as identified by nestin (E) or β-III tubulin (H), are positive for lamin A/C (F and I). Cardiomyocytes, as identified by α-actinin (K), or light meromyosin (MF-20) (N), are positive for lamin A/C (L and O). Images were captured with confocal microscopy. Scale bars equal 25 microns.

suggests that although B-type lamins are present in HSF-6 hES cells, the nuclear lamina structure at the periphery and throughout the nucleoplasm is relatively under-developed.

Our ability to detect lamin B2 protein using immunocytochemistry, but inability to detect lamin B2 mRNA using RT-PCR in HSF-6 hES cells seems contradictory. Cross-reactivity of the lamin B2 antibody with lamin B1 is highly unlikely, since it has been shown that the antibody does not detect lamin B1 in western analysis (Lehner et al., 1986), so we hypothesize two alternative explanations. First, lamin B2 mRNA might have a very short half-life, but sufficient protein accumulates for immunofluorescent detection. Second, hES cells might express a splice variant of lamin B2 that is recognized by the primary antibody, but lacks the region amplified by the PCR primers. For example, lamin B3 is a significantly smaller splice variant of lamin B2 that so far has only been detected in male germ cells (Furukawa and Hotta, 1993). However, if such a splice variant is present in hES cells, it is unlikely to be lamin B3 because the region of lamin B2 amplified by the PCR primers is shared by lamin B3 (Furukawa and Hotta, 1993). Therefore it is possible that hES cells express a unique, previously unidentified splice variant of lamin B2.
Both RT-PCR and immunofluorescence analysis demonstrate that HSF-6 hES cells (Figure 3C, lane 2 and Figure 5C, F, I, L) and 129/SVEV mES cells (Figure 5O) do not express lamin A/C. Further, our results show that lamin A/C expression is activated in neuronal lineages (Figure 8F, I) and cardiomyocytes (Figure 8L, O) differentiated from HSF-6 hES cells. This is consistent with previous reports that have detected lamin A/C only in differentiated cell types (Lourim and Lin, 1989b; Peter and Nigg, 1991; Prather et al., 1991; Prather et al., 1989; Rober et al., 1989; Schatten et al., 1985; Stewart and Burke, 1987). Interestingly, cells at the periphery of some HSF-6 hES cell colonies, where spontaneous differentiation sometimes occurs (our observations), express both Oct-4 (Figure 8B) and lamin A/C (Figure 8C). The intensity of Oct-4 and lamin A/C labeling varied within individual peripheral cells that had both present, but no statistically significant relationship could be established; we observed cells that had high intensity labeling for both, low intensity labeling for both, or high intensity for one and low intensity for the other. The different combinations of Oct-4 and lamin A/C expression in individual cells suggests that either protein is not directly influenced by the other. Interestingly, different Oct-4 to

lamin A/C ratios could represent cells undertaking alternate differentiation pathways. Thus, it appears that lamin A/C is activated prior to complete Oct-4 down-regulation during the *in vitro* differentiation process, suggesting that lamin A/C expression is an earlier indicator of ES cell differentiation. However, we did not observe similar co-labeling of lamin A/C with Tra-1-60, Tra-1-81, or SSEA-4, suggesting that these pluripotency markers are down-regulated before the activation of lamin A/C expression, *in vitro*.

Taken together, our results identify the absence of A-type lamins as a novel marker of undifferentiated ES cells in culture and positive expression as an indicator of differentiation. The presence of B-type lamins but absence of A-type lamins in ES cells demonstrates another similarity between ES cell lines and the inner cell mass cells from which they are derived. However, during murine development, Oct-4 is down-regulated in somatic tissues well before lamin A/C expression is detected in any cell type. We describe lamin A/C expression prior to Oct-4 down-regulation in HSF-6 hES cells, suggesting that *in vitro* differentiation of ES cell lines might not mimic the consecutive steps that lead to tissue specification during embryonic development *in vivo*. Lastly, our results are in accordance with a possible role for A-type lamins in the maintenance of the differentiated state.

How could A-type lamins maintain cells in a differentiated state? Once expressed, A-type lamins could "lock" the nucleus of differentiated cells in particular gene expression patterns. This would be a simple way to maintain transcriptional and phenotypic stability in specialized, terminally differentiated cells. A-type lamins could accomplish this by increasing nuclear rigidity, which could constrain chromatin remodeling. Several lines of evidence support this possibility. First, cells from patients with various *LMNA* mutations have an abnormally plastic nuclear morphology, marked by lobes and invaginations (Csoka et al., 2004a; Vigouroux et al., 2001). Second, it has been directly shown that lamin A/C deficiency reduces nuclear structural integrity under mechanical strain (Lammerding et al., 2004). Lastly, lamin A/C (Shoeman and Traub, 1990; Taniura et al., 1995) and lamin-associated proteins (LAPs) (Vlcek et al., 1999) can interact directly with chromatin by binding DNA directly, or via DNA associated proteins. Alternatively, lamin A/C could regulate the expression of specific genes that are involved in the

maintenance of a differentiated state as evidenced by observations that lamin A/C can interact with transcription factors such as MOK2 (Dreuillet et al., 2002) and SREBP1 (Lloyd et al., 2002), as well as retinoblastoma (Rb), which is involved in regulating cell cycle arrest and apoptosis (Johnson et al., 2004; Mancini et al., 1994; Ozaki et al., 1994). Lamin A/C might also have widespread effects on gene expression, since proper lamin A/C organization may be essential for polymerase II dependent transcription (Kumaran et al., 2002; Spann et al., 2002), and it has been found to co-localize with splicing factor speckles (Jagatheesan et al., 1999; Kumaran et al., 2002; Muralikrishna et al., 2001). The possibility should be considered that laminopathies arise because cells are unable to maintain their differentiated state as a result of a disorganized nuclear lamina caused by lamin A mutations. Cellular dysdifferentiation, previously postulated as a cause of cancer and aging (Cutler, 1991; Kator et al., 1985; Kirkland et al., 2002) would result in abnormal gene expression, reduced proliferation, and/or apoptosis. The devastating premature aging disease, Hutchinson-Gilford Progeria Syndrome, could be the ultimate example of such dysdifferentiation.

If A-type lamins maintain the differentiated state by “locking” cells in a specific gene expression pattern, whether directly through structural modification of the nuclear envelope or indirectly by influencing the expression of other genes, their absence in undifferentiated ES cells might be essential for pluripotentcy. The presence of a flexible nuclear envelope could be necessary for proper chromatin remodeling which occurs during differentiation. Interestingly, the low levels and/or altered organization of B-type lamins observed in HSF-6 hES cells (Figure 6C, F and 7C, F) could also contribute to nuclear envelope flexibility. In such a scenario, forced expression of lamin A/C or increased B-type lamin expression might “lock” ES cells in their natural undifferentiated state.

In conclusion, our results identify the lack of lamin A/C as a novel marker for undifferentiated ES cells, and lamin A/C expression as an early indicator of differentiation. These observations support the hypothesis that lamin A/C has a functional role in the maintenance of the differentiated state. Further, our results and the observation that undifferentiated ES have few nuclear pores (unpublisged data) suggests

that there are multiple structural differences between the nuclear envelopes of undifferentiated and differentiated cells that may be critical to the differentiation process.

2.6 MATERIALS AND METHODS

2.6.1 Cell Culture

Mouse ES Cells: 129/SVEV mES cells (Specialty Media, Phillipsburgh) were maintained in an undifferentiated state by co-culture with mitomycin (Sigma, St. Louis) -treated SNL mouse embryonic fibroblast (MEF) feeder cells (gift from Dr. Richard Chaillet, University of Pittsburgh) in DMEM medium with 15% FBS, 1% non-essential amino acids, 1mM L-Glutamine, 0.1mM β-mercaptoethanol, 1% nucleosides (all from Specialty Media), and 10^5 U/ml LIF (Chemicon, AU). Cells were passaged every 2-3 days and media was changed daily.

Human ES cells: HSF-6 hES cells (from UCSF, San Francisco under license) were maintained in an undifferentiated state by co-culture with mitomycin-treated CF-1 MEF feeder cells in DMEM medium with 20% Knockout serum replacer, 1% non-essential amino acids, 1mM L-Glutamine, and 4ng/ml FGF-2 (all from Invitrogen, Carlsbad, CA). Cells were passaged every 5-7 days and media was changed daily. WI-38 human embryonic lung fibroblasts (ATCC, Rockville, MD) were cultured in DMEM with15 % fetal bovine serum and 2mM L-Glutamine. Neuronal lineages and cardiomyocytes were obtained by culture of HSF-6 hES for five weeks on CF-1 MEF feeder cells without passage. Media were changed every 2 days.

2.6.2 RNA Isolation and RT-PCR:

The centers of undifferentiated HSF-6 colonies, cultured for 5 days under optimal conditions, were gently scraped with pulled pasteur pipets (see Figure 1A and B). Whole colonies of HSF-6 cells, which had begun to naturally differentiate after ten days in culture, were scraped as well. WI-38 cells were trypsinized. All cells were spun at 200 x g for 5 min and then washed twice with PBS. Cell pellets were immediately frozen in liquid nitrogen and stored at –80^{o}C. RNA was isolated using RNAqueous 4-PCR (Ambion, TX) and cDNA was generated using the Reverse Transcription System (Promega, WI) following the manufacturer's instructions. Spectrophotometry was used to verify quantity and quality of RNA and cDNA. Semiquantitative PCR was performed with 50ng of cDNA in a final concentration of: 0.02 U Biolase DNA polymerase, 1X NH4 buffer, 2.5mM MgCl2 (Bioline, Randolph, MA), 0.2mM dNTPs (Roche), 0.2μM primers (Invitrogen). PCR conditions were: 95 ^{o}C for 3 min followed by 35 cycles at 95 ^{o}C for 35 sec, 55 ^{o}C for 40 sec, and 72 ^{o}C for 45 sec and a final extension at 72 ^{o}C for 7 min. Human specific primers used for each gene:

Lamin A/C forward: AATGATCGCTTGGCGGTCTAC,

Lamin A/C reverse: CTTCTTGGTATTGCGCGCTTT (255bp);

Lamin B1 forward: AAAAGACAACTCTCGTCGCAT,

Lamin B1 reverse: CCGCTTTCCTCTAGTTGTACG (256bp);

Lamin B2 forward: ATTCAGAATCCAGGCGTCGAC,

Lamin B2 reverse: TTATTGTTGTGACAGGTCTTACGACG (339bp);

B-actin forward: TGGCACCACACCTTCTACAATGAGC,

B-actin reverse: GCACAGCTTCTCCTTAATGTCACGC (400bp);

Oct-4 forward: CGRGAAGCTGGAGAAGGAGAAGCTG,

Oct-4 reverse: AAGGGCCGCAGCTTACACATGTTC (230bp).

2.6.3 Wide-Field and Confocal Microscopy and Immunocytochemistry

hES and mES cells were passaged 4-5 days and 2 days, respectively, prior to fixation. Cells were fixed with 100% methanol for 20 minutes at –20°C or 2% formaldehyde for 45 minutes. Cells were subsequently washed twice with PBS, permeabilized with 0.1% Triton X-100, and incubated for one hour at 25°C with combinations of the following primary antibodies: monoclonal mouse anti-human Oct-4 (1:50), polyclonal rabbit anti-human lamin A/C (1:100) (both from Santa Cruz Biotechnology, Santa Cruz), monoclonal mouse anti-human lamin B1 (1:50) and B2 (1:50) (both from Zymed, San Francisco), monoclonal mouse anti-β-III tubulin (1:250), mouse anti-nestin (1:200) (both from Covance, Berkley), mouse anti-sarcomeric α-actinin (EA-53) (1:100) (from Sigma, Saint Louis), mouse anti-SSEA-4, mouse anti- TRA-160, mouse anti-TRA-180, and mouse anti-light meromyosin (MF-20) (1:3) (all obtained from the Developmental Studies Hybridoma Bank under the auspices of the NICHID, The University of Iowa, Department of Biological Sciences, Iowa City). Cells were washed three times with PBS and the primary antibodies were detected with Alexa Fluor 488, Alexa Fluor 546, and Alexa Fluor 568 secondary antibodies (all 1:100) (all from Molecular Probes, Oregon) for one hour at 25°C. DNA was visualized with TOTO-3 (1:1000) (Molecular Probes, Eugene), which was added to the secondary antibody mix. Cells were washed three times in PBS and mounted onto glass slides with Vectashield mounting medium (Vector Laboratories, Burlingame). Confocal images were captured with a Leica TCS SP2, using proprietary Leica software.

2.7 ACKOWLEDGEMENTS

I thank Esther Jane, Patti Petrosko, Amy Mucka, and Hina Qidwai for maintaining the 129/SVEV mouse and HSF-6 human ES cell lines, Richard Chaillet for donating immortalized SNL MEF feeder cells, Leah Kauffman for editing the manuscript, and Chris Navara and Vanessa Y. Rawe for helpful discussion.

CHAPTER TWO: DEFECTIVE DOUBLE-STRAND BREAK REPAIR CORRELATES WITH ABNORMAL NUCLEAR MORPHOLOGY AND IS IMPROVED WITH FTI TREATMENT IN HUTCHINSON-GILFORD PROGERIA SYNDROME FIBROBLASTS.

3.1. RATIONALE

There are multiple lines of evidence indicating that HGPS cells exhibit elevated DNA damage levels. Firstly, HGPS cells demonstrate limited proliferative capacity in culture, early onset of senescence, and increased apoptosis rates (Bridger and Kill, 2004), all of which can be caused by DNA damage. Secondly, it has been shown that DNA damage response pathways exhibit elevated activity in HGPS cells (Liu et al., 2006; Varela et al., 2005). Lastly, the most direct evidence of elevated DNA damage comes from a study that showed that HGPS have a DSB repair defect that may be specific to homologous recombination (HR) repair (Liu et al., 2005). DNA damage accumulation due to compromised repair is a possible molecular mechanism responsible for the increased apoptosis rate and early onset of senescence observed in HGPS and in turn the accelerated aging phenotype.

3.2. ABSTRACT

Impaired DSB repair has been implicated as a molecular mechanism contributing to the accelerating aging phenotype in Hutchinson-Gilford Progeria Syndrome (HGPS), but neither the extent nor the cause of the repair deficiency have been fully elucidated. Here we perform a quantitative analysis of the steady-

state number of DSBs and the repair kinetics of IR-induced DSBs in HGPS cells. We report a higher steady-state number of DSBs and impaired repair of IR-induced DSBs, both of which correlated strongly with abnormal nuclear morphology. Expression of GFP-Progerin in human coronary artery endothelial cells (hCAECs) resulted in impaired repair of IR-induced DSBs which also correlated with abnormal nuclear morphology. Farnesyl transferase inhibitor (FTI) treatment improved the repair of IR-induced DSBs, but only in HGPS cells whose nuclear morphology was also normalized. Interestingly, FTI treatment did not result in a statistically significant reduction in the higher steady-state number of DSBs. There is also report a delay in localization of phospho-NBS1 and MRE11, MRN complex repair factors necessary for homologous recombination (HR) repair, to DSBs in HGPS cells. Our results demonstrate a strong correlation between nuclear structural abnormalities and the DSB repair defect in HGPS and GFP-Progerin positive cells, suggesting a mechanistic link that may involve delayed repair factor localization to DNA damage. Further, our results show that similar to other HGPS phenotypes, FTI treatment has a beneficial effect on DSB repair.

3.3. INTRODUCTION

HGPS is a rare genetic disorder that causes rapid premature aging shortly after birth, recapitulating multiple pathologies associated with aging and resulting in a median lifespan of 13 years (Reviewed in [1]). The disease is caused by de novo mutations within exon 11 of the LMNA gene which partially activate a cryptic splice donor site, resulting in deletion of 50 amino acids from exon 11, with subsequent production of a truncated form of lamin A termed, Progerin or lamin AD50 [2, 3]. LMNA encodes the A-type nuclear lamins, primarily lamins A and C. Along with the primary B-type lamins, lamin B1 and lamin B2, the A-type lamins form the nuclear lamina [4, 5], a scaffold-like structure that lines the inner nuclear membrane and also contribute to a nuclear matrix [6]. Multiple LMNA mutations produce nuclear

structural irregularities, demonstrating that A-type lamins are intricately involved in nuclear structural organization (Reviewed in [7]). Furthermore, there are multiple lines of evidence indicating a central role for A-type lamins in chromatin organization (Reviewed in [7]).

Accordingly, HGPS cells exhibit altered nuclear structural characteristics and chromatin organization. Nuclear structural irregularities include changes in the spatial distribution of nuclear pore complexes [8] as well modifications of the nuclear lamina [8, 9] that are likely responsible for the abnormal nuclear morphology observed in primary HGPS cells [2, 3, 8]. These structural irregularities are accompanied by functional changes, including reduced deformability of the nuclear lamina [9], increased nuclear stiffness and sensitivity to mechanical stress [10], and mitotic defects, including abnormal chromosome segregation, delays in cytokinesis and nuclear reassembly, and binucleation [11, 12]. Multiple chromatin organization changes have been described as well. Particularly, HGPS cells exhibit loss of peripheral heterochromatin [8, 13] that may be due to epigenetic changes, including up-regulation of H3K9me3 and H4K20me3, which define constitutative heterochromatin and downregulation of H3K27me3 which defines facultative heterochromatin [13-15]. In addition to epigenetic changes, HP1a, which is usually associated with H3K9me3 is down-regulated and partially dissociated [14, 15]. It is likely that these abnormalities influence nuclear biological processes that dependent on proper nuclear structure and chromatin organization.

It has been demonstrated that the nuclear morphological changes and altered chromatin characteristics are not caused by lamin A haploinsufficiency, but by the presence of Progerin in a dominant gain-of-function fashion, possibly through its accumulation at the inner nuclear membrane (INM) [8, 14], where it appears to alter nuclear lamina structure [9]. In accordance, reduction of the farnesylated form of Progerin using farnesyl transferase inhibitors (FTIs) [16-22] and reduction of Progerin using antisense morpholinos [14] improves nuclear abnormalities in HGPS cells as well as various disease phenotypes in HGPS mouse models. The success of FTIs in these studies and the current lack of any other therapeutic

approach for HGPS has lead to a current phase II clinical trial examining the beneficial effect of FTIs in HGPS patients (ClinicalTrials.gov identifier: NCT00425607).

Interestingly, several lines of evidence indicate that HGPS cells have a higher steady-state number of DSBs. HGPS cells demonstrate limited proliferative capacity in culture, early onset of senescence, and increased apoptosis [23], all of which can be caused by accumulation of DSBs. Further, HGPS cells exhibit elevated activity of DNA damage response pathways [19]. Interestingly, the elevated activity of DNA damage response pathways was not reduced after 48 hours of FTI treatment even though nuclear morphology was improved, suggesting that the two phenotypes occur independently, and that FTIs may not be able to reduce the steady-state level of DSBs [19]. DSB accumulation appears to be due at least in part to impaired localization of DSB repair factors including, Rad51 and Rad50 [24]. It has also been shown that xeroderma pigmentosum group A (XPA), a nucleotide excision repair protein (NER), aberrantly localizes to a subset of DSBs in HGPS cells through interaction with chromatin and inhibits the localization of Rad51 and Rad50, perhaps through steric hindrance [24]. There is evidence to suggest that XPA does not localize to camptothecin (CPT) induced DSBs, indicating that XPA-localized DSBs may be functionally different in origin or repair [24]. However, XPA mediated interference with DSB repair does not fully explain the DSB repair problem in HGPS cells since repair of CPT-induced DSBs in HGPS cells is slower compared to wildtpye cells [24].

In this study we performed a quantitative analysis of the steady-state number of DSBs and the repair kinetics of IR-induced DSBs in HGPS fibroblasts. We also examined whether the observed deviations from wildtype for these characteristics correlated with abnormal nuclear morphology and were caused by Progerin. Further, we examined whether FTI treatment can decrease the steady-state DSB level and improve the repair kinetics of IR-induced DSBs in HGPS cells. Lastly, in order to expand on previous studies which showed that localization of repair factors to DSBs is impaired, we performed a quantitative analysis of the localization kinetics of the MRN repair complex factors, phospho-NBS1 and MRE1, to g-irradiation induced DSBs.

3.4. RESULTS

3.4.1. HGPS fibroblasts with an abnormal nuclear morphology have elevated steady-state levels of DSBs and demonstrate impaired repair of IR-induced DSBs.

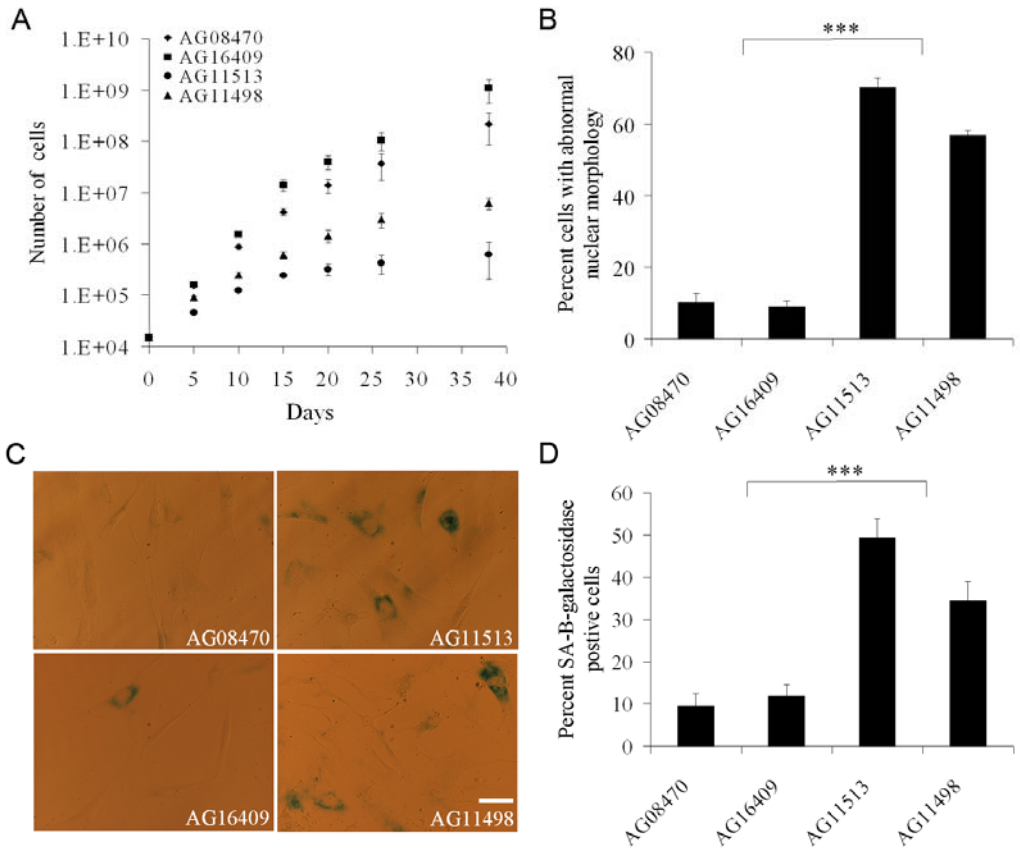

Figure 9. HGPS fibroblasts exhibit limited proliferative capacity, abnormal nuclear morphology, and early onset of senescence. A) Characterization of wildtype and HGPS fibroblast proliferation in culture for 38 days. B) HGPS cultures exhibited a higher percentage of cells with an abnormal nuclear morphology. C) Light microscopy images of SA β-galactosidase activity, a marker of senescence, in wildtype (left two panels) and HGPS cultures (right two panels). D) Quantification of the percentage of cells exhibiting SA β-galactosidase activity. Scale bar equals 25 μm.

To investigate DNA damage repair in HGPS cells, we examined primary dermal fibroblasts derived from two HGPS patients (AG11513 and AG11498) and two apparently healthy individuals (AG08470 and AG16409) of similar age (Figure 15A). Since there is evidence that HGPS cellular phenotypes increase in severity with increasing passage number [8], we used HGPS and wildtype cells of similar population doubling (Fig. 15A). The HGPS fibroblasts used in these experiments display classical HGPS phenotypes including decreased proliferative capacity (Fig. 9A), abnormal nuclear morphology (Fig 9B), and increased (SA) β-galactosidase activity, indicating a higher percentage of senescent cells (Fig. 9C, D).

In order to examine the difference in the steady-state number of DSBs between HGPS and wildtype fibroblasts, we quantified the average number of DSBs per cell using the γ-H2AX foci assay. H2AX is phosphorylated specifically at DSBs within minutes and is dephosphorylated after repair [25-28]. The formation and disappearance of γ-H2AX foci has been routinely used as a measure of DSB formation and repair, respectively [24-30]. A population of HGPS fibroblasts consists of cells that exhibit the characteristic abnormal nuclear morphology associated with HGPS, characterized by lobes and invaginations in the nuclear lamina, as well as cells that exhibit a normal nuclear morphology [8]. In order to examine whether the level of DSBs correlates with the abnormal nuclear morphology, we separated HGPS fibroblasts into two categories based on nuclear structure: normal (HGPSN) and abnormal (HGPSAB) cells. The nuclear envelope can be seen in the top panels in figure 10A using immunofluorescent labeling of lamin A, and whereas the nuclei in control cells are ovoid with the lamins circumscribing the inner nuclear surface, there are two types of nuclei in the HGPS fibroblasts: normal nuclei that appear similar to wildtype (AG11513N and AG11498N) and others which display abnormal nuclear structure (AG11513AB and AG11498AB). Although about 10% percent of AG08470 and AG16409 wildtype fibroblasts have an abnormal nuclear morphology (Fig. 9B), it is not due to the HGPS mutation, and thus we grouped together total wildtype cells irrespective of nuclear morphology

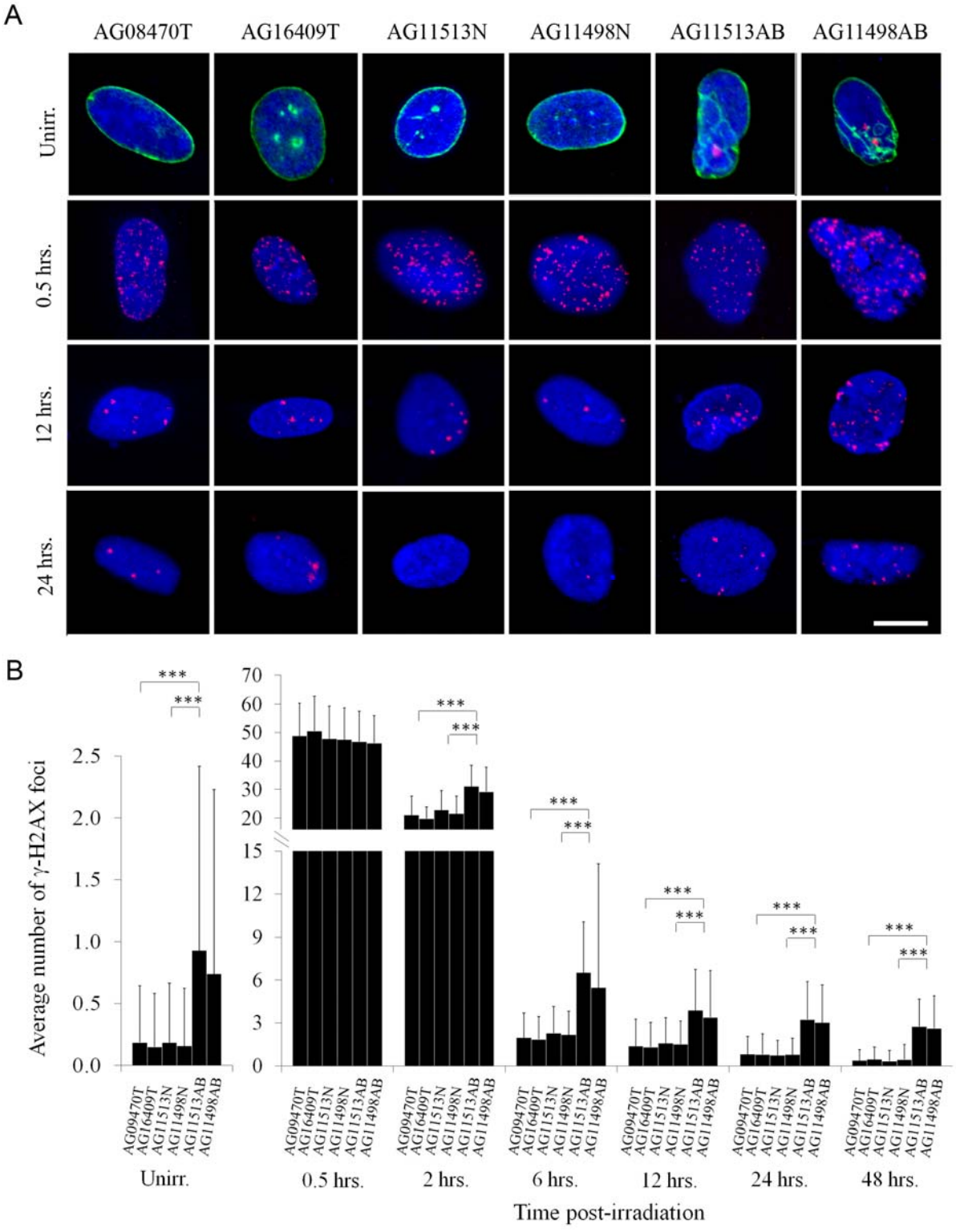
A
AG08470T
AG16409T
AG11513N
AG11498N
AG11513AB
AG11498AB
Unirr.
0.5 hrs.
12 hrs.
24 hrs.
B
Average number of γ-H2AX foci
***
AG09470T
AG16409T
AG11513N
AG11498N
AG11513AB
AG11498AB
Unirr.
0.5 hrs.
2 hrs.
6 hrs.
12 hrs.
24 hrs.
48 hrs.
Time post-irradiation

Figure 10. Steady-state level of DSBs and repair kinetics of g-irradiation induced DSBs in HGPS fibroblasts. Immunocytochemistry was performed for γ-H2AX and lamin A/C in unirradiated cells and at 0.5, 2, 6, 12, 24, and 48 hours after 2 Gy ionizing radiation. A) Representative confocal immunofluorescent images of γ-H2AX foci (red) and DNA (blue) at representative timepoints after irradiation show easily identifiable γ-H2AX foci. Lamin A/C (green) was included in the top row of panels to show the characteristic abnormal nuclear morphology that was used to differentiate between HGPS normal and abnormal cells. AG11513N and AG11498N are HGPS fibroblasts exhibiting normal nuclear morphology. AG11513AB and AG11498AB are HGPS fibroblasts exhibiting abnormal nuclear morphology. B) γ-H2AX foci were visually detected and the average number of foci per cell was calculated for the indicated timepoints. "T" = total cells including those with normal and abnormal nuclear morphologies. "N" = cells with a normal morphology. "AB" = cells with an abnormal morphology. Data is form three different experiments. At least 100 cells were examined per timepoint. For statistical analysis, cells form multiple experiments were pooled together for each experimental group and a one-way ANOVA test was performed followed by a Tukey post-test to obtain p-values for the differences between specific pairs of means. Error bars represent the standard deviation (SD) of the number of γ-H2AX foci per cell in order to highlight the large variance from cell to cell. Confocal images were captured using a Leica TCS SP2 using Leica software. Scale bar equals 10 μm. * = $p < 0.05$, ** = $p < 0.01$, and *** = $p < 0.001$.

(AG08470T and AG16409T). Averaged together, HGPSAB fibroblasts exhibited a 4.9-fold greater average number of γ-H2AX foci per cell compared to wildtype fibroblasts (Fig. 10B and 15B). There was no statistically significant difference in the average number of γ-H2AX foci per cell between HGPSN and wildtype fibroblasts (Fig. 10B and 15B). These results indicate that only HGPS cells with an abnormal nuclear morphology exhibit a higher steady-state average number of DSBs per cell compared to wildtype cells, demonstrating a correlation between the two phenotypes.

The higher steady-state level of DSBs in HGPSAB fibroblasts could be due to an increased rate in DSB formation or to impaired DSB repair. In order to test the latter hypothesis, we performed the γ-H2AX foci assay at 0.5, 2, 6, 12, 24, and 48 hours after irradiation to determine the kinetics of repair (Fig. 10). As for unirradiated cells, we visually distinguished between HGPSN (Fig. 10A, middle two columns) and HGPSAB fibroblasts (Fig. 10A, right two columns) and grouped together total wildtype fibroblasts (Fig. 10A, left two columns). The average number of γ-H2AX foci per cell was quantified in figure 1B. At 0.5 hours after irradiation (Fig. 10B and 15B), which has been previously reported to reflect the apex of γ-H2AX foci formation and represent the maximal number of DSBs formed [25, 26, 31], HGPSAB fibroblasts exhibited no statistically significant difference compared to wildtype and HGPSN fibroblasts,

indicating that H2AX phosphorylation occurs properly (Fig. 10B and 15B). However, at 2, 6, 12, 24, and 48 hours after irradiation, HGPSAB fibroblasts had a 1.5-fold, 3.1-fold, 2.7-fold, 3.9-fold, and 6.5-fold higher average number of γ-H2AX foci per cell compared to wildtype fibroblasts, respectively (Fig. 10B and 15B). There was no statistically significant difference in the average number of γ-H2AX foci between HGPSN and wildtype fibroblasts at any timepoint after irradiation (Fig. 10B and 15B). Further, whereas

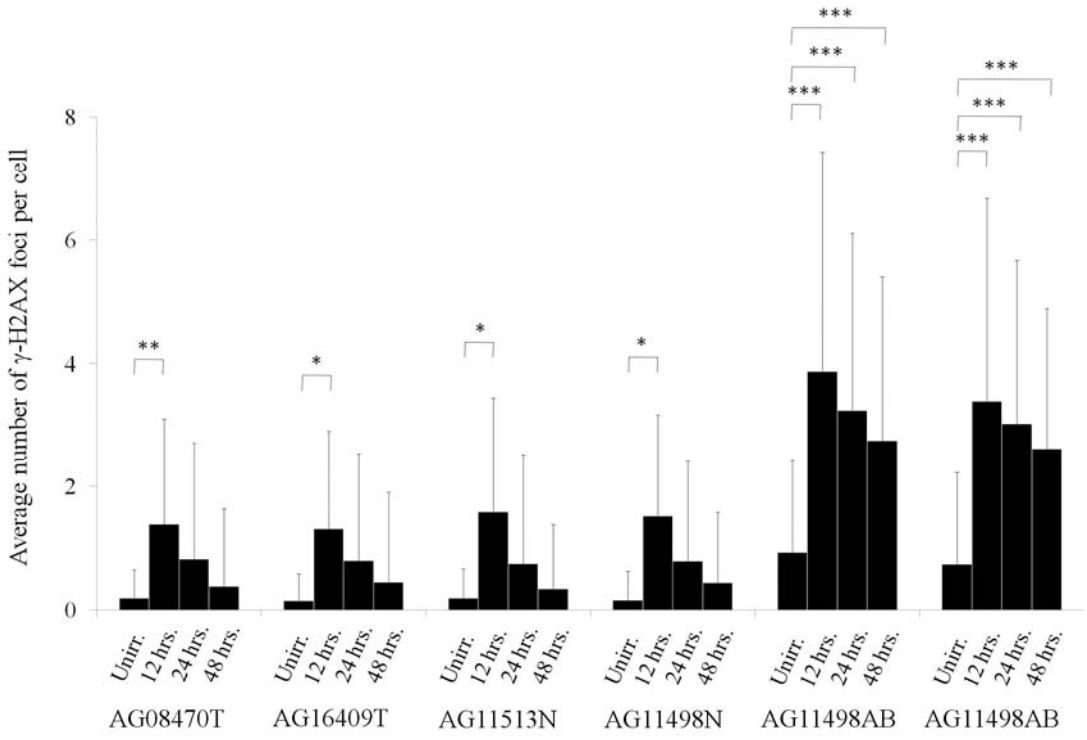

Figure 11. HGPS cells exhibit persistent IR-induced DSBs. Immunocytochemistry was performed for γ-H2AX and lamin A/C in unirradiated cells and at 0.5, 2, 6, 12, 24, and 442 hours after 2 Gy g-irradiation and the average number of γ-H2AX foci per cell was calculated. Examination of late repair kinetics shows that whereas wildtype fibroblasts (AG08470 and AG16409) return to steady-state DSB levels within 24 hours post-irradiation, HGPS cells continue to exhibit statistically significant higher levels of DSBs at 24 and 48 hours post-irradiation. Data is form three different experiments. At least 100 cells were examined per timepoint. For statistical analysis, cells form multiple experiments were pooled together for each experimental group and a one-way ANOVA test was performed followed by a Tukey post-test to obtain p-values for the differences between specific pairs of means. Error bars represent the standard deviation (SD) of the number of γ-H2AX foci per cell in order to highlight the large variance from cell to cel. * = $p < 0.05$, ** = $p < 0.01$, and *** = $p < 0.001$.

wildtype and HGPSN fibroblasts exhibited a return to steady-state DSB levels within 24 hours, HGPSAB fibroblasts still exhibited statistically significant differences even at 48 hours post-irradiation. (Fig. 11). These results indicate that repair of IR-induced DSBs is compromised specifically in HGPS cells with an abnormal nuclear morphology, highlighting a correlation between the two phenotypes.

3.4.2. Impaired repair of IR-induced DSBs is due to production of Progerin and is present only in Progerin positive cells with an abnormal nuclear morphology.

The abnormal nuclear morphology observed in HGPS cells is caused by the presence of Progerin in a dominant gain-of-function fashion [8, 15]. To examine whether Progerin is fundamentally responsible for the elevated steady-state number of DSBs and the impaired repair of IR-induced DSBs in HGPS cells, we expressed GFP-Progerin in normal hCAECs using lentiviral transduction (Fig. 12A, right columns). We also expressed GFP-LMNA to control for overexpression of a lamin A-like protein (Fig. 12A; middle left column). Expression of GFP-Progerin resulted in GFP-Progerin positive hCAECs with normal (Fig. 12A, middle right column) or abnormal nuclear morphologies (Fig 12A, right column) similar to what is seen in HGPS fibroblasts. Expression of GFP-LMNA had little to no effect on nuclear morphology (Fig. 12A, middle left column), similar to previous reports [8]. As before, we categorized GFP-Progerin positive hCAECs as having normal (GFP-HGPSN) or abnormal (GFP-HGPSAB) nuclear morphology. Unirradiated GFP-HGPSAB cells exhibited a 4.9-fold higher average number of γ-H2AX foci per cell compared to wildtype cells (Fig. 12B and 15C), indicating that expression of GFP-Progerin increases the higher steady-state number of DSBs. Analysis of the repair of IR-induced DSBs shows that expression of GFP-Progerin in wildtype hCAECs compromises DSB repair. At 0.5 hours post-irradiation, all cell types had a similar average number of γ-H2AX foci per cell (Fig. 12B, and 15C), indicating that GFP-Progerin has no effect on H2AX phosphorylation. At 12 and 24 hours post-irradiation GFP-HGPSAB cells exhibited a 2-fold and 4.3-fold higher average number of γ-H2AX foci per cell compared to wildtype cells (Fig. 12B and 15C), indicating that GFP-Progerin interferes with repair of IR-induced DSBs. There was

no statistically significant difference between wildtype and GFP-HGPSN cells (Fig. 12B and 15C), indicating that steady-state DSB levels were elevated and DSB repair was compromised only in cells whose nuclear morphology was altered. Further, no statistically significant differences were detected between wildtype and GFP-LMNA positive cells (Fig. 12B and 15C), indicating that overexpression of lamin A had little or no effect on DSB repair. Altogether, these results indicate that Progerin is fundamentally responsible for the elevated steady-state levels of DSBs and defective repair of IR-induced DSBs in HGPS in a dominant gain-of-function manner and that both phenotypes strongly correlate with the abnormal nuclear morphology.

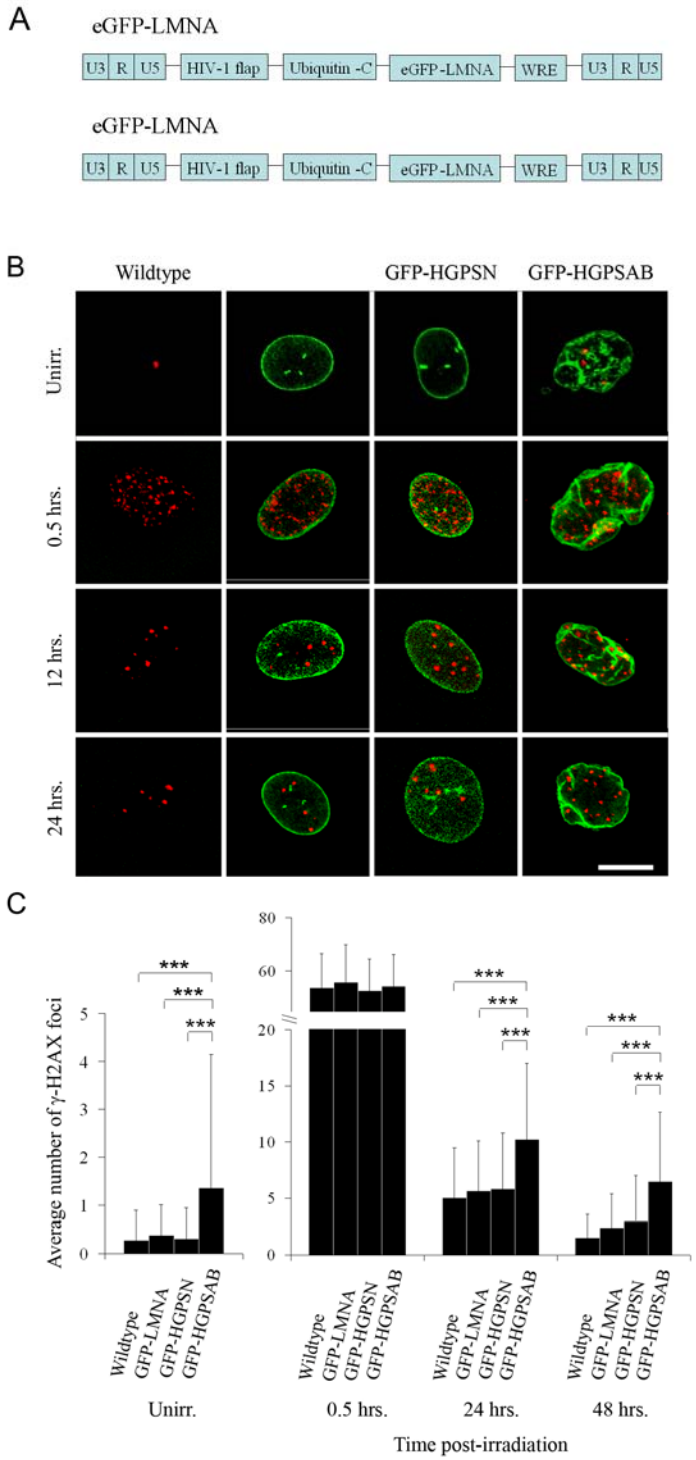

Figure 12. GFP-Progerin expression increases the steady-state level of DSBs and impairs repair of IR-induced DSBs in normal hCAECs. A) Immunocytochemistry was used to examine wildtype, GFP-LMNA positive, GFP-HGPSN positive (normal nuclear morphology), and GFP-HGPSAB positive (abnormal nuclear morphology) hCAECs for γ-H2AX (red). GFP fluorescence was captured (green). Stable expression of the GFP constructs was achieved using lentiviral transduction. Only GFP-Progerin positive cells were examined. B) γ-H2AX foci were visually detected and the average number of foci per cell was calculated for the indicated timepoints. Data is from two different experiments. At least 50 cells were examined per timepoint. For statistical analysis, cells form multiple experiments were pooled together for each experimental group and a one-way ANOVA test was performed followed by a Tukey post-test to obtain p-values for the differences between specific pairs of means. Error bars represent the standard deviation (SD) of the number of γ-H2AX foci per cell in order to highlight the large variance from cell to cell.Confocal images were captured using a Leica TCS SP2 using Leica software. Scale bar equals 10 μm. * = $p < 0.05$, ** = $p < 0.01$, and *** = $p < 0.001$.

3.4.3. FTI treatment improves nuclear morphology and repair of IR-induced DSBs, but does not reduce the steady-state level of DSBs in HGPS fibroblasts.

FTI treatment, which inhibits the maturation of Progerin, improves some of the nuclear abnormalities associated with HGPS both in vitro and in animal models [16-22]. To examine whether FTI treatment reduces steady-state DSB levels, we quantified the average number of γ-H2AX foci per cell after 72 hours of treatment. To examine whether FTI treatment improves the repair kinetics of IR-induced DSBs, we quantified the average number of γ-H2AX foci per cell at 0.5, 24, and 48 hours post-irradiation. For this purpose, FTI treatment was initiated 72 hours prior to irradiation and continued until the cells were assayed with cells examined 24 and 48 hours post-irradiation receiving a total of 96 and 120 hours of FTI treatment, respectively.

First, FTI treatment resulted in a statistically significant reduction in the percentage of HGPS fibroblasts with an abnormal nuclear morphology, as determined using immunofluorescence microscopy to visualize lamin A/C (Fig. 13A and 15D), similar to previous reports [16, 17, 22]. The decrease in the percentage of cells with an abnormal morphology correlated with the length of FTI treatment. Unirradiated FTI-treated AG11513 and AG11498 HGPS fibroblasts (72 hours total treatment) exhibited a 36% and 41% reduction in the percentage of cells with an abnormal nuclear morphology, respectively compared to non-treated cells (Fig. 13A, white bars). FTI-treated AG11513 and AG11498 fibroblasts examined 24 hours post-irradiation (96 hours total treatment) showed a 39% and 44% reduction, respectively (Figure 13A, gray bars). FTI-treated AG11513 and AG11498 fibroblasts examined 48 hours post-irradiation (120 hours total treatment) showed a 49% and 47% reduction, respectively (Fig. 13A, black bars). The percentage of FTI-treated HGPS fibroblasts with abnormal nuclear morphology remained statistically higher than wildtype fibroblasts for unirradiated cells as well as cells examined post-irradiation, indicating that FTI treatment does not restore normal morphology to all HGPS fibroblasts in the time periods examined, consistent with other reports [16, 17, 22].

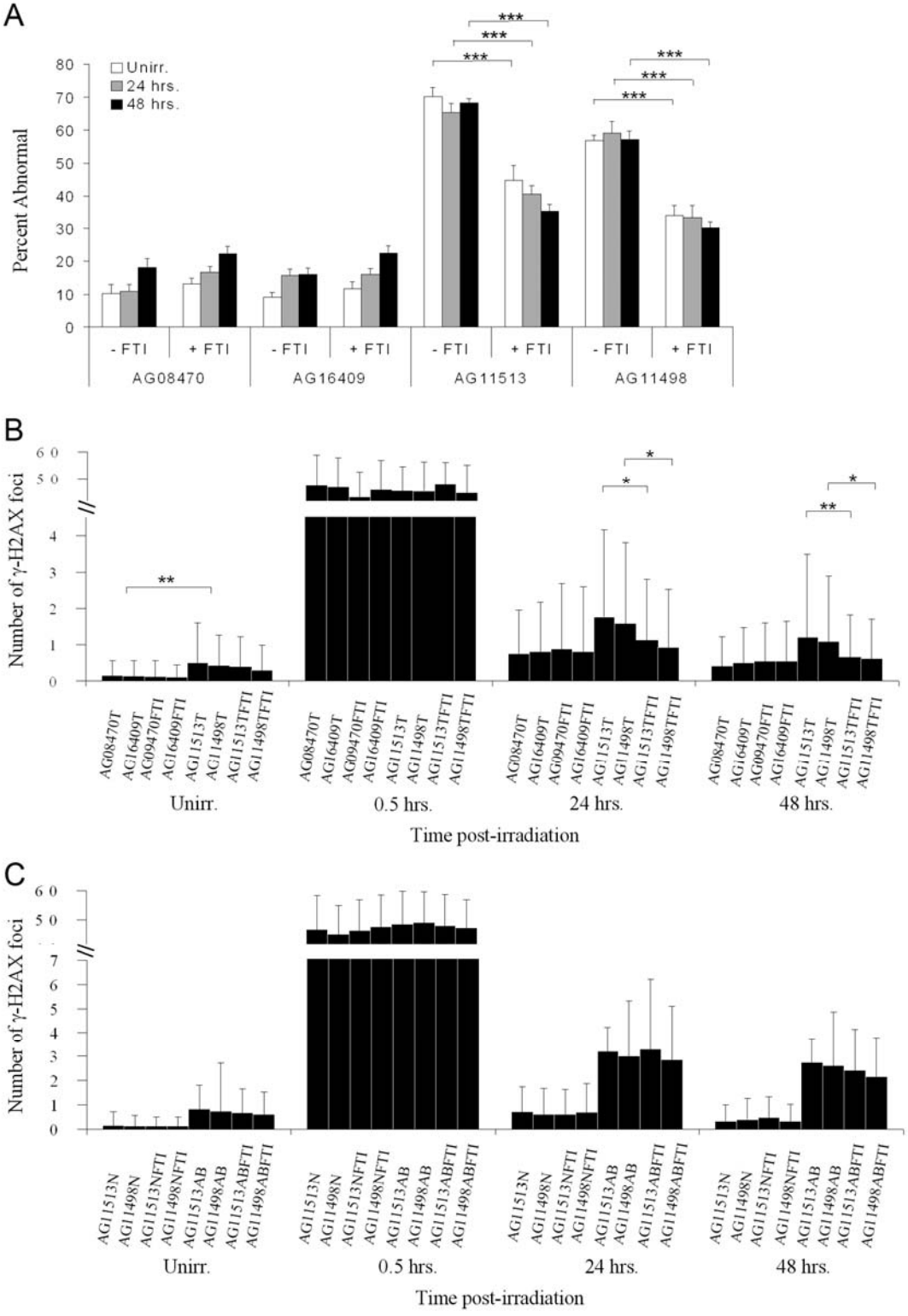
A
Percent Abnormal
Unirr.
24 hrs.
48 hrs.
- FTI
+ FTI
AG08470
AG16409
AG11513
AG11498
B
Number of γ-H2AX foci
Unirr.
0.5 hrs.
24 hrs.
48 hrs.
Time post-irradiation
C
Number of γ-H2AX foci
Unirr.
0.5 hrs.
24 hrs.
48 hrs.
Time post-irradiation

Figure 13. FTI treatment improves nuclear morphology and repair of IR-induced DSBs in HGPS fibroblasts, but has no effect on the steady-state level of DSBs. HGPS cells and cells from healthy individuals were treated for 72 hours with 5 uM FTI L-744832. Cells used in irradiation studies were treated with the FTI post-irradiation until assayed. Immunocytochemistry was performed for γ-H2AX and lamin A at the indicated timepoints after 2 Gy g-irradiation. A) Percentage of unirradiated (white bars), 24 hrs. post-irradiation (gray bars), and 48 hrs. post-irradiation (black bars) fibroblasts exhibiting an abnormal nuclear morphology in the presence (+) or absence (-) of FTI. Data is from experiments. At least 200 total cells were examined per group. Error bars represent the standard error of the mean (SEM). B) Examination of the average number of γ-H2AX foci per cell shows a statistically significant reduction in FTI-treated HGPS cells at 24 and 48 hours post-irradiation compared to non-treated HGPS cells. The differences between FTI-treated and non-treated unirradiated HGPS cells were not statistically significant. "T" = total cells including those with normal and abnormal nuclear morphologies. "TFTI" = FTI-treated total cells including those with normal and abnormal nuclear morphologies. D) Examination of the average number of γ-H2AX foci shows no change in HGPSN and HGPSAB populations after FTI treatment, suggesting that the overall decrease in HGPS cells is due to correction of the nuclear morphology defect. "N" = cells with normal nuclear morphology. "NFTI" = FTI-treated cells with normal morphology. "AB" = cells with abnormal nuclear morphology. "ABFTI" = FTI-treated cells with abnormal nuclear morphology. The data presented in B and C were obtained from three experiments. For statistical analysis, cells form multiple experiments were pooled together for each experimental group and a one-way ANOVA test was performed followed by a Tukey post-test to obtain p-values for the differences between specific pairs of means. Error bars represent the standard deviation (SD) of the number of γ-H2AX foci per cell in order to highlight the large variance from cell to cell. Confocal images were captured using a Leica TCS SP2 using Leica software. * = $p < 0.05$, ** = $p < 0.01$, and *** = $p < 0.001$.

To analyze the effect of FTI treatment on the steady-state level of DSBs and repair of IR- induced DSBs in HGPS cells, we used total HGPS (HGPST) cells instead of distinguishing between those with normal and abnormal morphology because FTIs improve nuclear morphology, which we have shown is correlated with the DSB repair defect and may cause erroneous interpretation of the results. First, grouping HGPS cells with normal and abnormal morphologies together still resulted in a statistically significant higher average number of γ-H2AX foci per cell compared to wildtype cells, for both unirradiated cells and cells examined 24 and 48 hours post irradiation (Fig 13B and 15E). Averaged together, HGPST fibroblast cultures exhibited a 3.2–fold higher steady-state average number of γ-H2AX foci per cell compared to wildtype cultures (Fig 13B and 15E). After irradiation, no statistically significant differences were observed at 0.5 hours between HGPST and wildtype cultures, but HGPST cultures did exhibit 2.15–fold and 2.3–fold higher average numbers of γ-H2AX foci per cell at 24 and 48 hours after irradiation, respectively (Fig 13B and 15E).

Quantification of the average number of γ-H2AX foci per cell for unirradiated FTI-treated HGPST (AG11513TFTI and AG11498TFTI) fibroblasts resulted in a statistically insignificant reduction compared to untreated HGPST (AG11513T and AG11498T) fibroblasts (Fig. 13B and 15E). This indicates that FTI treatment for 72 hours does not result in a detectable reduction in the steady-state number of DSBs in HGPST fibroblasts under our experimental conditions. At 0.5 hours after irradiation there was no statistically significant difference in the average number of IR-induced γ-H2AX foci between FTI-treated and non-treated HGPST fibroblasts (AG11513T and AG11498T) (Fig 13B and 15E). However, at 24 and 48 hours post-irradiation, FTI-treated HGPST fibroblasts (AG11513TFTI and AG11498TFTI) exhibited a statistically significant reduction in the average number of IR-induced γ-H2AX foci per cell compared to non-treated HGPST fibroblasts (AG11513T and AG11498T) (Fig. 13B and 15E), indicating that FTI treatment for 96 or 120 hours improves DSB repair. The differences in the average number of γ-H2AX foci per cell for FTI-treated HGPS fibroblasts (AG11513TFTI and AG11498TFTI) and wildtype fibroblasts were not statistically significant at 24 and 48 hours after irradiation under our experimental conditions (Fig. 13B and 15E), indicating that FTI treatment improves repair of IR-induced DSBs in HGPST fibroblasts to an efficiency that is indistinguishable from wildtype cells. Altogether, these results indicate that although FTI treatment can improve repair of IR-induced DSBs, it may not be able to reduce the steady-state level of DSBs in HGPS cells.

We hypothesized that the improvement in repair of IR-induced DSBs in HGPST cells may represent an improvement in all cells independent of nuclear morphology or may occur specifically in cells whose nuclear morphology was normalized. The latter hypothesis is supported by our earlier results, which indicate a correlation between abnormal nuclear morphology and impaired repair of IR-induced DSBs. If there is no correlation between abnormal nuclear morphology and the DSB repair defect, we would expect to see the following two outcomes: First, we would expect to see an FTI-dependent reduction in the average number of γ-H2AX foci per cell in HGPSAB fibroblasts due to individual HGPSAB fibroblasts that experience an improvement in DSB repair, but not in nuclear morphology. We did not observe this;

FTI-treated HGPSAB fibroblasts exhibited the same average number of γ-H2AX foci per cell as the non-treated HGPSAB fibroblasts (Fig. 13C and 15F), indicating that improvement in DSB repair only occurred in cells whose nuclear morphology was normalized. Second, we would expect to see an FTI-dependent increase in the average number of γ-H2AX foci per cell in HGPSN fibroblasts due to individual HGPSAB fibroblasts that experience an improvement in nuclear morphology, but not in DSB repair. We did not observe this either; FTI-treated HGPSN fibroblasts exhibited the same average number of γ-H2AX foci per cell as non-treated HGPSN fibroblasts (Fig. 13C and 15F), indicating that normalization of nuclear morphology was always accompanied by an improvement in DSB repair. These results demonstrate a strong correlation between nuclear morphology normalization and improvement in repair of IR-induced DSBs after FTI treatment.

3.4.4. MRN repair complex factor localization to IR-induced DSBs is delayed in HGPST cells and GFP-Progerin positive hCAECs with an abnormal nuclear morphology.

Previous reports suggest that the DSB repair deficiency observed in HGPS cells is specific to HR repair [29]. It has been reported that the localization of the DSB repair factors, Rad50 and Rad51 to XPA-localized DSBs is impaired in HGPS cells due to the aberrant localization of XPA, possibly through steric hindrance [24]. However, the localization of repair factors to IR-induced DSBs has not been clearly investigated in HGPS cells. Since the MRN (MRE11/Rad50/phospho-NBS1) repair complex is essential for DSB HR repair (Reviewed in [32]), we examined the protein levels of NBS1 and MRE11 as well as their colocalization kinetics to IR-induced γ-H2AX foci in total HGPS cells as well as GFP-Progerin positive hCAECs with an abnormal nuclear morphology (Fig. 14 and 15F,G). Immunocytochemistry was used to examine colocalization, identified by overlap of γ-H2AX shown in red and either phospho-NBS1 (Fig 14A) or MRE11 (Fig. 14B) shown in green. The percent of γ-H2AX foci that have either phospho-

NBS1 (Fig. 14C and 15G) or MRE11 (Fig 14D and 15H) colocalized at 0.5 and 2 hours post-irradiation was calculated. HGPS AG11513T (77%) and AG11498T (79%) fibroblasts and GFP-Progerin expressing

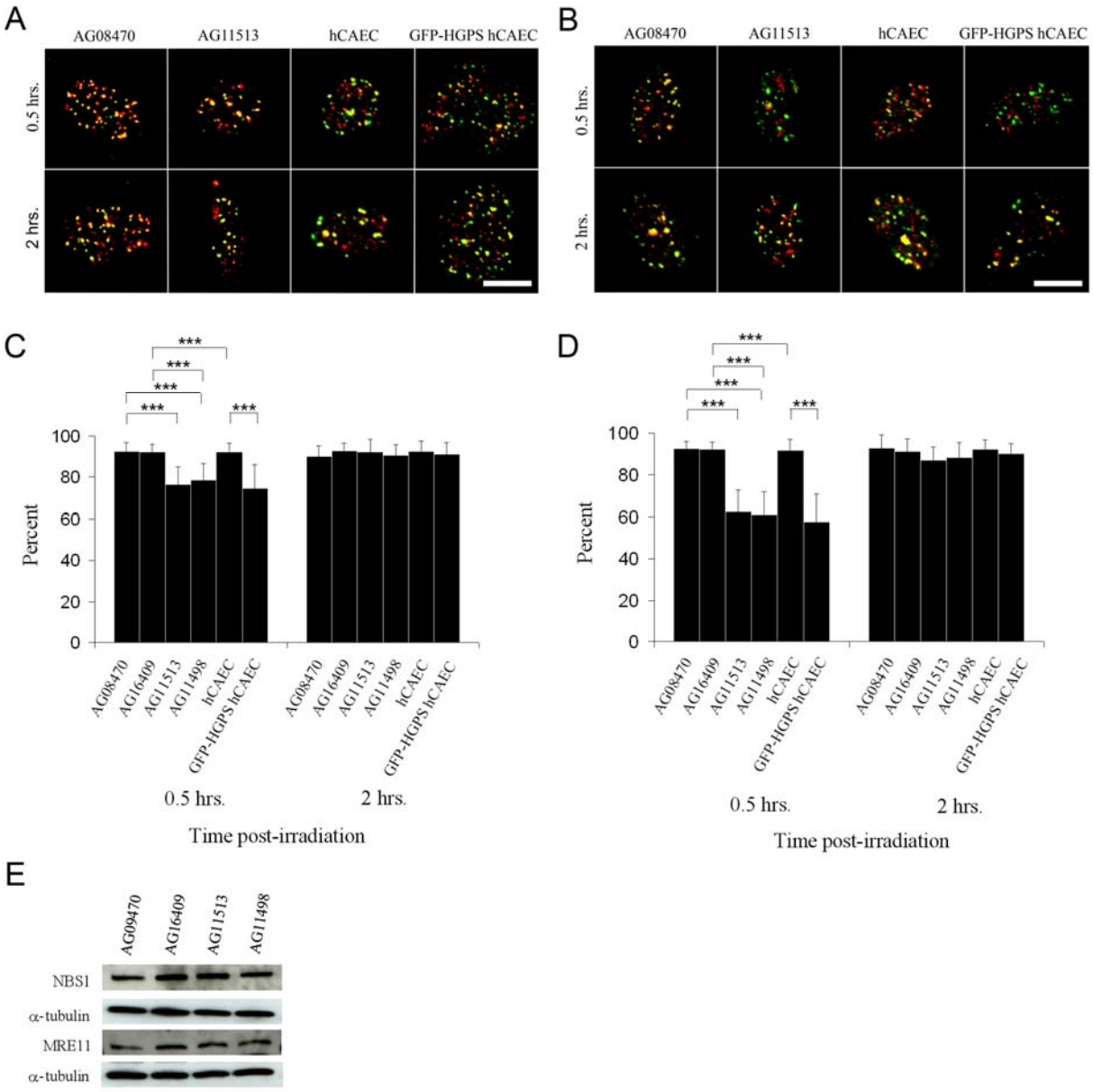

Figure 14. MRN repair complex factors exhibit delayed localization to IR-induced DSBs in total HGPS fibroblasts and GFP-Progerin expressing hCAECs with an abnormal nuclear morphology. Immunocytochemistry was performed for γ-H2AX and either phospho-NBS1 or MRE11 at various timepoints after g-irradiation and the percentage of γ-H2AX foci exhibiting phospho-NBS1 or MRE11 colocalization was determined. A) Immunocytochemistry for γ-H2AX (green) and phospho-NBS1 (red). B) Percentage of γ-H2AX foci exhibiting phospho-NBS1 colocalization. C) Immunocytochemistry for γ-H2AX (green) and MRE11 (red). D) Percentage of γ-H2AX foci exhibiting MRE11 colocalization. E) Western analysis of total NBS1 and MRE11. Data is from two experiments. Three experiments were performed. At least 1000 foci were examined for each timepoint. For statistical analysis, cells form multiple experiments were pooled together for each experimental group and a one-way ANOVA test was performed followed by a Tukey post-test to obtain p-values for the differences between specific pairs of means. Error bars represent the standard deviation (SD) in the percentage of γ-H2AX foci with phospho-NBS1 or MRE11 colocalized per cell. Confocal images were captured using a Leica TCS SP2 using Leica software. Scale bar equals 5 μm. * = $p < 0.05$, ** = $p < 0.01$, and *** = $p < 0.001$

hCAECs with an abnormal nuclear morphology (75%) exhibited statistically significant lower percentages of γ-H2AX foci colocalized with phospho-NBS1 at 0.5 hours after irradiation compared to wildtype AG08470T (93%) and AG16409T (92%) fibroblasts and wildtype hCAECs (92%) (Fig. 14C and 15G). Similarly, HGPS AG11513T (62%) and AG11498T (61%) fibroblasts and GFP-Progerin expressing hCAECs with an abnormal nuclear morphology (58%) exhibited a statistically significant lower percentage of γ-H2AX foci colocalized with MRE11 at 0.5hrs. post-irradiation compared to wildtype AG08470 (93%) and AG16409 (92%) fibroblasts and wildtype hCAECs (92%) (Fig. 14D and 15H). The differences in colocalization between HGPST fibroblasts and wildtype fibroblasts as well as between GFP-Progerin positive hCAECs with abnormal nuclear morphology and wildtype hCAECs disappeared by two hours after irradiation for both phospho-NBS1 (Fig. 14C and 15G) and MRE11 (Fig. 14D and 15H). Western blot analysis showed no substantial differences in the protein levels of total NBS1 and MRE11 between wildtype and HGPS fibroblasts (Fig. 14E). Altogether these results indicate that phospho-NBS1 and MRE11 localization to IR-induced DSBs may be delayed by as much as 2 hours. It is important to note that total HGPS cells were examined so the localization defect is likely to be even greater for HGPS cells with an abnormal nuclear morphology. Lastly, the observation that only select DSBs exhibit a lack of colocalization at 0.5 hours post-irradiation suggests that the delay only occurs at particular DSBs and is not a general phenomenon throughout the entire nucleus.

A

Characteristics of cells used					
Individual	Age	Sex	Cell Type	Genotype	PPD
AG08470	10 YR	F	Dermal fibroblast	Wildtype	10-15
AG16409	12 YR	M	Dermal fibroblast	Wildtype	10-15
AG11513	14 YR	M	Dermal fibroblast	G608G	10-15
AG11498	8 YR	F	Dermal fibroblast	G608G	15-20

B

Average number of γ-H2AX foci per cell						
	AG08470T	AG16409T	AG11513N	AG11498N	AG11513AB	AG11498AB
Unirr.	0.19 ± 0.46	0.15 ± 0.43	0.18 ± 0.48	0.16 ± 0.47	0.93 ± 1.49	0.74 ± 1.49
0.5 hrs.	48.83 ± 11.45	50.51 ± 12.28	47.80 ± 11.53	47.54 ±11.06	46.80 ± 10.67	46.30 ± 9.68
2 hrs.	21.07 ± 6.58	19.84 ± 4.16	22.81 ± 6.79	21.56 ± 6.15	31.05 ± 7.41	29.21 ± 8.45
6 hrs.	1.97 ± 1.71	1.86 ± 1.59	2.28 ± 1.86	2.17 ± 1.64	6.51 ± 3.56	5.47 ± 3.28
12 hrs.	1.38 ± 1.90	1.31 ± 1.74	1.59 ± 1.78	1.52 ± 1.62	3.87 ± 2.87	3.39 ± 2.65
24hrs.	0.82 ± 1.26	0.80 ± 1.45	0.74 ± 1.04	0.79 ± 1.14	3.24 ± 2.66	3.02 ± 2.27
48 hrs.	0.38 ± 0.77	0.45 ± 0.88	0.34 ± 0.74	0.44 ± 1.07	2.75 ± 1.92	2.62 ± 2.17

C

Average number of γ-H2AX foci per cell				
	Wildtype	GFP-LMNA	GFP-HGPSN	GFP-HGPSAB
Unirr.	0.28 ± 0.62	0.38 ± 0.63	0.30 ± 0.64	1.35 ± 2.79
0.5 hrs.	53.91 ± 12.47	55.88 ± 14.08	52.63 ± 11.77	54.36 ± 11.61
12 hrs.	5.07 ± 4.40	5.63 ± 4.45	5.85 ± 4.95	10.24 ± 6.76
24hrs.	1.51 ± 2.07	2.42 ± 2.99	2.99 ± 4.05	6.51 ± 6.13

D

Percent cells with abnormal nuclear morphology								
	AG08470		AG16409		AG11513		AG11498	
	- FTI	+ FTI	- FTI	+ FTI	- FTI	+ FTI	- FTI	+ FTI
Unirr.	10.21 ± 2.56	13.11 ± 1.78	9.06 ± 1.45	11.54 ± 2.08	70.24 ± 2.54	44.75 ± 4.49	56.88 ± 1.43	33.77 ± 3.03
24 hrs.	10.87 ± 2.01	16.59 ± 1.73	15.57 ± 1.90	16.04 ± 1.79	65.45 ± 2.71	40.62 ± 2.62	59.10 ± 3.50	33.13 ± 3.73
48 hrs.	18.13 ± 2.63	22.17 ± 2.28	15.97 ± 1.90	22.31 ± 2.43	68.31 ± 1.16	34.97 ± 2.27	57.16 ± 2.58	30.13 ± 1.72

E

Average number of γ-H2AX foci per cell								
	AG08470T	AG16409T	AG08470TFTI	AG16409TFTI	AG11513T	AG11498T	AG11513TFTI	AG11498TFTI
Unirr.	0.15 ± 0.41	0.14 ± 0.42	0.13 ± 0.43	0.11 ± 0.34	0.50 ± 1.11	0.43 ± 0.84	0.39 ± 0.83	0.30 ± 0.69
0.5 hrs.	47.48 ± 11.24	46.81 ± 11.06	43.14 ± 10.33	45.90 ± 10.90	45.14 ± 9.35	45.29 ± 10.98	47.86 ± 8.17	44.57 ± 10.33
24 hrs.	0.75 ± 1.20	0.81 ± 1.37	0.89 ± 1.80	0.81 ± 1.78	1.78 ± 2.39	1.58 ± 2.23	1.12 ± 1.68	0.93 ± 1.60
48 hrs.	0.42 ± 0.80	0.50 ± 0.96	0.55 ± 1.05	0.55 ± 1.10	1.21 ± 2.28	1.09 ± 1.80	0.66 ± 1.17	0.63 ± 1.07

F

Average number of γ-H2AX foci per cell								
	AG11513N	AG11498N	AG11513NFTI	11498NFTI	AG11513AB	AG11498AB	AG11513ABFTI	AG11498ABFTI
Unirr.	0.16 ± 0.56	0.13 ± 0.44	0.12 ± 0.38	0.12 ± 47.52	0.83 ± 1.60	0.74 ± 2.00	0.68 ± 0.97	0.59 ± 0.92
0.5 hrs.	46.71 ± 11.57	45.10 ± 9.83	46.33 ± 10.46	47.52 ± 10.94	48.48 ± 11.28	49.00 ± 10.54	47.95 ± 10.83	47.29 ± 9.52
24 hrs.	0.72 ± 1.03	0.61 ± 1.07	0.61 ± 1.02	0.71 ± 1.18	3.20 ± 2.74	3.03 ± 2.28	3.31 ± 2.90	2.87 ± 2.22
48 hrs.	0.32 ± 0.68	0.41 ± 0.86	0.49 ± 0.84	0.33 ± 0.69	2.75 ± 1.94	2.63 ± 2.23	2.42 ± 1.70	2.16 ± 1.62

G

Average percent of γ-H2AX foci exhibiting phospho-NBS1 colocalization						
	AG08470	AG16409	AG11513	AG11498	hCAEC	GFP-HGPS hCAEC
0.5 hrs.	92.49 ± 4.17	92.21 ± 3.76	76.52 ± 8.54	78.54 ± 7.82	92.32 ± 4.01	74.68 ± 11.24
2 hrs.	90.16 ± 4.99	92.90 ± 3.45	91.98 ± 6.47	90.57 ± 5.18	92.68 ± 4.84	90.99 ± 5.76

H

Average percent of γ-H2AX foci exhibiting MRE11 colocalization						
	AG08470	AG16409	AG11513	AG11498	hCAEC	GFP-HGPS hCAEC
0.5 hrs.	92.47 ± 3.41	92.24 ± 3.53	62.29 ± 10.47	61.15 ± 10.63	91.92 ± 4.95	57.76 ± 12.90
2 hrs.	92.77 ± 6.50	91.33 ± 5.83	86.88 ± 6.38	88.31 ±7.05	92.18 ± 4.60	90.18 ± 4.58

Figure 15. A) Cell type used in experiments: primary dermal fibroblasts of similar population doubling from age-matched healthy individuals (AG08470 and AG16409) and HGPS patients (AG08470 and AG11409). B-G) Tables providing exact values and standard deviations or standard errors as indicated in the figure legends for each figure as referenced in the text. B = Figure 10, C = Figure 12, D = Figure 13A. E = Figure 13B, F = Figure 13C. G = Figure 14C, and H = Figure 14B.

3.5. DISCUSSION

Recent reports have demonstrated an accumulation of DSBs in HGPS cells which may be due to defective DSB repair [19, 24, 29, 30]. These observations are interesting since DNA damage accumulation may contribute to the increased levels of apoptosis and senescence observed in HGPS cells and in turn to the accelerated aging phenotype. Here, we set forth to examine the severity of the DSB repair defect and investigate the mechanism/s responsible. Quantitative analysis showed that HGPS fibroblasts exhibit a higher steady-state number of DSBs and impaired repair of IR-induced DSBs compared to wildtype fibroblasts (Fig. 13B and 15E). The higher steady-state level of DSBs may be responsible for the elevated DNA damage signaling pathways reported in HGPS cells [19]. Our results are in accordance with two recent studies which showed that HGPS cells exhibit a higher steady-state level of DSBs [30]. Sedelnikova et al. reported that the average number of γ-H2AX foci per cell increases with passage in cultures. The authors detected 1.0, 1.2, and 1.9 average γ-H2AX foci per cell at passage 15, 26, and 38, respectively. Liu et al. also recently reported that passage 16 AG11513A HGPS primary fibroblast cultures exhibited about 10 average γ-H2AX foci per cell [24]. Our detection of 0.5 foci and 0.43 foci per cell for AG11513 and AG11498 HGPS cell cultures at passage 8-9 is in close agreement with the results obtained by Sedelnikova et al.

Ecoptic expression of GFP-Progerin in wildtype hCAECs produced similar phenotypes to HGPS primary fibroblast cultures. GFP Progerin positive cells displayed an increased steady-state level of DSBs (Fig 12A,B and 15C) and impaired repair of IR-induced DSBs (Figure 12A,B and 15C). In contrast, expression of a control GFP-LMNA construct resulted in minimal nuclear morphological changes and did not result in a statistically significant increase in steady-state DSB levels or a detectable defect in repair of IR-induced DSBs. This indicates that Progerin is fundamentally responsible for both phenotypes in a dominant gain-of-function manner similar to other HGPS cellular phenotypes [8, 14].

Separation of HGPS and GFP-Porgerin positive cells into groups with “normal” (N) or “abnormal” (AB) nuclear morphologies showed that the elevated steady-state level of DSBs and the DSB repair defect are only present in cells with an abnormal nuclear morphology (Fig 10A,B and 15B; Fig 12A,B and 15C). The strong correlation between the DSB associated defects and the abnormal nuclear morphology highlights the possibility of a mechanistic link even though it is possible that the two phenotypes occur independently through separate Progerin-dependent mechanisms. If there is a mechanistic link it is theoretically possible that the DSB-associated defects cause the abnormal nuclear morphology. However, this scenario is extremely unlikely because we did not observe any nuclear morphological changes similar to HGPS in wildtype fibroblasts in response to IR-induced DSBs. Further, there is no report to our knowledge suggesting that DSB formation leads to nuclear morphological changes similar to HGPS. Apoptosis, which can be caused by elevated levels of DSBs, does result in nuclear morphological changes, including chromatin condensation, nuclear shrinkage, and formation of apoptotic bodies, but these processes are characterized by a unique and different morphological pattern (Reviewed in [33]). Alternatively, the nuclear structural irregularities that underlie the abnormal nuclear morphology may cause the DSB repair defect. This last possibility is intriguing since it is becoming clear that the nucleus is a highly ordered compartment and that nuclear structure and chromatin organization are intricately linked to nuclear biological processes (Reviewed in [34, 35]).

How can nuclear structural irregularities impair DSB repair? Our observation along with those of others [24] which show that DSB repair factor localization to DSBs is compromised in HGPS cells highlights the possibility that abnormal nuclear structure impairs DSB repair by interfering with repair factor localization. We examined the kinetics of phospho-NBS1 (Fig. 14A,C and 15G) and MRE11 (Fig 14B,D and 15H) colocalization to IR-induced DSBs, and observed that both DSB repair factors exhibit an initial delay in localization to particular DSBs in HGPST cells. However, by two hours post-irradiation, both repair factors were localized to a similar percentage of DSBs in HGPST and wildtype cells. NBS1 and MRE11 protein levels were comparable in HGPS and wildtype cells. Similar colocalization delays to IR-induced DSBs were obtained in hCAECs expressing Progerin-GFP. There are multiple theoretical ways in which abnormal nuclear structure can interfere with DSB repair factor colocalization. First, the nuclear lobes and invaginations present in the nuclear envelope may compartmentalize the nucleus and thus restrict the motility or accessibility of repair factors to particular DSBs. A second possibility is that the local nuclear matrix which may be necessary for the formation of functional multi-protein repair complexes, and to which lamins have been proposed to contribute [6] is disrupted by the presence of Progerin. Third, local chromatin organization, which appears to be altered in HGPS cells [8, 15], may interfere with the formation of functional repair complexes. Interestingly, the changes in chromatin organization may themselves be due to more fundamental irregularities in nuclear structure. These scenarios could render local regions of the nucleus unfavorable to DSB repair, and DSBs that randomly occur in unfavorable regions may experience delayed or incomplete repair.

Interestingly, it has been recently proposed that among the multiple roles the MRN complex has in DSB repair is a tethering function that acts in two ways. First, the MRN complex tethers the two ends of the broken chromosome together and second, it also tethers the broken chromosome to the sister chromatid or other homologous genomic region that is to be used for homologous recombination repair (Reviewed in [32]). It is easily conceivable that a delay in the formation of such tethering units may lead to separation of the broken ends at a DSB, which may slow down or preclude further repair.

How can the accumulation of DSBs lead to the accelerated aging phenotype observed at the organismal level in HGPS? First, the prolonged presence of individual DSBs can activate DNA damage response pathways whose activity levels have been shown to be elevated in HGPS cells [19, 36]. Hyperactive DNA damage response pathways can lead to higher rates of apoptosis and senescence which have also been reported in HGPS cells. Even a delay of 1-2 hours as observed for phospho-NBS1 and MRE11 localization may be sufficient to lead to apoptosis or senescence. The importance of early response to DNA damage for cell survival is highlighted by a recent study, which showed that the radiosensitization caused by a one hour delay in activation of ATM after g-irradiation accounts for 70% of the radiosensitization caused by a 17 hour delay [37]. Finally, higher levels of apoptosis and senescence can lead to accelerated tissue/organ degeneration over time perhaps in part through exhaustion of adult stem cell pools as has been proposed (Reviewed in [38]).

We also demonstrate that FTI treatment, which has been shown to improve multiple HGPS phenotypes [16-22], also improves repair of IR-induced DSBs in HGPS cells. Interestingly, although we observed a reduction in the steady-state average number of DSBs per cell (non-IR-induced), it was not statistically significant, indicating that FTI treatment may not be able to reduce the level of steady-state DSBs. This observation is consistent with a previous report, which showed that FTI treatment did not reduce the elevated levels of DNA damage signaling pathways in HGPS cells [19]. There are several possible explanations for the discrepancy in the effect of FTI treatment on the repair of IR-induced DSBs and steady-state DSB levels. One possibility is that irradiated cells underwent longer FTI treatment (as described in the materials and methods) which may have resulted a greater beneficial effect on DSB repair. Another possible explanation is that FTI treatment creates a nuclear environment in which novel-DSBs (IR-induced) undergo normal repair, but pre-existing DSBs that formed in the context of nuclear structural irregularities remain irreparable. Lastly, there is evidence to suggest that some endogenous DSBs in HGPS cells (those observed at steady-state) appear to have XPA aberrantly localized and may be functionally different in origin and/or repair from those induced ectopically [24]. In this scenario, it is possible that FTIs improve the repair of ectopically-induced DSBs, but that the presence of XPA or other

characteristics of particular engogenous DSBs detected in non-irradiated cells may resist the FTI-based improvement. Further investigation is necessary to elucidate this matter. Such investigation is essential because if FTIs do not improve endogenously occurring DSBs in HGPS cells, then FTI treatment may not have significant clinical benefit.

HGPS research is motivated by the objective to develop therapeutic approaches for individuals with HGPS as well as by the rationale that the mechanism/s underlying the accelerated aging phenotype will increase our understanding of normal aging and age-associated disease. Regarding the former, our findings offer mixed results. On the one hand we show that FTI treatment can improve the DSB repair of radiologically-induced DSBs in HGPS cells. On the other hand, our results and those of others suggest that a subset of endogenously occurring DSBs (XPA-localized) may be functionally distinct and resistant to FTI-based repair improvement. In terms of HGPS research expanding our understanding of normal aging, our results suggest that, similar to other progeroid syndromes, HGPS pathology occurs due to an amplification of a biological process already believed to contribute to normal aging, namely DNA damage accumulation. The possibility that DNA damage accumulation is amplified by nuclear structural irregularities, as identified by our results, suggests that maintenance of proper nuclear structural organization is important for longevity.

3.6. MATERIAL AND METHODS

3.6.1. Cell Culture

Primary dermal fibroblasts, AG80470, AG16409, AG11513, and AG11498 (Coriell Cell Repository; Camden, NJ) were grown in Dulbecco's modified Eagles's medium (DMEM) supplemented with 15% fetal bovine serum, 1mM L-glutamine, 1% Pen/Strep, 1% MEM Non-essential amino acids. Cells were passaged every 4-6 days and media was changed every 2 days. Primary human coronary artery endothelial cells (Cambrex; East Rutherford, NJ) were cultured in endothelial cell basal medium (EBM) supplemented with the EGM-MV bullet kit (Cambrex). Cells were passaged every 6-8 days and media changed every 2 days.

3.6.2. FTI treatment

Cells were passaged and the media was replaced 24 hours later with media containing 5 uM FTI L-744832 (Biomol, Plymouth Meeting, PA). FTI media was replaced every 24 hours for 72 hours as described. For irradiated cells, treatment was continued every 24 hours post-irradiation until cells were assayed.

3.6.3. Western Analysis

Western immunoblotting was performed according to established protocols. Briefly, 10ug of protein was loaded onto Tris-HCL 4-15% linear gradient gels (Bio-Rad Laboratories; Hercules, CA) and individual gels were run at 60mA, 200V. Proteins were transferred to PVDF membrane for one hour at 350mA, 100V. PVDF membrane was blocked for one hour in Tris-Buffered Saline (TBS) containing 5% non-fat dry milk and 0.1% Tween-20. The following primary antibodies were diluted in blocking solution and used as needed: mouse anti-human MRE-11 monoclonal antibody (Novus Biologicals; Littleton, CO) and rabbit anti-human NBS1 polyclonal antibody (Millipore; Billerica, MA). Anti-mouse (Zymed Laboratories; San Francisco, CA) and anti-rabbit (Invitrogen; Carlsbad, CA) HRP-conjugated goat secondary antibodies were used and detected via chemi-luminescence using an ECL Advance Western Blotting Detection Kit (GE Healthcare; Buckinghamshire, UK).

3.6.4. Immunocytochemistry

Briefly, cells were passaged onto glass slides and fixed using –20°C methanol or 2% paraformaldehyde, as appropriate. The cells were washed 2X in PBS and 1X in Triton-X PBS and blocked for 30 minutes in BSA(0.3%)/goat serum(5%) at room temperature. Cells were then incubated with the following primary antibodies were as needed for one hour at room temperature: rabbit anti-human (pS353) polyclonal antibody, mouse anti-human MRE-11 monoclonal antibody, rabbit anti-human γ -H2AX polyclonal antibody (Novus Biologicals; Littleton, CO), mouse-anti-human γ -H2AX monoclonal antibody (Upstate; Lake Placid, NY). The cells were washed 2X in PBS and 1X in Triton-X PBS. The cells were incubated with anti-mouse and anti-rabbit Alexa fluor-488, -568, -633 secondary antibodies as appropriate (Molecular Probes; Eugene, Oregon). DNA was visualized with TOTO-3 as needed (Molecular Probes Inc; Eugene, OR). The cells were washed 2X in PBS and 1X in Triton-X PBS and mounted using VectaShield mounting medium (Vector Laboratories; Burlingame, CA). Confocal microscopy was performed with a Leica TCS SP2 confocal microscope.

3.6.5. Lentivirus Production and Transduction

Lamin A-GFP and Progerin-GFP fourth generation replication-incompetent HIV-1-based lentivirus was produced using the ViraPower™ Lentivirus Expression System following the manufacturer's instructions (Invitrogen, Carlsbad, CA). Briefly, 293FT cells were simultaneously transfected with ViraPower Packaging Mix and either GFP-LMNA or GFP-HGPS plasmids using Superfect transfection reagent (Invitorgen) according to the manufacturer's instructions (The ViraPower Packaging Mix contains the necessary structural and replication components in trans on three separate plasmids. The GFP-LMNA and GFP-HGPS plasmids contain elements that allow packaging of the gene constructs into virions. The gene constructs are under the control of the ubiquitin promoter). Supernatant was collected 60 hours

post-transfection. The virus was concentrated via ultra-centrifugation at 50,000G for 3 hours. Cells were transduced at an MOI of 20 for 18 hours.

3.7. ACKOWLEDGEMENTS

We would like to thank Dr. Ahmi Ben-Yehudah, Sandra Tavares-Varum, and Olga Momcilovic for helpful discussion. This research was supported by a grant from the National Institute of Child Health and Hukman Development, 1PO1HD047675.

CHATPTER THREE: SUMMARY AND CONCLUSIONS

4.1. Summary of results

The aim of the research presented in this doctoral disseration was to investigate the molecular and cellular mechanisms contributing to the "premature aging" phenotype in HGPS. Two approaches have been used to investigate such mechanisms. One approach examined whether LMNA, the mutated gene in HGPS, is expressed in pluripotent ES cells in order to determine whether the adverse effects caused by Progerin begin during embryonic development. The second approach examined whether DSB repair is compromised in HGPS cells in order to determine whether impaired repair is a molecular mechanism that contributes to the accelerated aging phenotype.

The research presented in Chapter One examined whether A-type and B-type lamins are expressed in undifferentiated mESCs and hESCs. The results show that although lamins B1 and B2 are expressed in undifferentiated mESCs and hESCs, lamin A/C is not (Figures 3, 4, and 5). However, lamin A/C expression is detected after in vitro differentiation of hESCs (mESC cells were not examined), indicating that as hESCs differentiate, lamin A/C expression is activated (Figure 8). This is in accordance with other reports that have shown that although B-type lamins are present during mouse embryonic development, lamin A/C is not expressed until the latter half of development (Prather et al., 1991; Prather et al., 1989; Rober et al., 1989; Schatten et al., 1985; Stewart and Burke, 1987). Similarly, lamin A/C is not expressed or expressed at low levels in undifferentiated EC cells (Peter and Nigg, 1991; Stewart and Burke, 1987). Altogether, these results suggest that lamin A is not expressed during early human embryonic

development, but is activated as cells differentiate. Thus, Progerin is probably absent during early human development, but accumulates concomitantly with LMNA expression at later developmental stages at which point it may exert a detrimental effect on the developmental process and produce the developmental defects present in HGPS patients. Furthermore, the fact that some tissues show developmental defects while others are spared may be due to different initiation of LMNA expression in different tissues. Similarly, the onset of LMNA expression in different tissues may influence the severity of the degenerative phenotype manifested by those tissues. More experimentation is needed to fully elucidate the pathological role of Progerin during human development.

The research presented in Chapter Two examines whether DSB repair is compromised in HGPS cells. First, examination of the steady-state level of DSBs showed that HGPS cells have a higher level compared to wildtype cells (Figure 10 and 15B). Experiments examining the repair IR-induced DSBs showed that the elevated steady-state level of DSBs in HGPS cells is due at least partly to impaired DSB repair (Figure 10 and 15B). HGPS cells exhibit impaired repair of DSBs within two hours of irradiation, indicating an early repair defect. This early repair defect may be due to impaired localization of DSB repair factors to DSBs. Colocalization experiments post-irradiation showed up to a two hour delay in the localization of the DSB repair factor NBS1 and MRE11 to a percentage of DSBs (Figure 14 and 15G,H). The observation that localization of these repair factors was not impaired across the board, but only to particular DSBs, suggests that the local environment may contribute to the mislocalization. Further, whereas wildtpye cells return to the steady-state level of DSBs by 24 hours post-irradiation, HGPS cells still exhibit statistically significant higher numbers of IR–induced DSBs remaining at 24 and 48 hours post-irradiation (Figure S2), indicating that HGPS cells have difficulty or are unable to repair particular IR-induced DSBs. The accumulation of such irreparable DSBs could certainly lead to the activation of DNA damage response pathways and subsequently to apoptosis or senescence.

Both the elevated steady-state level of DSBs and the impaired DSB repair of IR-induced DSBs were reproduced in healthy cells when Progerin was expressed (Figure 12 and 15C), indicating that Progerin

produces these phenotypes in a dominant gain-of-function fashion, similar to other HGPS phenotypes (Goldman et al., 2004; Scaffidi and Misteli, 2005). Accordingly, FTI-treatment, which has been shown to reduce progerin levels and improve nuclear morphology in HGPS cultures (Capell et al., 2005; Fong et al., 2006a; Glynn and Glover, 2005; Liu et al., 2006; Toth et al., 2005; Yang et al., 2006; Yang et al., 2008), also improves the repair kinetics of DSBs post-irradiation (Figure 13B and 15E). Although a decrease in the number steady-state DSBs was detected in HGPS cells after FTI treatment, the reduction was not statistically significant. Possible explanations for this apparent discreptency are discussed in Chapter Two. Further experimentation needs to be performed to verify whether or not FTI treatment can reduce the elevated steady-state level of DSBs in HGPS cells.

Interestingly, the DSB repair defect correlates strongly with the abnormal nuclear morphology (Figure 10 and 15E). This correlation may or may not be mechanistically significant as it is possible that both phenotypes are independently caused by some Progerin-dependent mechanism. However, if such a mechanistic link exists between the two phenotypes, it is possible that structural irregularities cause the DSB repair defect and elevated levels of DSBs since it is accepted that DSB repair requires not only enzymatic, but also structural components (Assenmacher and Hopfner, 2004; de Jager et al., 2004; Hopfner et al., 2001). The mechanism through which structural irregularities may interfere with DSB repair is discussed in detail in Chapter Two. Briefly, progerin-induced irregularities in local nuclear and/or chromatin structure could physically interfere with the proper formation of DSB repair complexes. Such a scenario could render local regions of the nucleus unfavorable to DSB repair. DSBs that randomly occur in such structurally unfavorable regions may experience delayed or incomplete repair. Such a possibility is supported by the structural role the MRN repair complex is proposed to have during DSB repair (Reviewed in (Assenmacher and Hopfner, 2004; Williams et al., 2007)). As discussed in the introduction, the MRN complex is believed to function as a tethering scaffold that holds the two chromosome ends at a DSB and/or the recombinational partner strand in the case of HR repair in close proximity and prevents their physical separation. The observed delayed localization of MRE11 and phospho-NBS1 to DSBs in HGPS cells may result in physical separation of the chromosome ends at DSBs and prohibit repair. Thus,

even though by two hours post-irradiation phospho-NBS1 and MRE11 were localized to a similar percentage of DSBs in HGPS and wildtype cells, the initial localization delay in HGPS cells may render those particular DSBs irreparable.

4.2. MECHANISTIC HYPOTHESES FOR HGPS PATHOLOGY

Several hypotheses have been proposed for the molecular and cellular pathogenesis in HGPS, and it is quite possible that the total pathological effect is due to a combination of these mechanisms working in concert. Interestingly, particular tissues or cell types may be more susceptible to different mechanism which may contribute to the segmental nature of HGPS. One possibility is that since lamin A mutations including the HGPS mutation result in loss of nuclear structural integrity (Lammerding et al., 2004), the lack of nuclear structural support leads to physical cellular damage which may result in loss of function or cell death. Obviously, HGPS does not lead to complete failure of nuclear structural integrity, but resulting structural weakness may be sufficient to affect tissues that are consistently subjected to physical stress such as blood vessel walls. Indeed, HGPS patients do display various vascular abnormalities (Reviewed in (Hennekam, 2006)) and the primary cause of death is due to complications associated with the rapid onset of atherosclerosis. However, it is difficult to imagine how such a mechanism would explain the development of lypodystrophy and multiple other HGPS features that affect tissues which are not under significant physical stress. To investigate this hypothesis further, it would be interesting to examine whether vascular endothelial cells expressing Progerin show any gene expression or functional differences compared to wildtype cells in response to various forms of physical force in vitro.

Another possible mechanistic hypothesis is that the accelerated aging phenotype in HGPS is due to gene expression changes. In support of this hypothesis lamin A has been shown to interact with particular transcription factors, including MOK2 (Dreuillet et al., 2002) and SREBP1 (Lloyd et al., 2002), as well as with retinoblastoma (Rb), which is involved in regulating cell cycle arrest and apoptosis (Johnson et al., 2004; Mancini et al., 1994; Ozaki et al., 1994). It is possible that lamin A influences the activity of these factors and that the HGPS mutation alters their activity and as a consequence gene expression. This is an interesting possibility since it would suggest that any genes whose expression is specifically altered by the HGPS mutation may also contribute to physiologic aging. Alternatively, mutation in lamin A which leads to nuclear lamin disorganization appears to negatively affect polymerase II mediated transcription, suggesting that a mutated form of LMNA may lead to global transcriptional changes (Spann et al., 2002). Indeed multiple gene array experiments have demonstrated global changes in gene expression, although the changes have not been very consistent across different experiments (Csoka et al., 2004b; Ly et al., 2000; Park et al., 2001). This suggests that, with the exception of particular genes whose expression may be affected through modification of transcription factor activity, the HGPS mutation does not result in consistent changes to a cell's genetic expression profile, instead having a stochastic affect on gene expression. Since lamin A expression appears to be confined to differentiated cells, it has been proposed that one of the functions of lamin A is to maintain the differentiated state, that is to "lock" cells into tissue specific gene expression patterns when they become terminally differentiated, most likely though structural control of local as well as global chromatin organization. Indeed, as previously discussed, mutations in LMNA including the HGPS mutation result in chromatin epigenetic changes that may occur due to structural alterations in the nuclear lamina and nuclear matrix and can influence gene expression. Thus, the premature aging phenotype may not be due to specific gene expression changes that mimic physiological aging, but may simply be due to stochastically altered expression that renders cells unable to fulfill the their tissue-specific functional roles or that may result in cellular death and that ultimately lead to tissue/organ degeneration and failure.

A third mechanistic hypothesis that has gained momentum recently proposes that DNA damage accumulation is responsible for the premature aging phenotype in HGPS. This is a logical conclusion considering that DNA damage is believed to contribute to physiological aging. Research form other laboratories along with the results presented here demonstrates that the steady-state level of DSBs is elevated in HGPS and that the elevated levels are due at least partly to impaired DSB repair. The accumulation of DSBs may be sufficient to produce the elevated levels of DNA damage response pathways as well as the elevated levels of apoptosis and senescence that have been described in HGPS cells. If this is the case, the accelerated aging phenotype observed in HGPS is simply due to the amplification of one of the central contributors to physiological aging, DNA damage accumulation.

But how would these mechanisms, working alone or in concert, produce the accelerated aging phenotype in HGPS patients? It is likely that all three result in cellular dysfunction and/or cell loss through increased apoptosis or senescence. Such cellular loss would increase the cellular turnover rate and could exhaust regenerative stem cell pools prematurely. It is commonly accepted that most, if not all, human tissues maintain cellular homeostasis through continual regeneration from tissue-specific stem cell pools. It has even been hypothesized that functional loss of adult tissue-specific stem cell pools contributes to normal aging (Reviewed in (Rossi et al., 2008; Sharpless and DePinho, 2007)). In HGPS, adult tissue-specific stem cell pools are expected to be under a higher pressure to maintain tissue homeostasis due to increased cell loss through apoptosis and senescence caused by compromised nuclear structural integrity, altered gene expression, and/or inefficient DSB repair. The higher rate of tissue cellular depletion may be too great for the regenerative capacity of stem cell pools to cope with causing gradual tissue degeneration. Alternatively, it has been shown that some and perhaps all adult tissue-specific stem cells have limited proliferative capacity. An increased rate of tissue turnover in HGPS could exhaust the proliferative capacity of adult tissue-specific stem cell pools more quickly, at which point the tissue will undergo degeneration. Lastly, the adult stem cell pools themselves may be directly affected by the DSB repair defect, resulting in stem cell loss. This last possibility needs to be investigated further, since there are contradictory reports regarding the expression of lamin A in undifferentiated cells (Constantinescu et

al., 2006; Lourim and Lin, 1989a; Rober et al., 1989; Soutoglou and Misteli, 2008). In light of these possible scenarios the segmental nature of HGPS can easily be attributed to tissue-specific differences in LMNA expression, rates of DSB formation, tissue turnover, and available adult stem cell pools.

BIBLIOGRAPHY

Aebi, U., J. Cohn, L. Buhle, and L. Gerace. 1986. The nuclear lamina is a meshwork of intermediate-type filaments. *Nature*. 323:560-4.

Allsopp, R.C., H. Vaziri, C. Patterson, S. Goldstein, E.V. Younglai, A.B. Futcher, C.W. Greider, and C.B. Harley. 1992. Telomere length predicts replicative capacity of human fibroblasts. *Proc Natl Acad Sci U S A*. 89:10114-8.

Andrews, P.W., G. Banting, I. Damjanov, D. Arnaud, and P. Avner. 1984. Three monoclonal antibodies defining distinct differentiation antigens associated with different high molecular weight polypeptides on the surface of human embryonal carcinoma cells. *Hybridoma*. 3:347-361.

Assenmacher, N., and K.P. Hopfner. 2004. MRE11/RAD50/NBS1: complex activities. *Chromosoma*. 113:157-66.

Aubert, G., and P.M. Lansdorp. 2008. Telomeres and aging. *Physiol Rev*. 88:557-79.

Bergo, M.O., B. Gavino, J. Ross, W.K. Schmidt, C. Hong, L.V. Kendall, A. Mohr, M. Meta, H. Genant, Y. Jiang, E.R. Wisner, N. Van Bruggen, R.A. Carano, S. Michaelis, S.M. Griffey, and S.G. Young. 2002. Zmpste24 deficiency in mice causes spontaneous bone fractures, muscle weakness, and a prelamin A processing defect. *Proc Natl Acad Sci U S A*. 99:13049-54.

Biamonti, G., M. Giacca, G. Perini, G. Contreas, L. Zentilin, F. Weighardt, M. Guerra, G. Della Valle, S. Saccone, S. Riva, and et al. 1992. The gene for a novel human lamin maps at a highly transcribed locus of chromosome 19 which replicates at the onset of S-phase. *Mol Cell Biol*. 12:3499-506.

Bosco, E.E., C.N. Mayhew, R.F. Hennigan, J. Sage, T. Jacks, and E.S. Knudsen. 2004. RB signaling prevents replication-dependent DNA double-strand breaks following genotoxic insult. *Nucleic Acids Res*. 32:25-34.

Bracken, A.P., D. Pasini, M. Capra, E. Prosperini, E. Colli, and K. Helin. 2003. EZH2 is downstream of the pRB-E2F pathway, essential for proliferation and amplified in cancer. *Embo J*. 22:5323-35.

Brawley, C., and E. Matunis. 2004. Regeneration of male germline stem cells by spermatogonial dedifferentiation in vivo. *Science*. 304:1331-1334.

Bridger, J.M., and I.R. Kill. 2004. Aging of Hutchinson-Gilford progeria syndrome fibroblasts is characterised by hyperproliferation and increased apoptosis. *Exp Gerontol*. 39:717-24.

Bridger, J.M., I.R. Kill, M. O'Farrell, and C.J. Hutchison. 1993. Internal lamin structures within G1 nuclei of human dermal fibroblasts. *J Cell Sci*. 104 (Pt 2):297-306.

Broers, J.L., B.M. Machiels, H.J. Kuijpers, F. Smedts, R. van den Kieboom, Y. Raymond, and F.C. Ramaekers. 1997. A- and B-type lamins are differentially expressed in normal human tissues. *Histochem Cell Biol*. 107:505-17.

Burke, B. 1990. On the cell-free association of lamins A and C with metaphase chromosomes. *Exp Cell Res*. 186:169-76.

Burke, B., and L. Gerace. 1986. A cell free system to study reassembly of the nuclear envelope at the end of mitosis. *Cell*. 44:639-52.

Burke, B., and C.L. Stewart. 2002. Life at the edge: the nuclear envelope and human disease. *Nat Rev Mol Cell Biol*. 3:575-85.

Cao, B., B. Zheng, R.J. Jankowski, S. Kimura, M. Ikezawa, B. Deasy, J. Cummins, M. Epperly, Z. Qu-Petersen, and J. Huard. 2003. Muscle stem cells differentiate into haematopoietic lineages but retain myogenic potential. *Nat Cell Biol*. 5:640-646.

Cao, K., B.C. Capell, M.R. Erdos, K. Djabali, and F.S. Collins. 2007. A lamin A protein isoform overexpressed in Hutchinson-Gilford progeria syndrome interferes with mitosis in progeria and normal cells. *Proc Natl Acad Sci U S A*. 104:4949-54.

Capanni, C., V. Cenni, E. Mattioli, P. Sabatelli, A. Ognibene, M. Columbaro, V.K. Parnaik, M. Wehnert, N.M. Maraldi, S. Squarzoni, and G. Lattanzi. 2003. Failure of lamin A/C to functionally assemble in R482L mutated familial partial lipodystrophy fibroblasts: altered intermolecular interaction with emerin and implications for gene transcription. *Exp Cell Res*. 291:122-34.

Capell, B.C., M.R. Erdos, J.P. Madigan, J.J. Fiordalisi, R. Varga, K.N. Conneely, L.B. Gordon, C.J. Der, A.D. Cox, and F.S. Collins. 2005. Inhibiting farnesylation of progerin prevents the characteristic nuclear blebbing of Hutchinson-Gilford progeria syndrome. *Proc Natl Acad Sci U S A*. 102:12879-84.

Carney, J.P., R.S. Maser, H. Olivares, E.M. Davis, M. Le Beau, J.R. Yates, 3rd, L. Hays, W.F. Morgan, and J.H. Petrini. 1998. The hMre11/hRad50 protein complex and Nijmegen breakage syndrome: linkage of double-strand break repair to the cellular DNA damage response. *Cell*. 93:477-86.

Chaudhuri, J., U. Basu, A. Zarrin, C. Yan, S. Franco, T. Perlot, B. Vuong, J. Wang, R.T. Phan, A. Datta, J. Manis, and F.W. Alt. 2007. Evolution of the immunoglobulin heavy chain class switch recombination mechanism. *Adv Immunol*. 94:157-214.

Chen, F., A. Nastasi, Z. Shen, M. Brenneman, H. Crissman, and D.J. Chen. 1997. Cell cycle-dependent protein expression of mammalian homologs of yeast DNA double-strand break repair genes Rad51 and Rad52. *Mutat Res*. 384:205-11.

Clements, L., S. Manilal, D.R. Love, and G.E. Morris. 2000. Direct interaction between emerin and lamin A. *Biochem Biophys Res Commun*. 267:709-14.

Columbaro, M., C. Capanni, E. Mattioli, G. Novelli, V.K. Parnaik, S. Squarzoni, N.M. Maraldi, and G. Lattanzi. 2005. Rescue of heterochromatin organization in Hutchinson-Gilford progeria by drug treatment. *Cell Mol Life Sci*. 62:2669-78.

Constantinescu, D., H.L. Gray, P.J. Sammak, G.P. Schatten, and A.B. Csoka. 2006. Lamin A/C expression is a marker of mouse and human embryonic stem cell differentiation. *Stem Cells*. 24:177-85.

Corrigan, D.P., D. Kuszczak, A.E. Rusinol, D.P. Thewke, C.A. Hrycyna, S. Michaelis, and M.S. Sinensky. 2005. Prelamin A endoproteolytic processing in vitro by recombinant Zmpste24. *Biochem J*. 387:129-38.

Csoka, A.B., H. Cao, P.J. Sammak, D. Constantinescu, G.P. Schatten, and R.A. Hegele. 2004a. Novel lamin A/C gene (LMNA) mutations in atypical progeroid syndromes. *J Med Genet*. 41:304-8.

Csoka, A.B., S.B. English, C.P. Simkevich, D.G. Ginzinger, A.J. Butte, G.P. Schatten, F.G. Rothman, and J.M. Sedivy. 2004b. Genome-scale expression profiling of Hutchinson-Gilford progeria syndrome reveals widespread transcriptional misregulation leading to mesodermal/mesenchymal defects and accelerated atherosclerosis. *Aging Cell*. 3:235-43.

Cutler, R.G. 1991. Recent progress in testing the longevity determinant and dysdifferentiation. *Arch Gerontology Geriatr*. 12:75-98.

Dabauvalle, M.C., K. Loos, H. Merkert, and U. Scheer. 1991. Spontaneous assembly of pore complex-containing membranes ("annulate lamellae") in Xenopus egg extract in the absence of chromatin. *J Cell Biol*. 112:1073-82.

Dahl, K.N., P. Scaffidi, M.F. Islam, A.G. Yodh, K.L. Wilson, and T. Misteli. 2006. Distinct structural and mechanical properties of the nuclear lamina in Hutchinson-Gilford progeria syndrome. *Proc Natl Acad Sci U S A*. 103:10271-6.

de Jager, M., K.M. Trujillo, P. Sung, K.P. Hopfner, J.P. Carney, J.A. Tainer, J.C. Connelly, D.R. Leach, R. Kanaar, and C. Wyman. 2004. Differential arrangements of conserved building blocks among homologs of the Rad50/Mre11 DNA repair protein complex. *J Mol Biol*. 339:937-49.

De Sandre-Giovannoli, A., R. Bernard, P. Cau, C. Navarro, J. Amiel, I. Boccaccio, S. Lyonnet, C.L. Stewart, A. Munnich, M. Le Merrer, and N. Levy. 2003. Lamin a truncation in Hutchinson-Gilford progeria. *Science*. 300:2055.

Dechat, T., B. Korbei, O.A. Vaughan, S. Vlcek, C.J. Hutchison, and R. Foisner. 2000. Lamina-associated polypeptide 2alpha binds intranuclear A-type lamins. *J Cell Sci*. 113 Pt 19:3473-84.

Dechat, T., T. Shimi, S.A. Adam, A.E. Rusinol, D.A. Andres, H.P. Spielmann, M.S. Sinensky, and R.D. Goldman. 2007. Alterations in mitosis and cell cycle progression caused by a mutant lamin A known to accelerate human aging. *Proc Natl Acad Sci U S A*. 104:4955-60.

Delbarre, E., M. Tramier, M. Coppey-Moisan, C. Gaillard, J.C. Courvalin, and B. Buendia. 2006. The truncated prelamin A in Hutchinson-Gilford progeria syndrome alters segregation of A-type and B-type lamin homopolymers. *Hum Mol Genet*. 15:1113-22.

Dessev, G., C. Iovcheva-Dessev, J.R. Bischoff, D. Beach, and R. Goldman. 1991. A complex containing p34cdc2 and cyclin B phosphorylates the nuclear lamin and disassembles nuclei of clam oocytes in vitro. *J Cell Biol*. 112:523-33.

Dreuillet, C., J. Tillit, M. Kress, and M. Ernoult-Lange. 2002. In vivo and in vitro interaction between human transcription factor MOK2 and nuclear lamin A/C. *Nucleic Acids Res*. 30:4634-42.

Dronkert, M.L., H.B. Beverloo, R.D. Johnson, J.H. Hoeijmakers, M. Jasin, and R. Kanaar. 2000. Mouse RAD54 affects DNA double-strand break repair and sister chromatid exchange. *Mol Cell Biol*. 20:3147-56.

Eriksson, M., W.T. Brown, L.B. Gordon, M.W. Glynn, J. Singer, L. Scott, M.R. Erdos, C.M. Robbins, T.Y. Moses, P. Berglund, A. Dutra, E. Pak, S. Durkin, A.B. Csoka, M. Boehnke, T.W. Glover, and F.S. Collins. 2003. Recurrent de novo point mutations in lamin A cause Hutchinson-Gilford progeria syndrome. *Nature*. 423:293-8.

Fawcett, D.W. 1966. On the occurrence of a fibrous lamina on the inner aspect of the nuclear envelope in certain cells of vertebrates. *Am J Anat*. 119:129-45.

Filesi, I., F. Gullotta, G. Lattanzi, M.R. D'Apice, C. Capanni, A.M. Nardone, M. Columbaro, G. Scarano, E. Mattioli, P. Sabatelli, N.M. Maraldi, S. Biocca, and G. Novelli. 2005. Alterations of nuclear envelope and chromatin organization in mandibuloacral dysplasia, a rare form of laminopathy. *Physiol Genomics*. 23:150-8.

Fisher, D.Z., N. Chaudhary, and G. Blobel. 1986. cDNA sequencing of nuclear lamins A and C reveals primary and secondary structural homology to intermediate filament proteins. *Proc Natl Acad Sci U S A*. 83:6450-4.

Fong, L.G., D. Frost, M. Meta, X. Qiao, S.H. Yang, C. Coffinier, and S.G. Young. 2006a. A protein farnesyltransferase inhibitor ameliorates disease in a mouse model of progeria. *Science*. 311:1621-3.

Fong, L.G., J.K. Ng, J. Lammerding, T.A. Vickers, M. Meta, N. Cote, B. Gavino, X. Qiao, S.Y. Chang, S.R. Young, S.H. Yang, C.L. Stewart, R.T. Lee, C.F. Bennett, M.O. Bergo, and S.G. Young. 2006b. Prelamin A and lamin A appear to be dispensable in the nuclear lamina. *J Clin Invest*. 116:743-52.

Franco, S., F.W. Alt, and J.P. Manis. 2006. Pathways that suppress programmed DNA breaks from progressing to chromosomal breaks and translocations. *DNA Repair (Amst)*. 5:1030-41.

Furukawa, K., and Y. Hotta. 1993. cDNA cloning of a germ cell specific lamin B3 from mouse spermatocytes and analysis of its function by ectopic expression in somatic cells. *Embo J*. 12:97-106.

Furukawa, K., H. Inagaki, and Y. Hotta. 1994. Identification and cloning of an mRNA coding for a germ cell-specific A-type lamin in mice. *Exp Cell Res*. 212:426-30.

Gatz, S.A., and L. Wiesmuller. 2006. p53 in recombination and repair. *Cell Death Differ*. 13:1003-16.

Georgatos, S.D., A. Pyrpasopoulou, and P.A. Theodoropoulos. 1997. Nuclear envelope breakdown in mammalian cells involves stepwise lamina disassembly and microtubule-drive deformation of the nuclear membrane. *J Cell Sci*. 110 (Pt 17):2129-40.

Gerace, L., and G. Blobel. 1980. The nuclear envelope lamina is reversibly depolymerized during mitosis. *Cell*. 19:277-87.

Gilford, H. 1904. Progeria: a form of senilism. *Practitioner*. 73:188-217.

Glass, C.A., J.R. Glass, H. Taniura, K.W. Hasel, J.M. Blevitt, and L. Gerace. 1993. The alpha-helical rod domain of human lamins A and C contains a chromatin binding site. *Embo J*. 12:4413-24.

Glass, J.R., and L. Gerace. 1990. Lamins A and C bind and assemble at the surface of mitotic chromosomes. *J Cell Biol*. 111:1047-57.

Glynn, M.W., and T.W. Glover. 2005. Incomplete processing of mutant lamin A in Hutchinson-Gilford progeria leads to nuclear abnormalities, which are reversed by farnesyltransferase inhibition. *Hum Mol Genet*. 14:2959-69.

Goldman, A.E., R.D. Moir, M. Montag-Lowy, M. Stewart, and R.D. Goldman. 1992. Pathway of incorporation of microinjected lamin A into the nuclear envelope. *J Cell Biol*. 119:725-35.

Goldman, R.D., D.K. Shumaker, M.R. Erdos, M. Eriksson, A.E. Goldman, L.B. Gordon, Y. Gruenbaum, S. Khuon, M. Mendez, R. Varga, and F.S. Collins. 2004. Accumulation of mutant lamin A causes progressive changes in nuclear architecture in Hutchinson-Gilford progeria syndrome. *Proc Natl Acad Sci U S A*. 101:8963-8.

Gonzalo, S., M. Garcia-Cao, M.F. Fraga, G. Schotta, A.H. Peters, S.E. Cotter, R. Eguia, D.C. Dean, M. Esteller, T. Jenuwein, and M.A. Blasco. 2005. Role of the RB1 family in stabilizing histone methylation at constitutive heterochromatin. *Nat Cell Biol*. 7:420-8.

Gropp, M., P. Itsykson, O. Singer, T. Ben-Hur, E. Reinhartz, E. Galun, and B.E. Reubinoff. 2003. Stable genetic modification of human embryonic stem cells by lentiviral vectors. *Mol Ther*. 7:281-7.

Harborth, J., S.M. Elbashir, K. Bechert, T. Tuschl, and K. Weber. 2001. Identification of essential genes in cultured mammalian cells using small interfering RNAs. *J Cell Sci*. 114:4557-65.

Hennekam, R.C. 2006. Hutchinson-Gilford progeria syndrome: review of the phenotype. *Am J Med Genet A*. 140:2603-24.

Hofer, A.C., R.T. Tran, O.Z. Aziz, W. Wright, G. Novelli, J. Shay, and M. Lewis. 2005. Shared phenotypes among segmental progeroid syndromes suggest underlying pathways of aging. *J Gerontol A Biol Sci Med Sci*. 60:10-20.

Hoger, T.H., G. Krohne, and J.A. Kleinschmidt. 1991. Interaction of Xenopus lamins A and LII with chromatin in vitro mediated by a sequence element in the carboxyterminal domain. *Exp Cell Res*. 197:280-9.

Holaska, J.M., K.K. Lee, A.K. Kowalski, and K.L. Wilson. 2003. Transcriptional repressor germ cell-less (GCL) and barrier to autointegration factor (BAF) compete for binding to emerin in vitro. *J Biol Chem*. 278:6969-75.

Hopfner, K.P., A. Karcher, L. Craig, T.T. Woo, J.P. Carney, and J.A. Tainer. 2001. Structural biochemistry and interaction architecture of the DNA double-strand break repair Mre11 nuclease and Rad50-ATPase. *Cell*. 105:473-85.

Hozak, P., A.M. Sasseville, Y. Raymond, and P.R. Cook. 1995. Lamin proteins form an internal nucleoskeleton as well as a peripheral lamina in human cells. *J Cell Sci*. 108 (Pt 2):635-44.

Hutchinson, J. 1886. Congenital absence of hair and mammary glands with atrophic condition of the skin and its appendages in a boy whose mother had been almost totally bald from alopecia areata from the age of six. *Medicochirurgical Transactions*. 69:473-477.

Isaac, C.E., S.M. Francis, A.L. Martens, L.M. Julian, L.A. Seifried, N. Erdmann, U.K. Binne, L. Harrington, P. Sicinski, N.G. Berube, N.J. Dyson, and F.A. Dick. 2006. The retinoblastoma protein regulates pericentric heterochromatin. *Mol Cell Biol*. 26:3659-71.

Jagatheesan, G., S. Thanumalayan, B. Muralikrishna, N. Rangaraj, A.A. Karande, and V.K. Parnaik. 1999. Colocalization of intranuclear lamin foci with RNA splicing factors. *J Cell Sci*. 112 (Pt 24):4651-61.

Johnson, B.R., R.T. Nitta, R.L. Frock, L. Mounkes, D.A. Barbie, C.L. Stewart, E. Harlow, and B.K. Kennedy. 2004. A-type lamins regulate retinoblastoma protein function by promoting subnuclear localization and preventing proteasomal degradation. *Proc Natl Acad Sci U S A*. 101:9677-82.

Kadyk, L.C., and L.H. Hartwell. 1992. Sister chromatids are preferred over homologs as substrates for recombinational repair in Saccharomyces cerevisiae. *Genetics*. 132:387-402.

Kannagi, R., N.A. Cochran, F. Ishigami, S. Hakomori, P.W. Andrews, B.B. Knowles, and D. Solter. 1983. Stage-specific embryonic antigens (SSEA-3 and -4) are epitopes of a unique globo-series ganglioside isolated from human teratocarcinoma cells. *Embo J*. 2:2355-2361.

Kator, K., V. Cristofalo, R. Charpentier, and R.G. Cutler. 1985. Dysdifferentiative nature of aging: passage number dependency of globin gene. *Gerontology*. 31:355-361.

Keeney, S., and M.J. Neale. 2006. Initiation of meiotic recombination by formation of DNA double-strand breaks: mechanism and regulation. *Biochem Soc Trans*. 34:523-5.

Kennedy, B.K., D.A. Barbie, M. Classon, N. Dyson, and E. Harlow. 2000. Nuclear organization of DNA replication in primary mammalian cells. *Genes Dev*. 14:2855-68.

Kirkland, J.L., T. Tchkonia, T. Pirtskhalava, J. Han, and I. Karagiannides. 2002. Adipogenesis and aging: does aging make fat go MAD? *Exp Gerontol*. 37:757-767.

Kirkwood, T.B. 1977. Evolution of ageing. *Nature*. 270:301-4.

Kirkwood, T.B., and R. Holliday. 1979. The evolution of ageing and longevity. *Proc R Soc Lond B Biol Sci*. 205:531-46.

Kobayashi, J., K. Iwabuchi, K. Miyagawa, E. Sonoda, K. Suzuki, M. Takata, and H. Tauchi. 2008. Current topics in DNA double-strand break repair. *J Radiat Res (Tokyo)*. 49:93-103.

Kumaran, R.I., B. Muralikrishna, and V.K. Parnaik. 2002. Lamin A/C speckles mediate spatial organization of splicing factor compartments and RNA polymerase II transcription. *J Cell Biol*. 159:783-93.

Kurz, E.U., and S.P. Lees-Miller. 2004. DNA damage-induced activation of ATM and ATM-dependent signaling pathways. *DNA Repair (Amst)*. 3:889-900.

Lammerding, J., P.C. Schulze, T. Takahashi, S. Kozlov, T. Sullivan, R.D. Kamm, C.L. Stewart, and R.T. Lee. 2004. Lamin A/C deficiency causes defective nuclear mechanics and mechanotransduction. *J Clin Invest*. 113:370-8.

Lee, J.H., and T.T. Paull. 2005. ATM activation by DNA double-strand breaks through the Mre11-Rad50-Nbs1 complex. *Science*. 308:551-4.

Lehner, C.F., V. Kurer, H.M. Eppenberger, and E.A. Nigg. 1986. The nuclear lamin protein family in higher vertebrates. Identification of quantitatively minor lamin proteins by monoclonal antibodies. *J Biol Chem*. 261:13293-301.

Lenz-Bohme, B., J. Wismar, S. Fuchs, R. Reifegerste, E. Buchner, H. Betz, and B. Schmitt. 1997. Insertional mutation of the Drosophila nuclear lamin Dm0 gene results in defective nuclear envelopes, clustering of nuclear pore complexes, and accumulation of annulate lamellae. *J Cell Biol*. 137:1001-16.

Limoli, C.L., E. Giedzinski, W.M. Bonner, and J.E. Cleaver. 2002. UV-induced replication arrest in the xeroderma pigmentosum variant leads to DNA double-strand breaks, gamma -H2AX formation, and Mre11 relocalization. *Proc Natl Acad Sci U S A*. 99:233-8.

Liu, B., J. Wang, K.M. Chan, W.M. Tjia, W. Deng, X. Guan, J.D. Huang, K.M. Li, P.Y. Chau, D.J. Chen, D. Pei, A.M. Pendas, J. Cadinanos, C. Lopez-Otin, H.F. Tse, C. Hutchison, J. Chen, Y. Cao, K.S. Cheah, K. Tryggvason, and Z. Zhou. 2005. Genomic instability in laminopathy-based premature aging. *Nat Med*. 11:780-5.

Liu, Y., A. Rusinol, M. Sinensky, Y. Wang, and Y. Zou. 2006. DNA damage responses in progeroid syndromes arise from defective maturation of prelamin A. *J Cell Sci*. 119:4644-9.

Lloyd, D.J., R.C. Trembath, and S. Shackleton. 2002. A novel interaction between lamin A and SREBP1: implications for partial lipodystrophy and other laminopathies. *Hum Mol Genet*. 11:769-77.

Lombard, D.B., K.F. Chua, R. Mostoslavsky, S. Franco, M. Gostissa, and F.W. Alt. 2005. DNA repair, genome stability, and aging. *Cell*. 120:497-512.

Lourim, D., and G. Krohne. 1993. Membrane-associated lamins in Xenopus egg extracts: identification of two vesicle populations. *J Cell Biol*. 123:501-12.

Lourim, D., and J.J. Lin. 1989a. Expression of nuclear lamin A and muscle-specific proteins in differentiating muscle cells in ovo and in vitro. *J Cell Biol*. 109:495-504.

Lourim, D., and J.J. Lin. 1989b. Expression of nulcear lamin A and muscle-specific proteins in differentiating muscle cells in ovo and in vitro. *J Cll Biol*. 109:495-504.

Luo, G., M.S. Yao, C.F. Bender, M. Mills, A.R. Bladl, A. Bradley, and J.H. Petrini. 1999. Disruption of mRad50 causes embryonic stem cell lethality, abnormal embryonic development, and sensitivity to ionizing radiation. *Proc Natl Acad Sci U S A*. 96:7376-81.

Ly, D.H., D.J. Lockhart, R.A. Lerner, and P.G. Schultz. 2000. Mitotic misregulation and human aging. *Science*. 287:2486-92.

Machiels, B.M., A.H. Zorenc, J.M. Endert, H.J. Kuijpers, G.J. van Eys, F.C. Ramaekers, and J.L. Broers. 1996. An alternative splicing product of the lamin A/C gene lacks exon 10. *J Biol Chem*. 271:9249-53.

Magnuson, T., C.J. Epstein, L.M. Silver, and G.R. Martin. 1982. Pluripotent embryonic stem cell lines can be derived from tw5/tw5 blastocysts. *Nature*. 298:750-3.

Mancini, M.A., B. Shan, J.A. Nickerson, S. Penman, and W.H. Lee. 1994. The retinoblastoma gene product is a cell cycle-dependent, nuclear matrix-associated protein. *Proc Natl Acad Sci U S A*. 91:418-22.

Masny, P.S., U. Bengtsson, S.A. Chung, J.H. Martin, B. van Engelen, S.M. van der Maarel, and S.T. Winokur. 2004. Localization of 4q35.2 to the nuclear periphery: is FSHD a nuclear envelope disease? *Hum Mol Genet*. 13:1857-71.

McKeon, F.D., M.W. Kirschner, and D. Caput. 1986. Homologies in both primary and secondary structure between nuclear envelope and intermediate filament proteins. *Nature*. 319:463-8.

Meaburn, K.J., E. Cabuy, G. Bonne, N. Levy, G.E. Morris, G. Novelli, I.R. Kill, and J.M. Bridger. 2007. Primary laminopathy fibroblasts display altered genome organization and apoptosis. *Aging Cell*. 6:139-53.

Meier, J., K.H. Campbell, C.C. Ford, R. Stick, and C.J. Hutchison. 1991. The role of lamin LIII in nuclear assembly and DNA replication, in cell-free extracts of Xenopus eggs. *J Cell Sci*. 98 (Pt 3):271-9.

Merideth, M.A., L.B. Gordon, S. Clauss, V. Sachdev, A.C. Smith, M.B. Perry, C.C. Brewer, C. Zalewski, H.J. Kim, B. Solomon, B.P. Brooks, L.H. Gerber, M.L. Turner, D.L. Domingo, T.C. Hart, J. Graf, J.C. Reynolds, A. Gropman, J.A. Yanovski, M. Gerhard-Herman, F.S. Collins, E.G. Nabel, R.O. Cannon, 3rd, W.A. Gahl, and W.J. Introne. 2008. Phenotype and course of Hutchinson-Gilford progeria syndrome. *N Engl J Med*. 358:592-604.

Moir, R.D., T.P. Spann, H. Herrmann, and R.D. Goldman. 2000. Disruption of nuclear lamin organization blocks the elongation phase of DNA replication. *J Cell Biol*. 149:1179-92.

Mounkes, L., S. Kozlov, B. Burke, and C.L. Stewart. 2003. The laminopathies: nuclear structure meets disease. *Curr Opin Genet Dev*. 13:223-30.

Muralikrishna, B., J. Dhawan, N. Rangaraj, and V.K. Parnaik. 2001. Distinct changes in intranuclear lamin A/C organization during myoblast differentiation. *J Cell Sci*. 114:4001-11.

Navarro, C.L., P. Cau, and N. Levy. 2006. Molecular bases of progeroid syndromes. *Hum Mol Genet*. 15 Spec No 2:R151-61.

Newport, J., and T. Spann. 1987. Disassembly of the nucleus in mitotic extracts: membrane vesicularization, lamin disassembly, and chromosome condensation are independent processes. *Cell*. 48:219-30.

Newport, J.W., K.L. Wilson, and W.G. Dunphy. 1990. A lamin-independent pathway for nuclear envelope assembly. *J Cell Biol*. 111:2247-59.

Nielsen, S.J., R. Schneider, U.M. Bauer, A.J. Bannister, A. Morrison, D. O'Carroll, R. Firestein, M. Cleary, T. Jenuwein, R.E. Herrera, and T. Kouzarides. 2001. Rb targets histone H3 methylation and HP1 to promoters. *Nature*. 412:561-5.

Nikolova, V., C. Leimena, A.C. McMahon, J.C. Tan, S. Chandar, D. Jogia, S.H. Kesteven, J. Michalicek, R. Otway, F. Verheyen, S. Rainer, C.L. Stewart, D. Martin, M.P.

Feneley, and D. Fatkin. 2004. Defects in nuclear structure and function promote dilated cardiomyopathy in lamin A/C-deficient mice. *J Clin Invest*. 113:357-69.

Ottaviano, Y., and L. Gerace. 1985. Phosphorylation of the nuclear lamins during interphase and mitosis. *J Biol Chem*. 260:624-32.

Ouellette, M.M., L.D. McDaniel, W.E. Wright, J.W. Shay, and R.A. Schultz. 2000. The establishment of telomerase-immortalized cell lines representing human chromosome instability syndromes. *Hum Mol Genet*. 9:403-11.

Ozaki, T., M. Saijo, K. Murakami, H. Enomoto, Y. Taya, and S. Sakiyama. 1994. Complex formation between lamin A and the retinoblastoma gene product: identification of the domain on lamin A required for its interaction. *Oncogene*. 9:2649-53.

Park, W.Y., C.I. Hwang, M.J. Kang, J.Y. Seo, J.H. Chung, Y.S. Kim, J.H. Lee, H. Kim, K.A. Kim, H.J. Yoo, and J.S. Seo. 2001. Gene profile of replicative senescence is different from progeria or elderly donor. *Biochem Biophys Res Commun*. 282:934-9.

Pesce, M., M.K. Gross, and H.R. Scholer. 1998. In line with our ancestors: Oct-4 and the mammalian germ. *Bioessays*. 20:722-732.

Peter, M., J. Nakagawa, M. Doree, J.C. Labbe, and E.A. Nigg. 1990. In vitro disassembly of the nuclear lamina and M phase-specific phosphorylation of lamins by cdc2 kinase. *Cell*. 61:591-602.

Peter, M., and E.A. Nigg. 1991. Ectopic expression of an A-type lamin does not interfere with differentiation of lamin A-negative embryonal carcinoma cells. *J Cell Sci*. 100 (Pt 3):589-98.

Pollard, K.M., E.K. Chan, B.J. Grant, K.F. Sullivan, E.M. Tan, and C.A. Glass. 1990. In vitro posttranslational modification of lamin B cloned from a human T-cell line. *Mol Cell Biol*. 10:2164-75.

Prather, R.S., J. Kubiak, G.G. Maul, N.L. First, and G. Schatten. 1991. The expression of nuclear lamin A and C epitopes is regulated by the developmental stage of the cytoplasm in mouse oocytes or embryos. *J Exp Zool*. 257:110-4.

Prather, R.S., M.M. Sims, G.G. Maul, N.L. First, and G. Schatten. 1989. Nuclear lamin antigens are developmentally regulated during porcine and bovine embryogenesis. *Biol Reprod*. 41:123-32.

Puzianowska-Kuznicka, M., and J. Kuznicki. 2005. Genetic alterations in accelerated ageing syndromes. Do they play a role in natural ageing? *Int J Biochem Cell Biol*. 37:947-60.

Rankin, J., and S. Ellard. 2006. The laminopathies: a clinical review. *Clin Genet*. 70:261-74.

Reubinoff, B.E., M.F. Pera, C.Y. Fong, A. Trounson, and A. Bongso. 2000. Embryonic stem cell lines from human blastocysts: somatic differentiation in vitro. *Nat Biotechnol*. 18:399-404.

Rober, R.A., K. Weber, and M. Osborn. 1989. Differential timing of nuclear lamin A/C expression in the various organs of the mouse embryo and the young animal: a developmental study. *Development*. 105:365-78.

Rossi, D.J., C.H. Jamieson, and I.L. Weissman. 2008. Stems cells and the pathways to aging and cancer. *Cell*. 132:681-96.

Sabatelli, P., G. Lattanzi, A. Ognibene, M. Columbaro, C. Capanni, L. Merlini, N.M. Maraldi, and S. Squarzoni. 2001. Nuclear alterations in autosomal-dominant Emery-Dreifuss muscular dystrophy. *Muscle Nerve*. 24:826-9.

Scaffidi, P., and T. Misteli. 2005. Reversal of the cellular phenotype in the premature aging disease Hutchinson-Gilford progeria syndrome. *Nat Med*. 11:440-5.

Scaffidi, P., and T. Misteli. 2008. Lamin A-dependent misregulation of adult stem cells associated with accelerated ageing. *Nat Cell Biol*. 10:452-9.

Schatten, G., G.G. Maul, H. Schatten, N. Chaly, C. Simerly, R. Balczon, and D.L. Brown. 1985. Nuclear lamins and peripheral nuclear antigens during fertilization and embryogenesis in mice and sea urchins. *Proc Natl Acad Sci U S A*. 82:4727-31.

Schmidt, M., and G. Krohne. 1995. In vivo assembly kinetics of fluorescently labeled Xenopus lamin A mutants. *Eur J Cell Biol*. 68:345-54.

Sedelnikova, O.A., I. Horikawa, D.B. Zimonjic, N.C. Popescu, W.M. Bonner, and J.C. Barrett. 2004. Senescing human cells and ageing mice accumulate DNA lesions with unrepairable double-strand breaks. *Nat Cell Biol*. 6:168-70.

Sharpless, N.E., and R.A. DePinho. 2007. How stem cells age and why this makes us grow old. *Nat Rev Mol Cell Biol*. 8:703-13.

Shoeman, R.L., and P. Traub. 1990. The in vitro DNA-binding properties of purified nuclear lamin proteins and vimentin. *J Biol Chem*. 265:9055-61.

Shrivastav, M., L.P. De Haro, and J.A. Nickoloff. 2008. Regulation of DNA double-strand break repair pathway choice. *Cell Res*. 18:134-47.

Shumaker, D.K., T. Dechat, A. Kohlmaier, S.A. Adam, M.R. Bozovsky, M.R. Erdos, M. Eriksson, A.E. Goldman, S. Khuon, F.S. Collins, T. Jenuwein, and R.D. Goldman. 2006. Mutant nuclear lamin A leads to progressive alterations of epigenetic control in premature aging. *Proc Natl Acad Sci U S A*. 103:8703-8.

Shumaker, D.K., L.R. Vann, M.W. Goldberg, T.D. Allen, and K.L. Wilson. 1998. TPEN, a Zn2+/Fe2+ chelator with low affinity for Ca2+, inhibits lamin assembly, destabilizes nuclear architecture and may independently protect nuclei from apoptosis in vitro. *Cell Calcium*. 23:151-64.

Sinensky, M., K. Fantle, M. Trujillo, T. McLain, A. Kupfer, and M. Dalton. 1994. The processing pathway of prelamin A. *J Cell Sci*. 107 (Pt 1):61-7.

Sjogren, C., and K. Nasmyth. 2001. Sister chromatid cohesion is required for postreplicative double-strand break repair in Saccharomyces cerevisiae. *Curr Biol*. 11:991-5.

Smythe, C., H.E. Jenkins, and C.J. Hutchison. 2000. Incorporation of the nuclear pore basket protein nup153 into nuclear pore structures is dependent upon lamina assembly: evidence from cell-free extracts of Xenopus eggs. *Embo J*. 19:3918-31.

Soutoglou, E., and T. Misteli. 2008. Activation of the cellular DNA damage response in the absence of DNA lesions. *Science*. 320:1507-10.

Spann, T.P., A.E. Goldman, C. Wang, S. Huang, and R.D. Goldman. 2002. Alteration of nuclear lamin organization inhibits RNA polymerase II-dependent transcription. *J Cell Biol*. 156:603-8.

Spann, T.P., R.D. Moir, A.E. Goldman, R. Stick, and R.D. Goldman. 1997. Disruption of nuclear lamin organization alters the distribution of replication factors and inhibits DNA synthesis. *J Cell Biol*. 136:1201-12.

Steen, R.L., S.B. Martins, K. Tasken, and P. Collas. 2000. Recruitment of protein phosphatase 1 to the nuclear envelope by A-kinase anchoring protein AKAP149 is a prerequisite for nuclear lamina assembly. *J Cell Biol*. 150:1251-62.

Stewart, C., and B. Burke. 1987. Teratocarcinoma stem cells and early mouse embryos contain only a single major lamin polypeptide closely resembling lamin B. *Cell*. 51:383-92.

Stewart, G.S., R.S. Maser, T. Stankovic, D.A. Bressan, M.I. Kaplan, N.G. Jaspers, A. Raams, P.J. Byrd, J.H. Petrini, and A.M. Taylor. 1999. The DNA double-strand break repair gene hMRE11 is mutated in individuals with an ataxia-telangiectasia-like disorder. *Cell*. 99:577-87.

Stierle, V., J. Couprie, C. Ostlund, I. Krimm, S. Zinn-Justin, P. Hossenlopp, H.J. Worman, J.C. Courvalin, and I. Duband-Goulet. 2003. The carboxyl-terminal region common to lamins A and C contains a DNA binding domain. *Biochemistry*. 42:4819-28.

Strathern, J.N., B.K. Shafer, and C.B. McGill. 1995. DNA synthesis errors associated with double-strand-break repair. *Genetics*. 140:965-72.

Strom, L., C. Karlsson, H.B. Lindroos, S. Wedahl, Y. Katou, K. Shirahige, and C. Sjogren. 2007. Postreplicative formation of cohesion is required for repair and induced by a single DNA break. *Science*. 317:242-5.

Sullivan, T., D. Escalante-Alcalde, H. Bhatt, M. Anver, N. Bhat, K. Nagashima, C.L. Stewart, and B. Burke. 1999. Loss of A-type lamin expression compromises nuclear envelope integrity leading to muscular dystrophy. *J Cell Biol*. 147:913-20.

Taniura, H., C. Glass, and L. Gerace. 1995. A chromatin binding site in the tail domain of nuclear lamins that interacts with core histones. *J Cell Biol*. 131:33-44.

Thompson, L.J., M. Bollen, and A.P. Fields. 1997. Identification of protein phosphatase 1 as a mitotic lamin phosphatase. *J Biol Chem*. 272:29693-7.

Thomson, J.A., J. Itskovitz-Eldor, S.S. Shapiro, M.A. Waknitz, J.J. Swiergiel, V.S. Marshall, and J.M. Jones. 1998. Embryonic stem cell lines derived from human blastocysts. *Science*. 282:1145-7.

Toth, J.I., S.H. Yang, X. Qiao, A.P. Beigneux, M.H. Gelb, C.L. Moulson, J.H. Miner, S.G. Young, and L.G. Fong. 2005. Blocking protein farnesyltransferase improves nuclear shape in fibroblasts from humans with progeroid syndromes. *Proc Natl Acad Sci U S A*. 102:12873-8.

Varela, I., J. Cadinanos, A.M. Pendas, A. Gutierrez-Fernandez, A.R. Folgueras, L.M. Sanchez, Z. Zhou, F.J. Rodriguez, C.L. Stewart, J.A. Vega, K. Tryggvason, J.M. Freije, and C. Lopez-Otin. 2005. Accelerated ageing in mice deficient in Zmpste24 protease is linked to p53 signalling activation. *Nature*. 437:564-8.

Varga, R., M. Eriksson, M.R. Erdos, M. Olive, I. Harten, F. Kolodgie, B.C. Capell, J. Cheng, D. Faddah, S. Perkins, H. Avallone, H. San, X. Qu, S. Ganesh, L.B. Gordon, R. Virmani, T.N. Wight, E.G. Nabel, and F.S. Collins. 2006. Progressive vascular smooth muscle cell defects in a mouse model of Hutchinson-Gilford progeria syndrome. *Proc Natl Acad Sci U S A*. 103:3250-5.

Varon, R., C. Vissinga, M. Platzer, K.M. Cerosaletti, K.H. Chrzanowska, K. Saar, G. Beckmann, E. Seemanova, P.R. Cooper, N.J. Nowak, M. Stumm, C.M. Weemaes, R.A. Gatti, R.K. Wilson, M. Digweed, A. Rosenthal, K. Sperling, P. Concannon, and A. Reis. 1998. Nibrin, a novel DNA double-strand break repair protein, is mutated in Nijmegen breakage syndrome. *Cell*. 93:467-76.

Vergnes, L., M. Peterfy, M.O. Bergo, S.G. Young, and K. Reue. 2004. Lamin B1 is required for mouse development and nuclear integrity. *Proc Natl Acad Sci U S A*. 101:10428-33.

Vigouroux, C., M. Auclair, E. Dubosclard, M. Pouchelet, J. Capeau, J.C. Courvalin, and B. Buendia. 2001. Nuclear envelope disorganization in fibroblasts from lipodystrophic patients with heterozygous R482Q/W mutations in the lamin A/C gene. *J Cell Sci*. 114:4459-68.

Vijg, J. 2000. Somatic mutations and aging: a re-evaluation. *Mutat Res*. 447:117-35.

Vlcek, S., H. Just, T. Dechat, and R. Foisner. 1999. Functional diversity of LAP2alpha and LAP2beta in postmitotic chromosome association is caused by an alpha-specific nuclear targeting domain. *Embo J*. 18:6370-84.

Wallis, C.V., A.N. Sheerin, M.H. Green, C.J. Jones, D. Kipling, and R.G. Faragher. 2004. Fibroblast clones from patients with Hutchinson-Gilford progeria can senesce despite the presence of telomerase. *Exp Gerontol*. 39:461-7.

Williams, R.S., J.S. Williams, and J.A. Tainer. 2007. Mre11-Rad50-Nbs1 is a keystone complex connecting DNA repair machinery, double-strand break signaling, and the chromatin template. *Biochem Cell Biol*. 85:509-20.

Xiao, Y., and D.T. Weaver. 1997. Conditional gene targeted deletion by Cre recombinase demonstrates the requirement for the double-strand break repair Mre11 protein in murine embryonic stem cells. *Nucleic Acids Res*. 25:2985-91.

Yang, S.H., M.O. Bergo, J.I. Toth, X. Qiao, Y. Hu, S. Sandoval, M. Meta, P. Bendale, M.H. Gelb, S.G. Young, and L.G. Fong. 2005. Blocking protein farnesyltransferase improves nuclear blebbing in mouse fibroblasts with a targeted Hutchinson-Gilford progeria syndrome mutation. *Proc Natl Acad Sci U S A*. 102:10291-6.

Yang, S.H., M. Meta, X. Qiao, D. Frost, J. Bauch, C. Coffinier, S. Majumdar, M.O. Bergo, S.G. Young, and L.G. Fong. 2006. A farnesyltransferase inhibitor improves disease phenotypes in mice with a Hutchinson-Gilford progeria syndrome mutation. *J Clin Invest*. 116:2115-21.

Yang, S.H., X. Qiao, L.G. Fong, and S.G. Young. 2008. Treatment with a farnesyltransferase inhibitor improves survival in mice with a Hutchinson-Gilford progeria syndrome mutation. *Biochim Biophys Acta*. 1781:36-9.

You, Z., C. Chahwan, J. Bailis, T. Hunter, and P. Russell. 2005. ATM activation and its recruitment to damaged DNA require binding to the C terminus of Nbs1. *Mol Cell Biol*. 25:5363-79.

Yuan, J., G. Simos, G. Blobel, and S.D. Georgatos. 1991. Binding of lamin A to polynucleosomes. *J Biol Chem*. 266:9211-5.

Zhu, J., S. Petersen, L. Tessarollo, and A. Nussenzweig. 2001. Targeted disruption of the Nijmegen breakage syndrome gene NBS1 leads to early embryonic lethality in mice. *Curr Biol*. 11:105-9.